Verifica e Validazione di Risultati Numerici

Tiziano Ghisu

Cagliari, 5 novembre 2018

CONTENUTI

1) Note Preliminari
2) Errore e Incertezza in una Simulazione Numerica
3) Verifica e Validazione
4) Esempio 1 - Coefficiente di Portanza di un Profilo
5) Esempio 2 - Turbina Wells
6) Conclusioni

NOTE PRELIMINARI

NOTE PRELIMINARI (1)

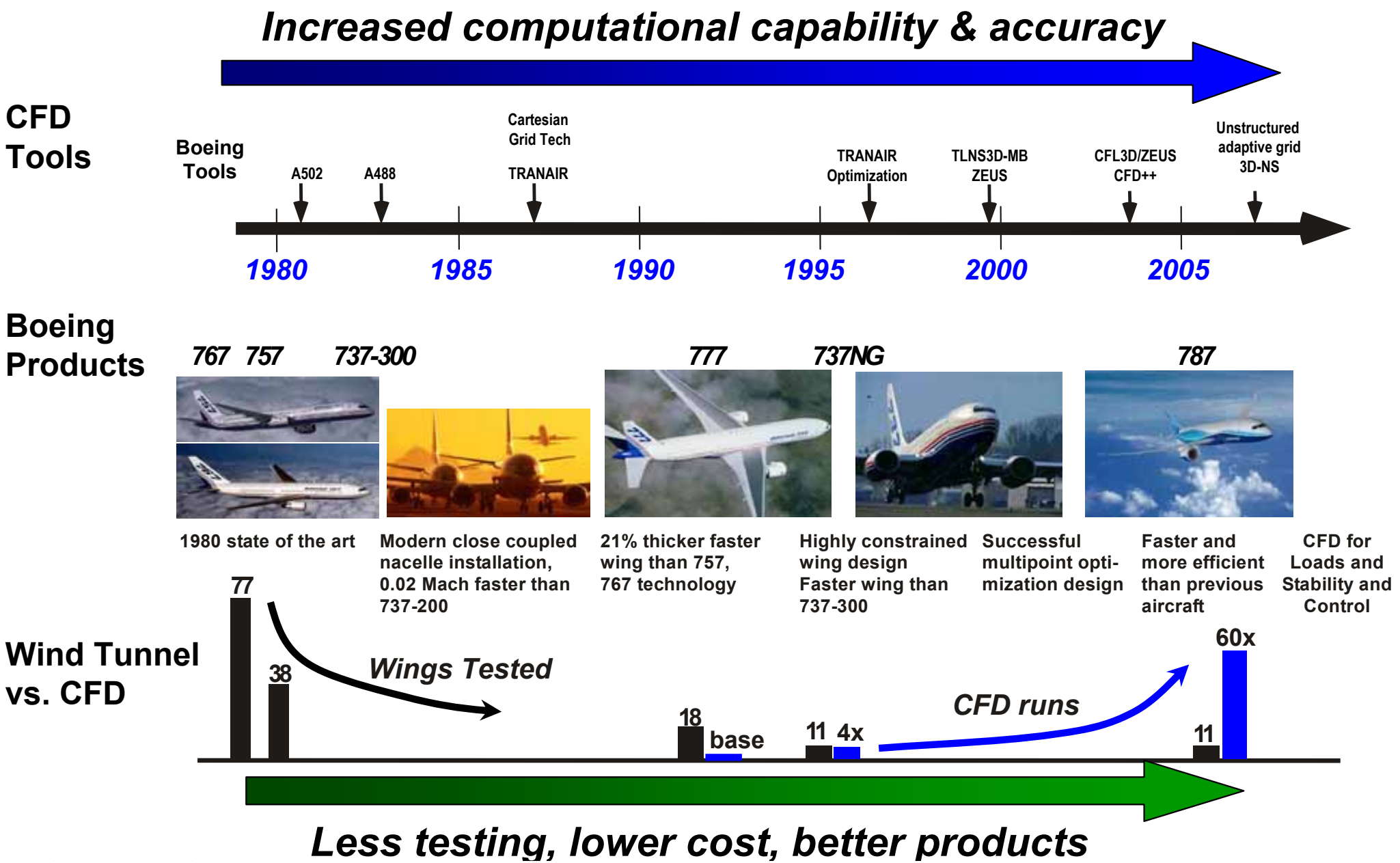

NOTE PRELIMINARI (2)

1970

1980

1990

2000

NOTE PRELIMINARI (3)

RR XWB (2010)

ERRORE E INCERTEZZA
IN UNA SIMULAZIONE NUMERICA

FASI DI UNA SIMULAZIONE NUMERICA

PROBLEMA FISICO

MODELLO MATEMATICO

$$\nabla \cdot \mathbf{u} = 0$$

$$\rho\frac{\partial \mathbf{u}}{\partial t} + \rho\nabla\cdot(\mathbf{u}\otimes\mathbf{u}) = \rho\frac{D\mathbf{u}}{Dt} = -\nabla p + \nabla\cdot\mathbf{\Pi} + \mathbf{a}$$

$$\rho\frac{\partial h}{\partial t} + \rho\nabla\cdot(\mathbf{u}h) = \rho\frac{Dh}{Dt} = -\nabla\cdot\mathbf{q} + \mathbf{\Pi}\colon\nabla\mathbf{u} + \frac{Dp}{Dt}$$

SOLUZIONE NUMERICA

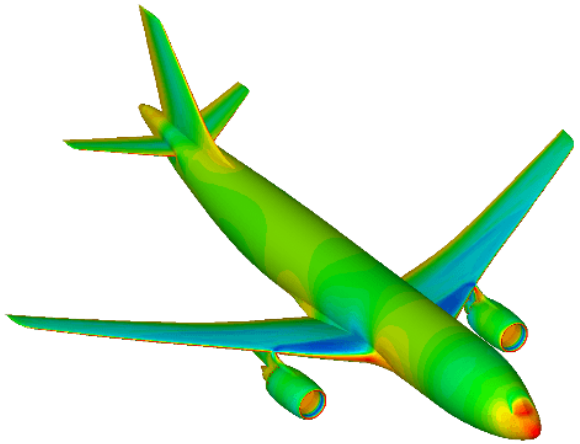

FASI DI UNA SIMULAZIONE NUMERICA

PROBLEMA FISICO

ERRORE MODELLO

MODELLO MATEMATICO

$$\nabla \cdot \mathbf{u} = 0$$

$$\rho\frac{\partial \mathbf{u}}{\partial t} + \rho\nabla\cdot(\mathbf{u}\otimes\mathbf{u}) = \rho\frac{D\mathbf{u}}{Dt} = -\nabla p + \nabla\cdot\mathbf{\Pi} + \mathbf{a}$$

$$\rho\frac{\partial h}{\partial t} + \rho\nabla\cdot(\mathbf{u}h) = \rho\frac{Dh}{Dt} = -\nabla\cdot\mathbf{q} + \mathbf{\Pi}\colon\nabla\mathbf{u} + \frac{Dp}{Dt}$$

ERRORE NUMERICO

SOLUZIONE NUMERICA

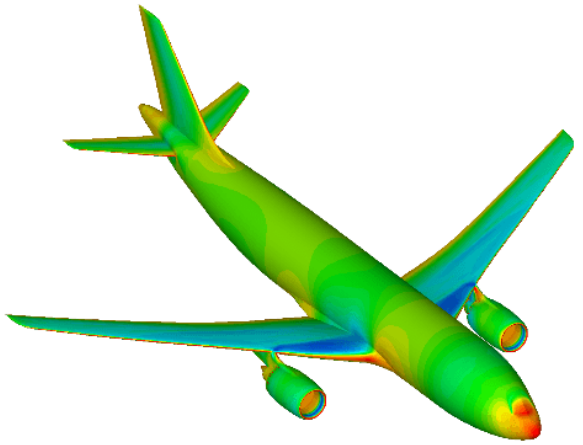

FASI DI UNA SIMULAZIONE NUMERICA

La **verifica** e **validazione** si occupano della valutazione degli errori e dell'incertezza introdotti nella soluzione numerica di un problema fisico.

FASI DI UNA SIMULAZIONE NUMERICA

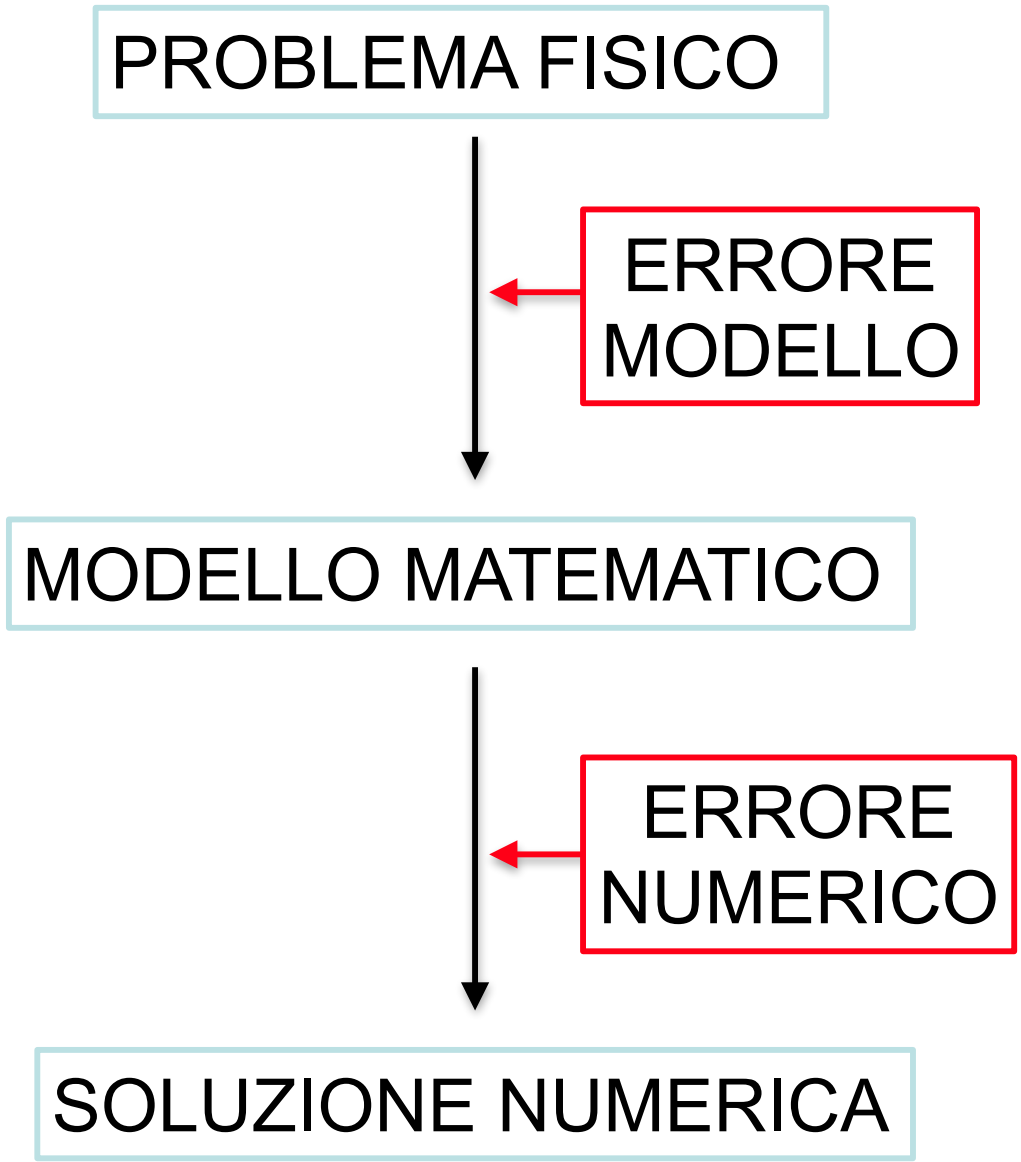

La **validazione** (validation) è la determinazione dell'accuratezza del modello matematico nel rappresentare il problema fisico sotto esame.

(stima dell'errore del modello)

La **verifica** (verification) è la determinazione dell'accuratezza dell'implementazione numerica di un modello e della sua soluzione.

(stima dell'errore numerico)

FASI DI UNA SIMULAZIONE NUMERICA

PROBLEMA FISICO

MODELLO MATEMATICO

$$\nabla \cdot \mathbf{u} = 0$$

$$\rho\frac{\partial \mathbf{u}}{\partial t} + \rho\nabla\cdot(\mathbf{u}\otimes\mathbf{u}) = \rho\frac{D\mathbf{u}}{Dt} = -\nabla p + \nabla\cdot\mathbf{\Pi} + \mathbf{a}$$

$$\rho\frac{\partial h}{\partial t} + \rho\nabla\cdot(\mathbf{u}h) = \rho\frac{Dh}{Dt} = -\nabla\cdot\mathbf{q} + \mathbf{\Pi}\colon\nabla\mathbf{u} + \frac{Dp}{Dt}$$

SOLUZIONE NUMERICA

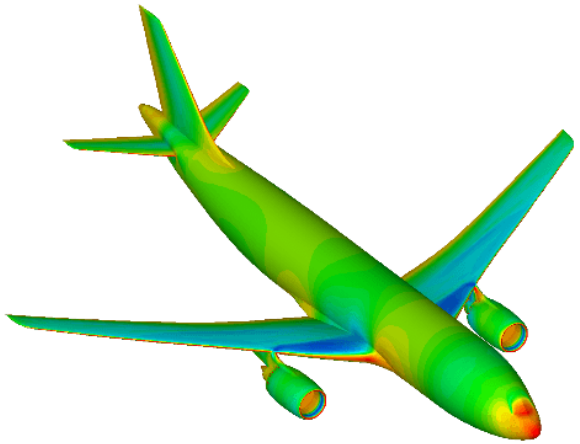

ERRORE E INCERTEZZA

1) SOLUZIONE NUMERICA

2) STIMA ERRORE NUMERICO (**VERIFICA**)

ERRORE E INCERTEZZA

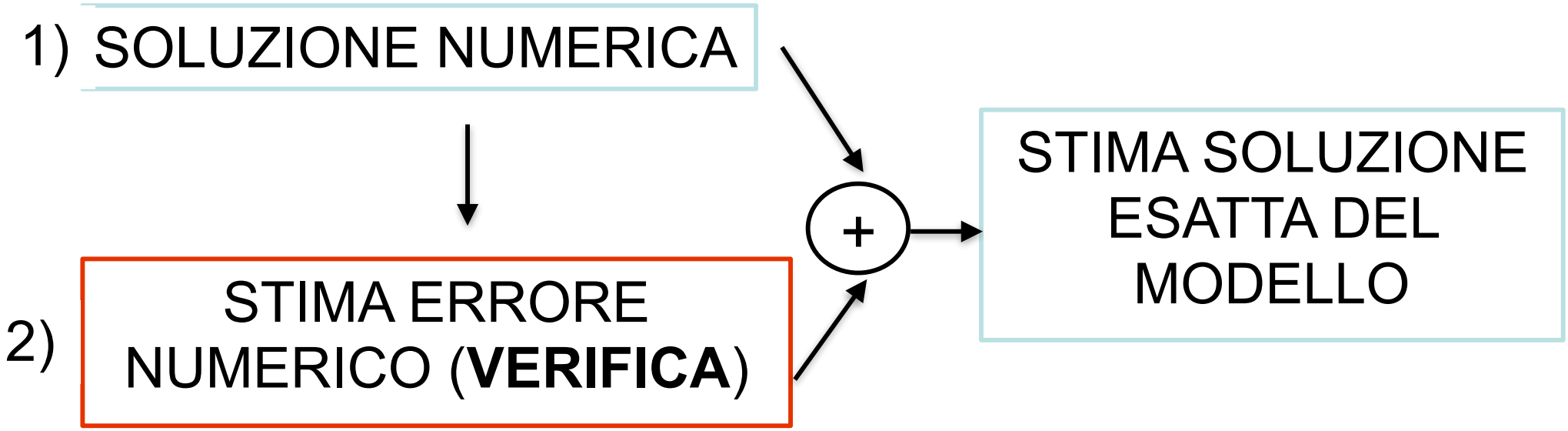

ERRORE E INCERTEZZA

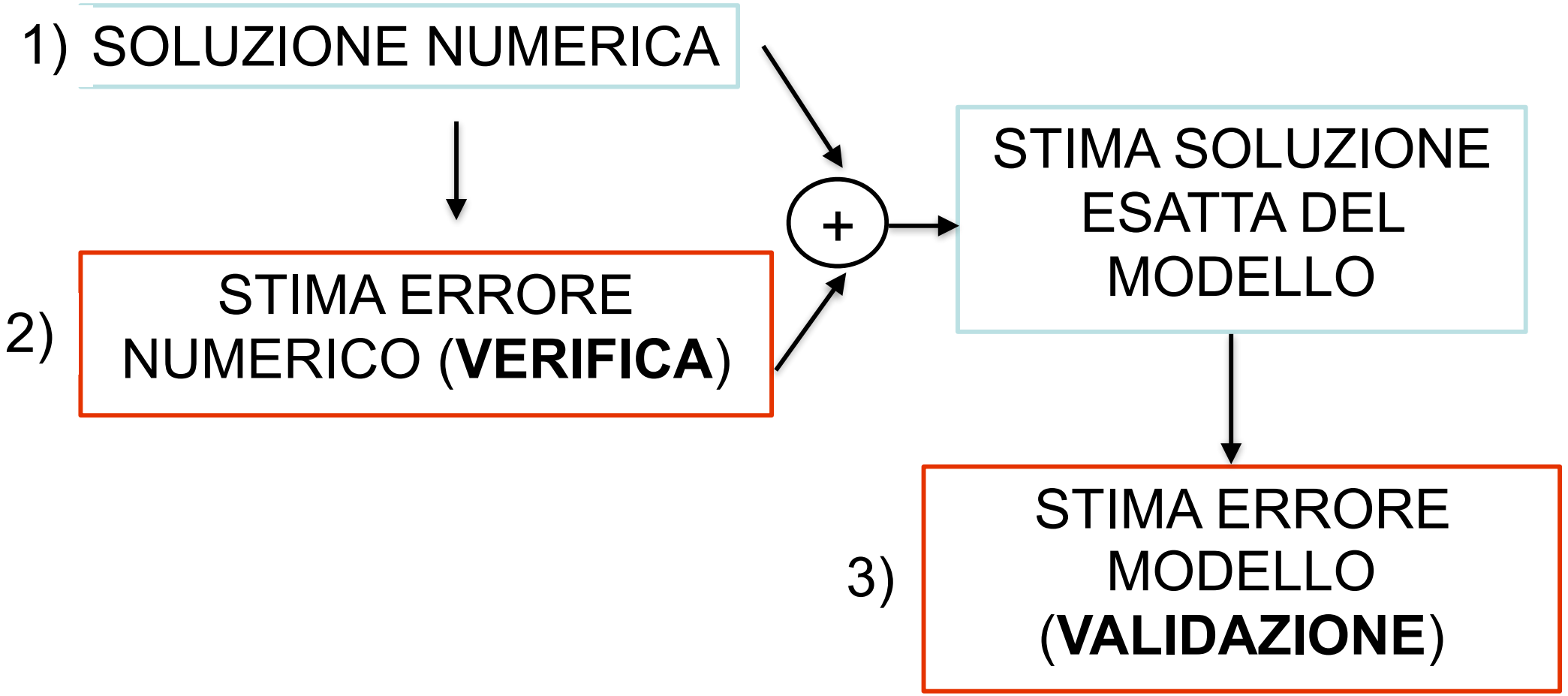

FASI DI UNA SIMULAZIONE NUMERICA

La **verifica** deve necessariamente precedere la **validazione**.

Non ci può essere **validazione** senza **verifica**.

Ci può essere **verifica** senza **validazione**.

ERRORE E INCERTEZZA

ERRORE E INCERTEZZA

1. Freitas, C. (1993). Journal of fluids engineering editorial policy statement on the control of numerical accuracy. *Journal of Fluids Engineering, Transactions of the ASME*, *115*(3), 339–340. doi:10.1115/1.2910144
2. Ferziger, J., & Perić, M. (1996). Further discussion of numerical errors in CFD. *International Journal for Numerical Methods in Fluids*, *23*(12), 1263–1274
3. Stern, F., Wilson, R., Coleman, H., & Paterson, E. (2001). Comprehensive approach to verification and validation of CFD simulations—part 1: Methodology and procedures. *Journal of Fluids Engineering, Transactions of the ASME*, *123*(4), 793–802. doi:10.1115/1.1412235
4. Oberkampf, W., Trucano, T., & Hirsch, C. (2003). Verification, validation, and predictive capability in computational engineering and physics. *Verification, Validation, and Predictive Capability in Computational Engineering and Physics*
5. Roache, P. (2003). Conservatism of the grid convergence index in finite volume computations on steady-state fluid flow and heat transfer. *Journal of Fluids Engineering, Transactions of the ASME*, *125*(4), 731–732. doi:10.1115/1.1588692
6. Stern, F., Wilson, R., & Shao, J. (2006). Quantitative V&V of CFD simulations and certification of cfd codes. *International Journal for Numerical Methods in Fluids*, *50*(11), 1335–1355. doi:10.1002/fld.1090
7. Celik, I., Ghia, U., Roache, P., Freitas, C., Coleman, H., & Raad, P. (2008). Procedure for estimation and reporting of uncertainty due to discretization in CFD applications. *Journal of Fluids Engineering, Transactions of the ASME*, *130*(7), 0780011–0780014. doi:10.1115/1.2960953
8. Editorial policy statement on numerical and experimental accuracy. (2014). *AIAA Journal*, *52*(1), 16. doi:10.2514/1.J053252
9. Roy, C., & Oberkampf, W. (2016). *Verification and validation in computational fluid dynamics*.

ERRORE E INCERTEZZA

DEFINIZIONI[1]**:**

- **ERRORE**: la differenza tra un valore "misurato" e il valore vero di una quantità

- **INCERTEZZA**: parametro che caratterizza la dispersione dei dati che potrebbero ragionevolmente essere misurati

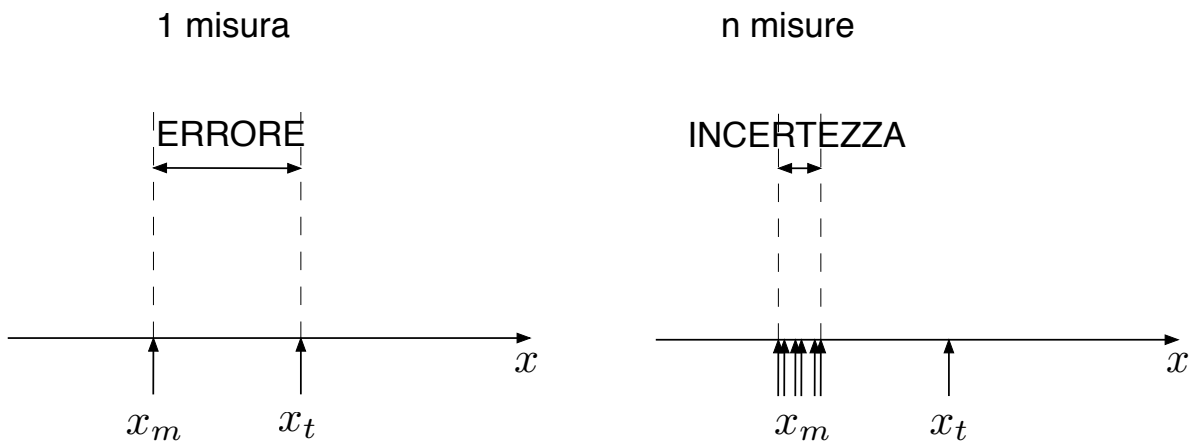

[1] De Bièvre, P. (2012). The 2012 international vocabulary of metrology: "VIM". *Accreditation and Quality Assurance*, *17*(2), 231–232. doi:10.1007/s00769-012-0885-3.

ERRORE E INCERTEZZA

VALORE MISURATO/SIMULATO x_m

VALORE VERO x_t

ERRORE $\delta_x = x_m - x_t$

INCERTEZZA U_{xm}

VALORE VERO (STIMA) $x_m - U_{mx} \leq \hat{x}_t \leq x_m + U_{mx}$

ERRORE E INCERTEZZA

$$\delta_s = \delta_{sm} + \delta_{sn} = S_n - T = (S_m - T) + (S_n - S_m)$$

δ_s	ERRORE GLOBALE DELLA SIMULAZIONE
δ_{sm}	ERRORE DEL MODELLO
δ_{sn}	ERRORE NUMERICO
S	RISULTATO SIMULAZIONE
T	DATO REALE

ERRORE E INCERTEZZA

$$\delta_s = \delta_{sm} + \delta_{sn} = S_n - T = (S_m - T) + (S_n - S_m)$$

$$|\delta_s| \leq |\delta_{sm}| + |\delta_{sn}|$$

$$|U_s| \leq |U_{sm}| + |U_{sn}|$$

δ_s	ERRORE GLOBALE DELLA SIMULAZIONE
δ_{sm}	ERRORE DEL MODELLO
δ_{sn}	ERRORE NUMERICO
S	RISULTATO SIMULAZIONE
T	DATO REALE
U_s	INCERTEZZA SIMULAZIONE
U_{sm}	INCERTEZZA MODELLO
U_{sn}	INCERTEZZA NUMERICA

ERRORE E INCERTEZZA

$$\delta_s = \delta_{sm} + \delta_{sn} = S_n - T = (S_m - T) + (S_n - S_m)$$

δ_{sm} (errore del modello) deriva da approssimazioni nella rappresentazione matematica del problema fisico:

- equazioni matematiche
- geometria
- condizioni al contorno
- modelli di turbolenza

δ_{sn} (errore numerico) da approssimazioni dovute alla soluzione numerica del problema matematico

- discretizzazione
- diffusione artificiale
- convergenza incompleta (iterativa o dovuta alla griglia)
- non-conservatività

STIMA ERRORE NUMERICO

$$\delta_{sn} = \sum_{i=1}^{N} \delta_{sn,i}$$

dove $\delta_{sn,i}$ rappresenta il contributo all'errore numerico dato dal parametro h_i. La stima di $\delta_{sn,i}$ avviene mediante studi di convergenza utilizzando soluzioni multiple con valori diversi del parametro h_i.

$$S_n = S_m + \left(\sum_{i=1, i \neq k}^{N} \delta_{sn,i} \right) + \delta_{sn,k}$$

dove

$$\delta_{sn,k} \simeq \sum_{j=1}^{g} f_j h_k^j$$

STIMA ERRORE NUMERICO

$$\sum_{j=1}^{d} f_j h_k^j = S_n(h_k) - \left[S_m + \left(\sum_{i=1, i \neq k}^{N} \delta_{sn,i} \right) \right] = S_n(h_k) - \hat{S}_n$$

La precedente contiene $d + 1$ incognite: gli f_j e $\hat{S}_n$ (la soluzione numerica "corretta", cioè depurata dell'errore dovuto al parametro h_k).
Alternativamente, l'equazione precedente può essere riscritta nel seguente modo:

$$f_p h_k^p + \epsilon(h_k) = f_p^* h_k^p = S_n - \hat{S}_n$$

dove $f_p h_k^p$ rappresenta il termine dominante nell'espansione in serie di Taylor, e $epsilon(h_k)$ è l'errore di troncamento.

STIMA ERRORE NUMERICO

Nella precedente equazione, le incognite sono: p, f_p^* e $\hat{S}_n$. Per determinarle, posso fare in modo di far sparire dalle equazioni il termine $\hat{S}_n$:

$$(f_p^* h_{k,1}^p) - (f_p^* h_{k,2}^p) = S_n(h_{k,1}) - S_n(h_{k,2})$$

dove $h_{k,1}$ e $h_{k,2}$ rappresentano due diversi valori del parametro h_k, e $S_n(h_{k,1})$ e $S_n(h_{k,2})$ le corrispondenti soluzioni numeriche. Essendo presenti due incognite (p e f_p^*), abbiamo bisogno di scrivere la stessa equazione per almeno due coppie di valori $h_{k,1}$ e $h_{k,2}$.

STIMA ERRORE NUMERICO

Ho dunque bisogno di almeno 3 soluzioni numeriche (con 3 valori del parametro h_k) per stimare l'errore numerico. Consideriamo il minimo numero di soluzioni:

$$(f_p^* h_{k,1}^p) - (f_p^* h_{k,2}^p) = S_n(h_{k,1}) - S_n(h_{k,2}) = \epsilon_{12}$$
$$(f_p^* h_{k,2}^p) - (f_p^* h_{k,3}^p) = S_n(h_{k,2}) - S_n(h_{k,3}) = \epsilon_{23}$$

Dividendo membro a membro:

$$\frac{h_{k,1}^p - h_{k,2}^p}{h_{k,2}^p - h_{k,3}^p} = \frac{\epsilon_{12}}{\epsilon_{23}}$$

$$\left(\frac{h_{k,2}}{h_{k,3}}\right)^p \frac{\left(\frac{h_{k,1}}{h_{k,2}}\right)^p - 1}{\left(\frac{h_{k,2}}{h_{k,3}}\right)^p - 1} = \frac{\epsilon_{12}}{\epsilon_{23}}$$

STIMA ERRORE NUMERICO

Dalle precedenti posso ricavare:

$$p = \frac{\log\left(\frac{\epsilon_{12}}{\epsilon_{23}}\right)}{\log\left(\frac{h_{k,2}}{h_{k,3}}\right)} + \frac{1}{\log\left(\frac{h_{k,2}}{h_{k,3}}\right)} \log\left[\frac{\left(\frac{h_{k,2}}{h_{k,3}}\right)^p - 1}{\left(\frac{h_{k,1}}{h_{k,2}}\right)^p - 1}\right]$$

$$f_p^* = \frac{\epsilon_{23}}{h_{k,2}^p - h_{k,3}^p} \qquad \delta_{sn,k}(h_{k,3}) = \frac{\epsilon_{23}}{\frac{h_{k,2}}{h_{k,3}}^p - 1}$$

Si possono presentare 3 situazioni:

1. $p > 0$ $\rightarrow$ La soluzione numerica converge con ordine p
2. p indefinito $\rightarrow$ La soluzione numerica oscilla
3. $p \leq 0$ $\rightarrow$ La soluzione numerica diverge

ERRORE E INCERTEZZA

Le equazioni viste finora ci consentono di effettuare delle "stime" sull'errore numerico. La quantificazione dell'incertezza (e quindi dell'affidabilità della stima) si basa su valutazioni teoriche, supportate da verifiche sperimentali.

1. $p > 0$ (soluzione numerica convergente)

$$U_{sn,k} = |1 - C_k|\delta_{sn,k} \qquad \text{dove } C_k = \frac{\left(\frac{h_{k,2}}{h_{k,3}}\right)^p - 1}{\left(\frac{h_{k,2}}{h_{k,3}}\right)_t^p - 1}$$

2. p indefinito (soluzione numerica oscillatoria)

$$U_{sn,k} = \frac{1}{2}\left(U_S - U_L\right)$$

dove

p_t	ordine di convergenza teorico
U_S	limite superiore
U_L	limite inferiore

ESEMPIO - PROFILO ALARE

ESEMPIO - PROFILO ALARE

Consideriamo un profilo alare investito da una corrente uniforme con un angolo di incidenza α.

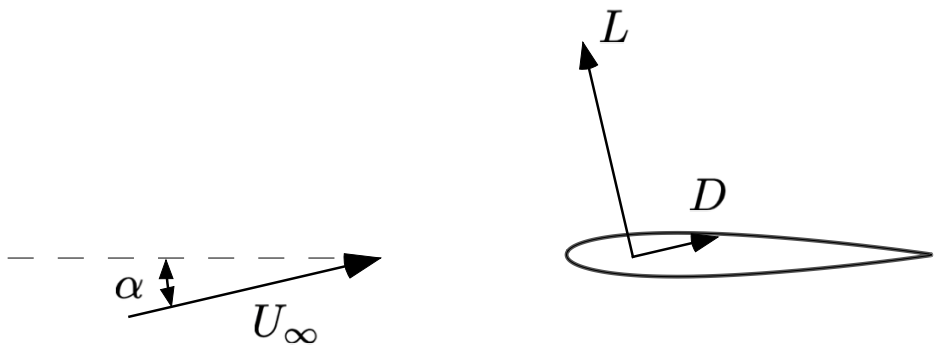

ESEMPIO - PROFILO ALARE

Risolviamo le equazioni costitutive (Navier-Stokes) utilizzando Ansys Fluent.

GRIGLIA (circa 8000 celle):

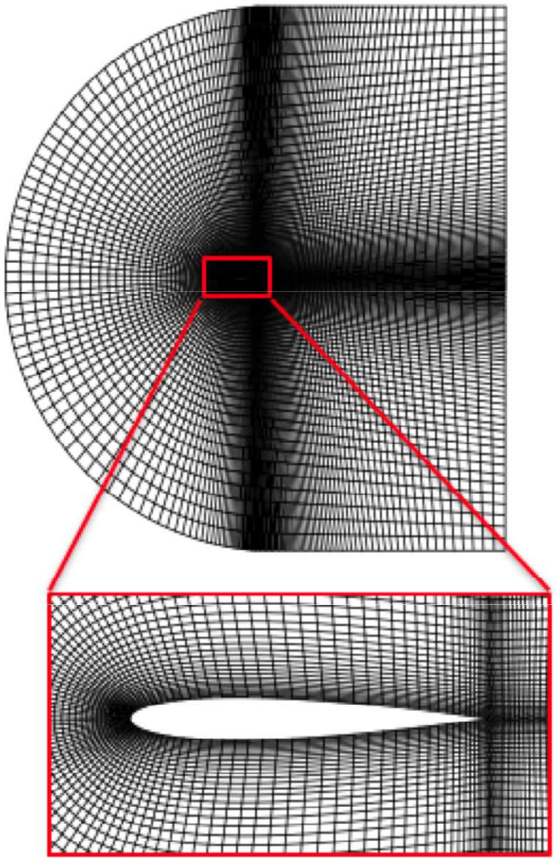

Ipotesi:

- flusso inviscido
- termini diffusivi e convettivi discretizzati con metodi del secondo ordine (upwind)
- SIMPLE per la correzione della pressione
- convergenza dei residui a 10^{-10} (errore iterativo trascurabile)

ESEMPIO - PROFILO ALARE

RISULTATI:

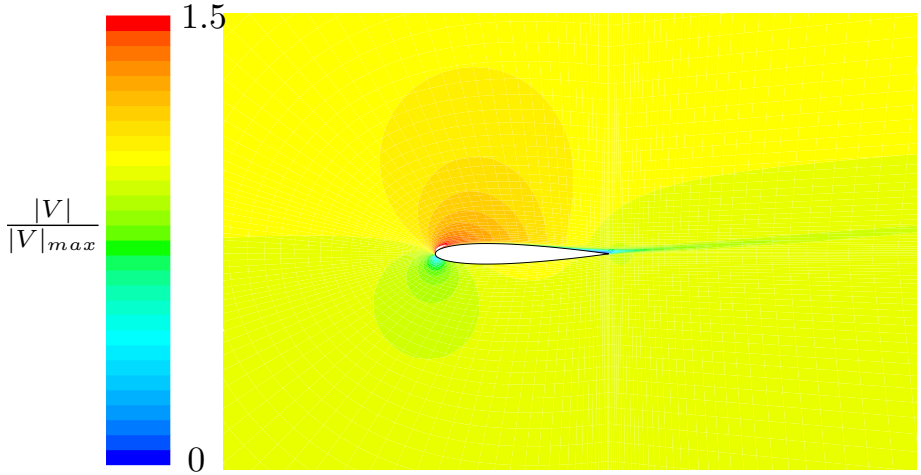

$$c_L = \frac{L}{\frac{1}{2}\rho V_\infty^2 S}$$

$$c_p = \frac{p - p_\infty}{\frac{1}{2}\rho V_\infty^2}$$

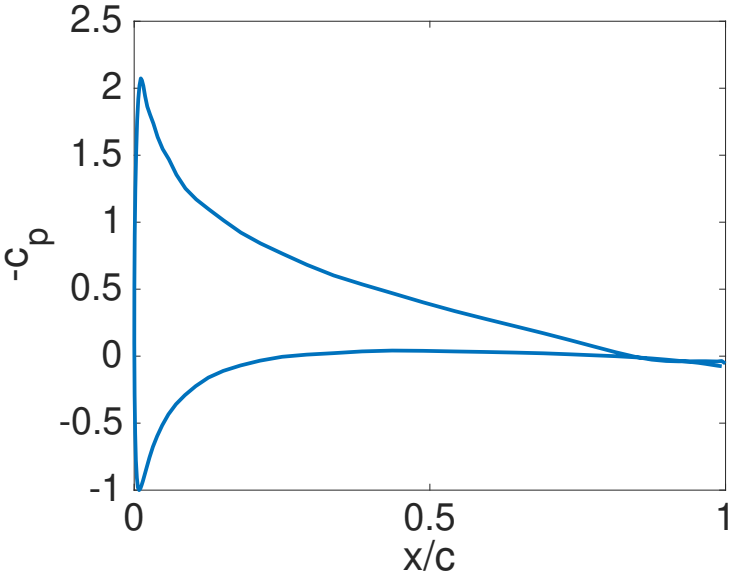

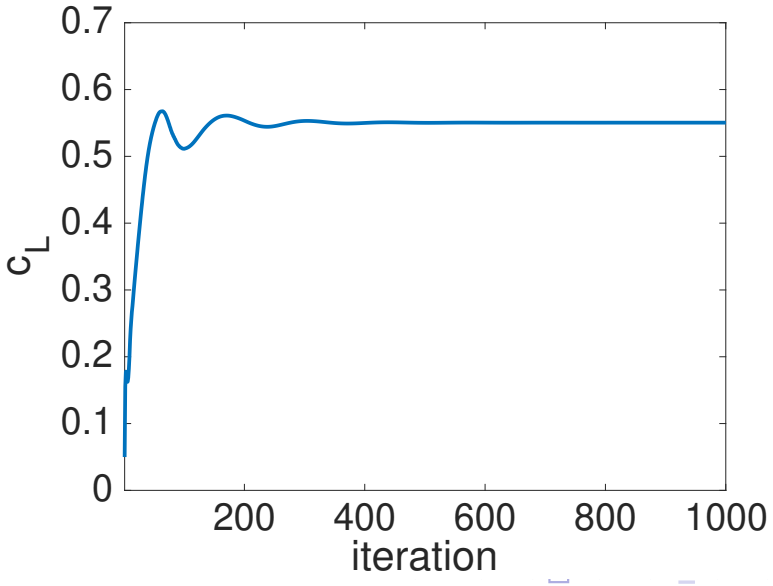

ESEMPIO - PROFILO ALARE

Utilizziamo 3 griglie con numero di celle crescente per verificare la soluzione numerica:

	GRIGLIA 1	GRIGLIA 2	GRIGLIA 3
N. CELLE	7799	17595	40040
h (-)	0.1132	0.0753	0.0499
c_l (-)	0.5560	0.6170	0.6545

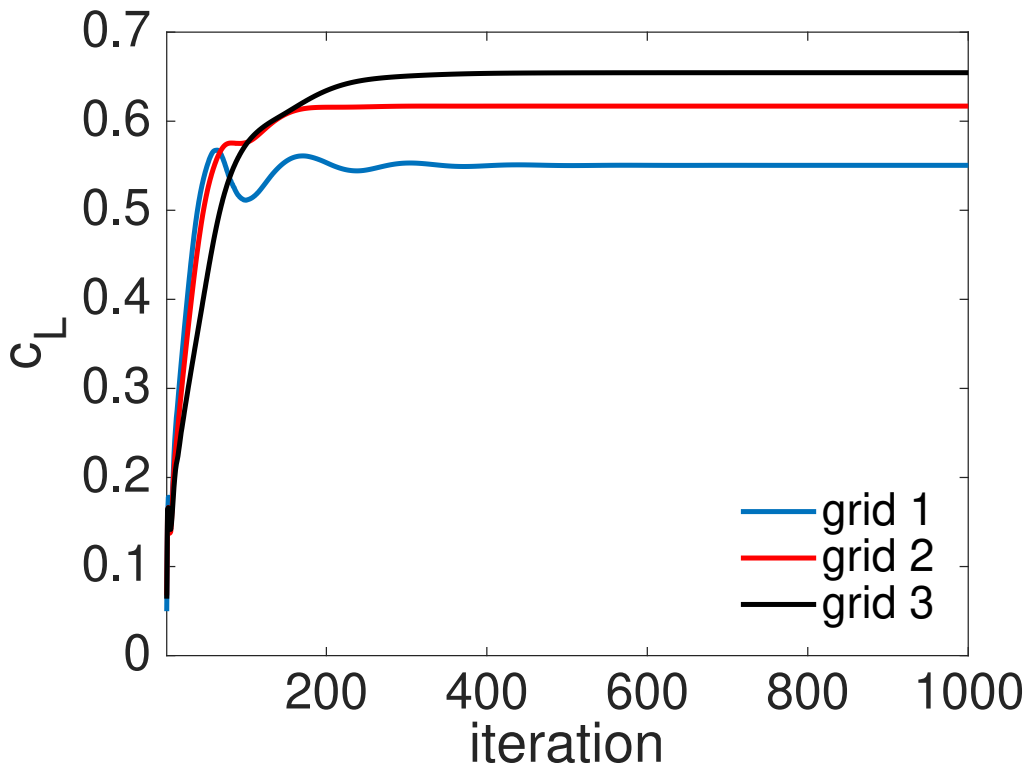

ESEMPIO - PROFILO ALARE

Utilizziamo 3 griglie con numero di celle crescente per verificare la soluzione numerica:

	GRIGLIA 1	GRIGLIA 2	GRIGLIA 3
N. CELLE	7799	17595	40040
h (-)	0.1132	0.0753	0.0499
c_l (-)	0.5560	0.6170	0.6545

$$p = \frac{\log\left(\frac{\epsilon_{12}}{\epsilon_{23}}\right)}{\log\left(\frac{h_{k,2}}{h_{k,3}}\right)} + \frac{1}{\log\left(\frac{h_{k,2}}{h_{k,3}}\right)} \log\left[\frac{\left(\frac{h_{k,2}}{h_{k,3}}\right)^p - 1}{\left(\frac{h_{k,1}}{h_{k,2}}\right)^p - 1}\right] = 1.21$$

$$f_p^* = \frac{\epsilon_{23}}{h_{k,2}^p - h_{k,3}^p} = -2.21 \qquad \delta_{sn,k}(h_{k,3}) = \frac{\epsilon_{23}}{\frac{h_{k,2}}{h_{k,3}}^p - 1} = -0.0578$$

$$C_k = \frac{\left(\frac{h_{k,3}}{h_{k,4}}\right)^p - 1}{\left(\frac{h_{k,3}}{h_{k,4}}\right)_t^p - 1} = 0.51 \qquad U_k = |(1-C_k)\delta_{sn,k}| = 0.028$$

$$\hat{S}_n = 0.712 \pm 0.028$$

ESEMPIO - PROFILO ALARE

Aggiungiamo una quarta griglia con un numero ancora maggiore di celle:

	GRIGLIA 1	GRIGLIA 2	GRIGLIA 3	GRIGLIA 4
N. CELLE	7799	17595	40040	71585
h (-)	0.1132	0.0753	0.0499	0.0374
c_l (-)	0.5560	0.6170	0.6545	0.66858

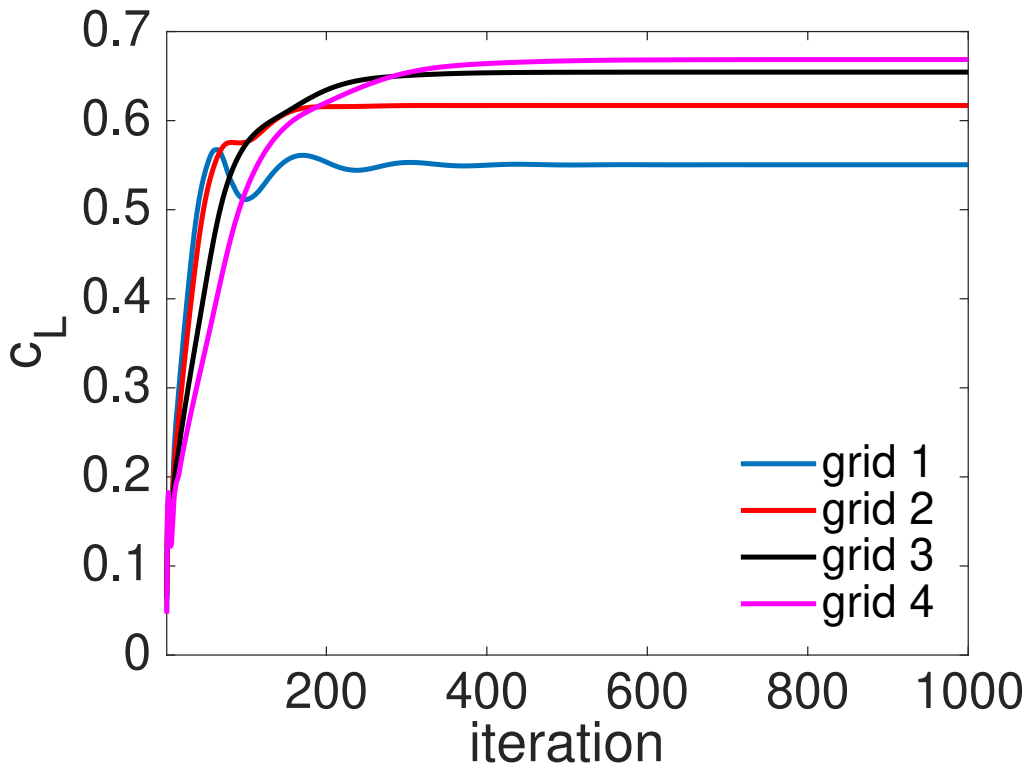

ESEMPIO - PROFILO ALARE

Aggiungiamo una quarta griglia con un numero ancora maggiore di celle:

	GRIGLIA 1	GRIGLIA 2	GRIGLIA 3	GRIGLIA 4
N. CELLE	7799	17595	40040	71585
h (-)	0.1132	0.0753	0.0499	0.0374
c_l (-)	0.5560	0.6170	0.6545	0.66858

$$p = \frac{\log\left(\frac{\epsilon_{23}}{\epsilon_{34}}\right)}{\log\left(\frac{h_{k,3}}{h_{k,4}}\right)} + \frac{1}{\log\left(\frac{h_{k,3}}{h_{k,4}}\right)} \log\left[\frac{\left(\frac{h_{k,3}}{h_{k,4}}\right)^p - 1}{\left(\frac{h_{k,2}}{h_{k,3}}\right)^p - 1}\right] = 1.76$$

$$f_p^* = \frac{\epsilon_{34}}{h_{k,3}^p - h_{k,4}^p} = -6.99 \qquad \delta_{sn,k}(h_{k,4}) = \frac{\epsilon_{34}}{\frac{h_{k,3}}{h_{k,4}}^p - 1} = -0.0210$$

$$C_k = \frac{\left(\frac{h_{k,3}}{h_{k,4}}\right)^p - 1}{\left(\frac{h_{k,3}}{h_{k,4}}\right)_t^p - 1} = 0.85 \qquad U_k = |(1-C_k)\delta_{sn,k}| = 0.003$$

$$\hat{S}_n = 0.690 \pm 0.003$$

ESEMPIO - PROFILO ALARE

VALIDAZIONE:

Reperiamo i dati sperimentali da: *Aerodynamic characteristics of NACA0012 airfoil section at angles of attack from 0° to 180°*. (1955).(Tech. rep. No. TN3361). National Advisory Committee for Aeronautics. Langley Aeronautical Laboratory Langley Field, Washington

$$T = 0.650 \pm 0.017$$

$$S_m = 0.690 \pm 0.003$$

$$\delta_{sm} = 0.040 \pm 0.020$$

ESEMPIO - TURBINA WELLS

TURBINA WELLS

TURBINA WELLS

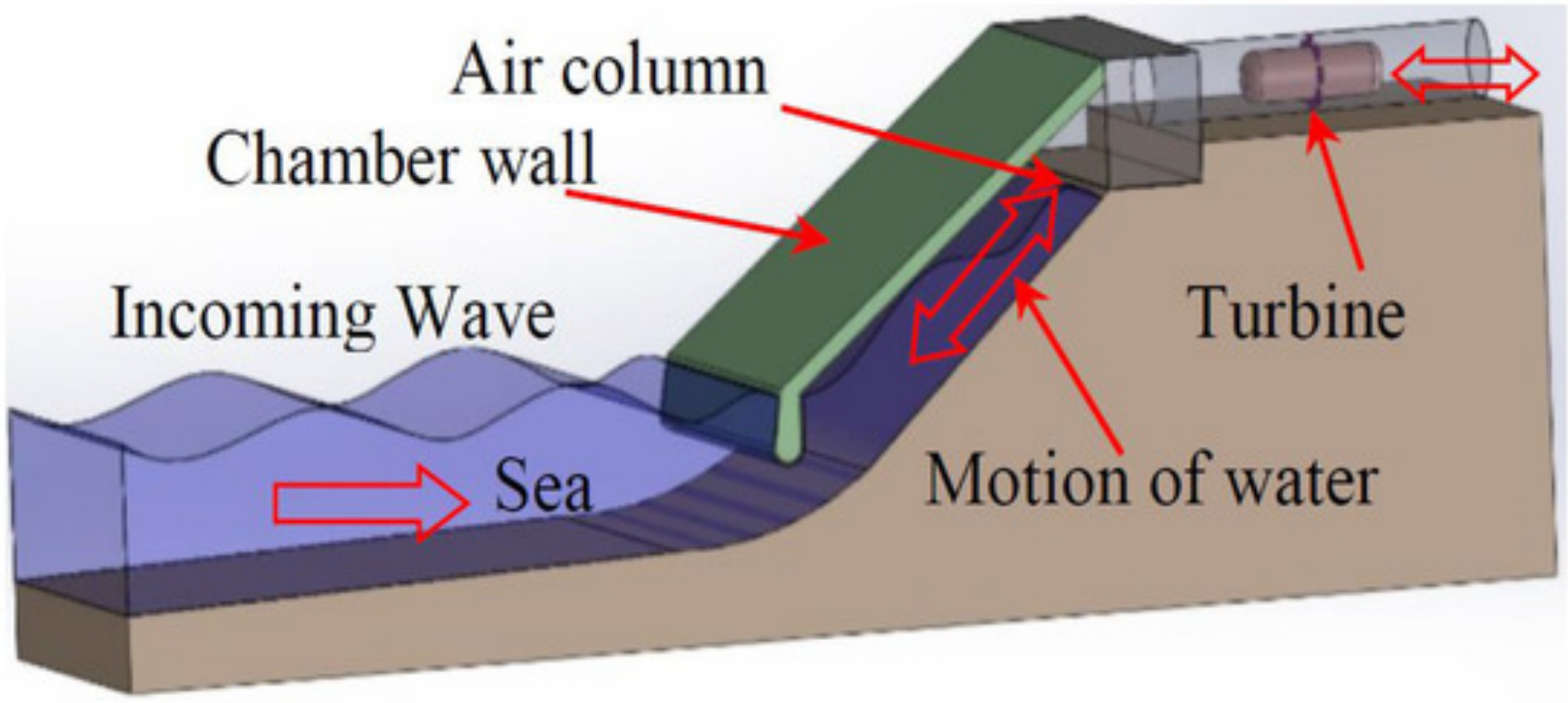

TURBINA WELLS

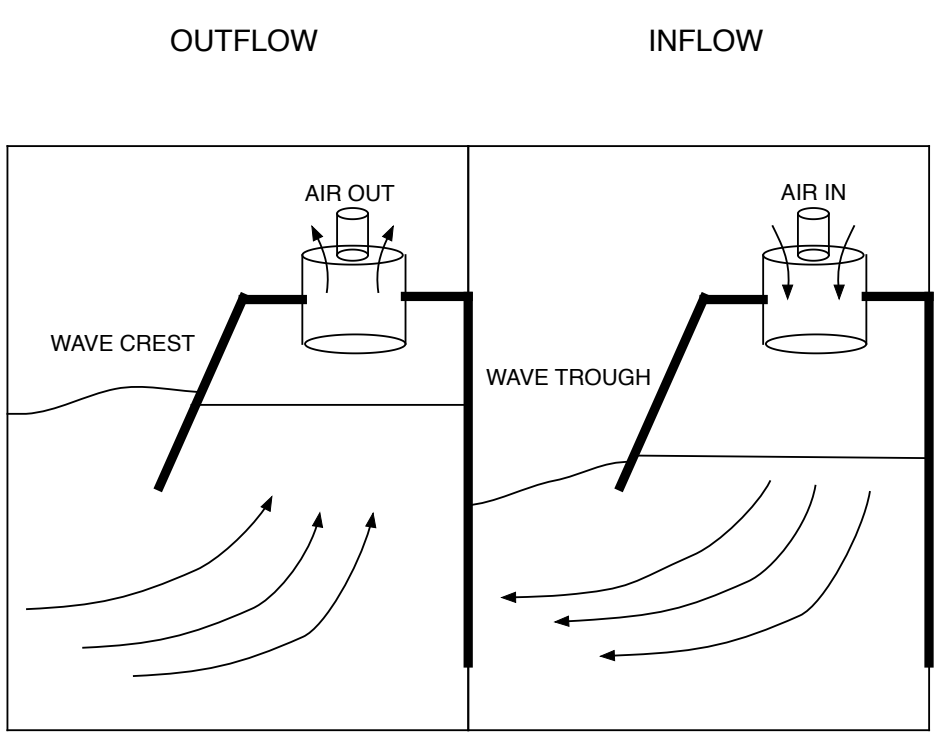

OWC system

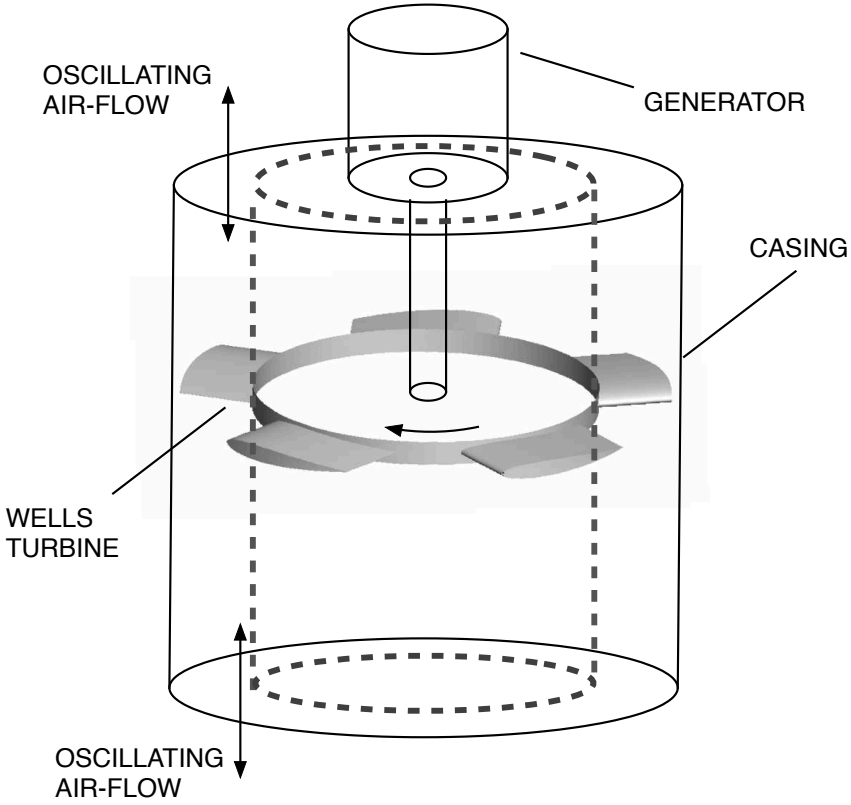

Wells turbine

TURBINA WELLS

Triangoli di velocità e forze aerodinamiche durante le fasi di inflow e outflow sono simmetrici:

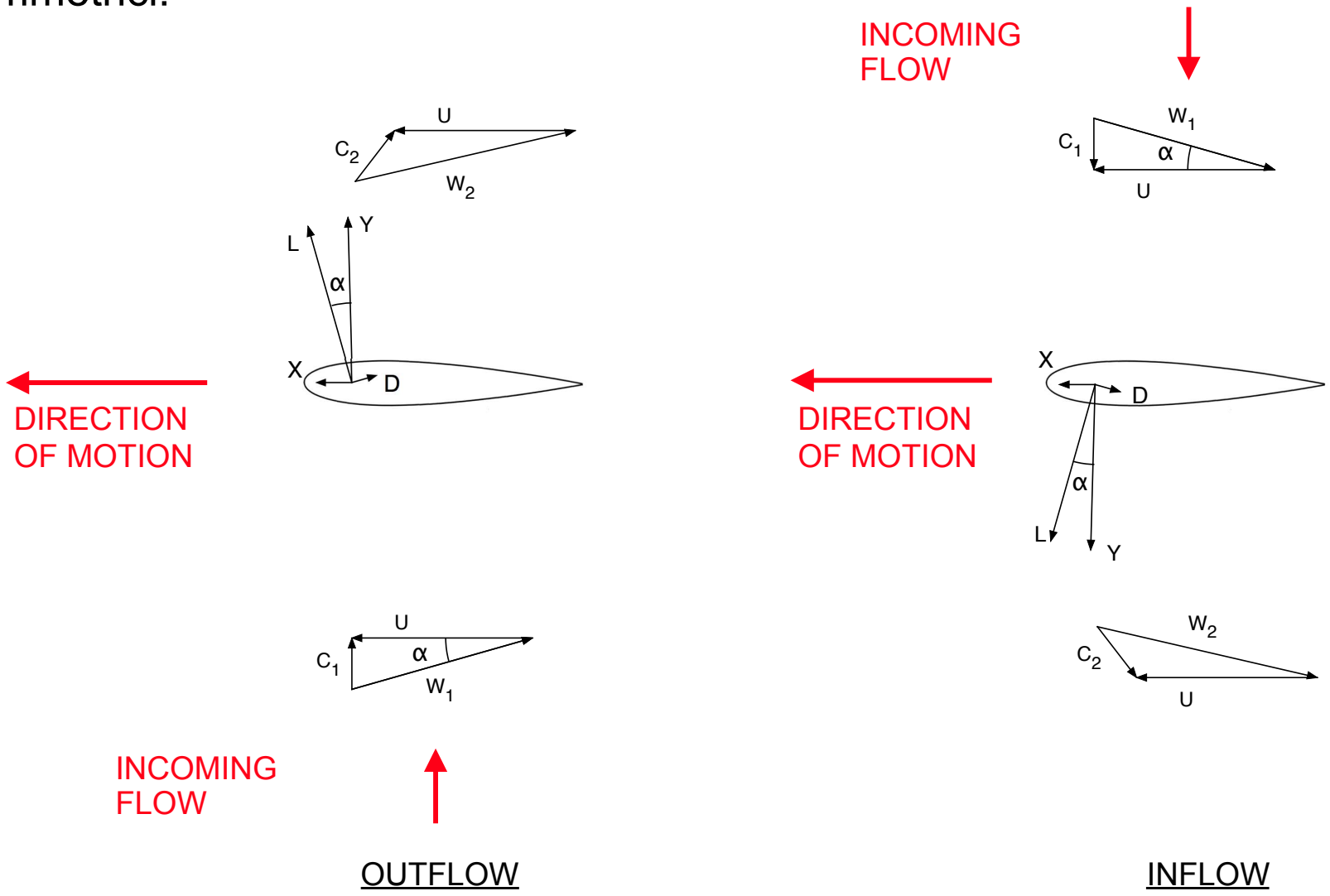

TURBINA WELLS

In una turbina Wells, il punto di lavoro cambia continuamente:

COEFFICIENTE DI FLUSSO

$$\phi = \frac{V_a}{\omega r_t}$$

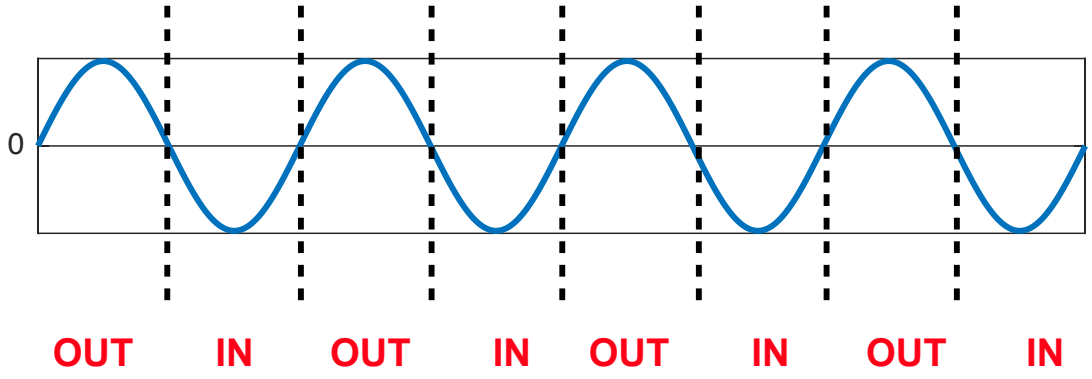

TURBINA WELLS

In una turbina Wells, il punto di lavoro cambia continuamente:

COEFFICIENTE DI FLUSSO

$$\phi = \frac{V_a}{\omega r_t}$$

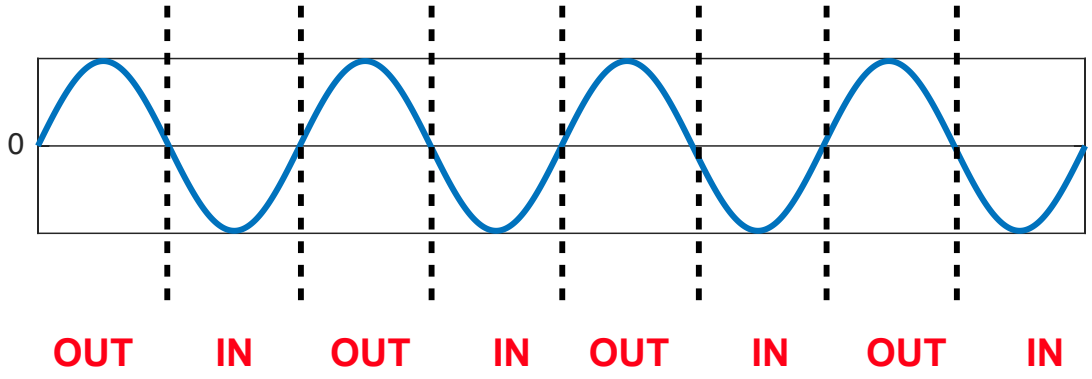

COEFFICIENTE DI PRESSIONE

$$P^* = \frac{\Delta P}{\rho \omega^2 r_t^2}$$

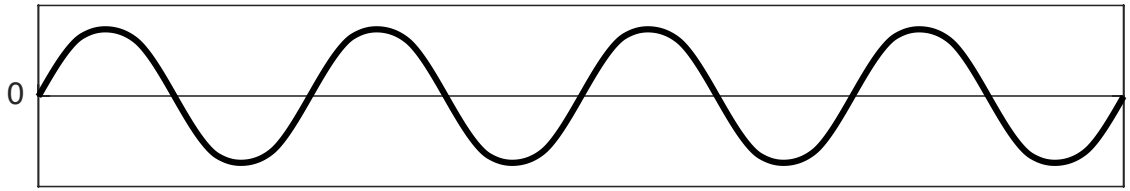

COEFFICIENTE DI COPPIA

$$T^* = \frac{T}{\rho \omega^2 r_t^5}$$

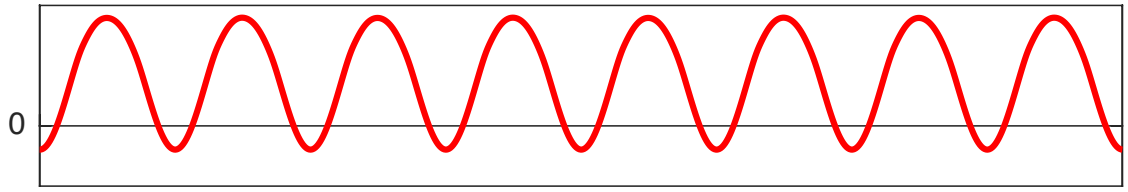

TURBINA WELLS - ISTERESI

In una turbina Wells, il punto di lavoro cambia continuamente:

COEFFICIENTE DI FLUSSO

$$\phi = \frac{V_a}{\omega r_t}$$

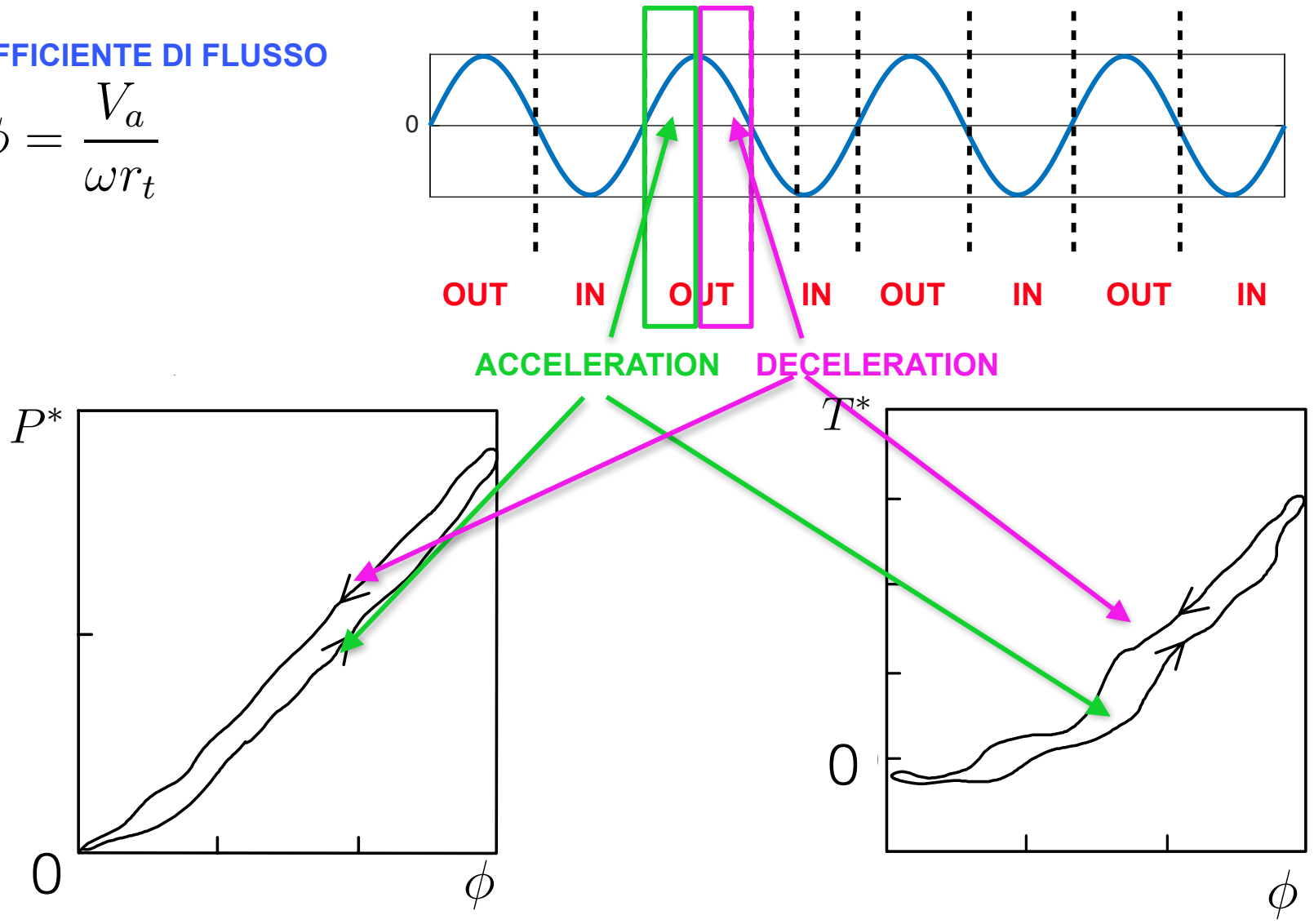

figure adattate da:

T. Setoguchi, M. Takao, and K. Kaneko. Hysteresis on wells turbine characteristics in reciprocating flow. *International Journal of Rotating Machinery*, 4(1):17–24, 1998.

TURBINA WELLS - ISTERESI

Il fenomeno dell'isteresi è stato discusso ampiamente nella letteratura scientifica:

[1] T. Setoguchi, M. Takao, and K. Kaneko. Hysteresis on wells turbine characteristics in reciprocating flow. *International Journal of Rotating Machinery*, 4(1):17–24, 1998.

[2] T.-H. Kim, Y. Kinoue, T. Setoguchi, and K. Kaneko. Effects of hub-to-tip ratio and tip clearance on **hysteretic** characteristics of wells turbine for wave power conversion. *Journal of Thermal Science*, 11(3):207–213, 2002.

[3] Y. Kinoue, T. Setoguchi, T.H. Kim, K. Kaneko, and M. Inoue. Mechanism of **hysteretic** characteristics of wells turbine for wave power conversion. *Journal of Fluids Engineering, Transactions of the ASME*, 125(2):302–307, 2003.

[4] T. Setoguchi, Y. Kinoue, T.H. Kim, K. Kaneko, and M. Inoue. **Hysteretic** characteristics of wells turbine for wave power conversion. *Renewable Energy*, 28(13):2113–2127, 2003.

[5] Y. Kinoue, T.H. Kim, T. Setoguchi, M. Mohammad, K. Kaneko, and M. Inoue. **Hysteretic** characteristics of monoplane and biplane wells turbine for wave power conversion. *Energy Conversion and Management*, 45(9-10):1617–1629, 2004.

[6] Y. Kinoue, T. Setoguchi, T.H. Kim, M. Mamun, K. Kaneko, and M. Inoue. **Hysteretic** characteristics of the wells turbine in a deep stall condition. *Proceedings of the Institution of Mechanical Engineers Part M: Journal of Engineering for the Maritime Environment*, 218(3):167–173, 2004.

[7] M. Mamun, Y. Kinoue, T. Setoguchi, T.H. Kim, K. Kaneko, and M. Inoue. **Hysteretic** flow characteristics of biplane wells turbine. *Ocean Engineering*, 31(11-12):1423–1435, 2004.

[8] M. Mamun, T. Setoguchi, Y. Kinoue, and K. Kaneko. Visualization of unsteady flow phenomena of wells turbine during **hysteresis** study. *Journal of Flow Visualization and Image Processing*, 12(2):111–123, 2005.

[9] Y. Kinoue, M. Mamun, T. Setoguchi, and K. Kaneko. **Hysteretic** characteristics of wells turbine for wave power conversion (effects of solidity and setting angle). *International Journal of Sustainable Energy*, 26(1):51–60, 2007.

TURBINA WELLS - ISTERESI

Il fenomeno dell'isteresi è stato discusso ampiamente nella letteratura scientifica:

… anche recentemente:

[10] A.S. Shehata, K.M. Saqr, Q. Xiao, M.F. Shehadeh, and A. Day. Performance Analysis of Wells Turbine Blades Using the Entropy Generation Minimization Method. *Renewable Energy*, 86:1123–1133, 2016.

[11] Ahmed S. Shehata, Qing Xiao, Mohamed El-Shaib, Ashraf Sharara, and Day Alexander. Comparative analysis of different wave turbine designs based on conditions relevant to northern coast of Egypt. *Energy*, 120:450–467, 2017.

[12] Ahmed S. Shehata, Qing Xiao, Khalid M. Saqr, Ahmed Naguib, and Day Alexander. Passive flow control for aerodynamic performance enhancement of airfoil with its application in Wells turbine – Under oscillating flow condition. *Ocean Engineering*, 136(March):31–53, 2017.

[13] A. S. Shehata, Q. Xiao, M. M. Selim, A. H. Elbatran, and D. Alexander. Enhancement of performance of wave turbine during stall using passive flow control: First and second law analysis. *Renewable Energy*, 113(December):369–392, 2017.

[14] Qiuhao Hu and Ye Li. Unsteady rans simulations of wells turbine under transient flow conditions. *ASME Journal of Offshore Mechanics and Arctic Engineering*, 140(1), 2018.

TURBINA WELLS - ISTERESI

La spiegazione dell'origine dell'isteresi è stata trovata tramite simulazioni CFD

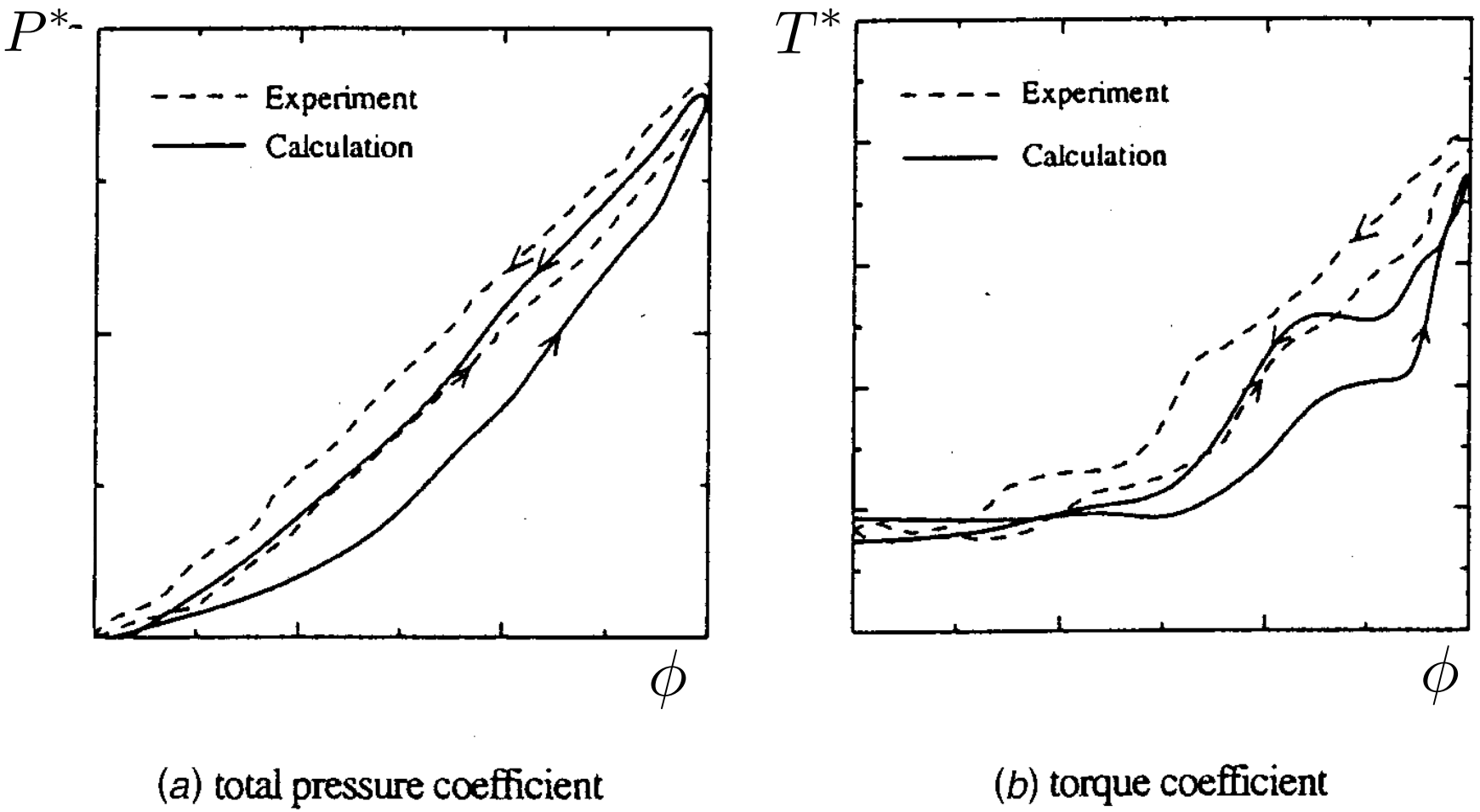

(*a*) total pressure coefficient

(*b*) torque coefficient

figure adattate da:

Y. Kinoue, T. Setoguchi, T.H. Kim, K. Kaneko, and M. Inoue. Mechanism of **hysteretic** characteristics of wells turbine for wave power conversion. *Journal of Fluids Engineering, Transactions of the ASME*, 125(2):302–307, 2003.

TURBINA WELLS - ISTERESI

La spiegazione dell'origine dell'isteresi è stata trovata tramite simulazioni CFD.
La causa è attribuita all'interazione dei vortici di scia con la circuitazione della pala.

ACCELERAZIONE

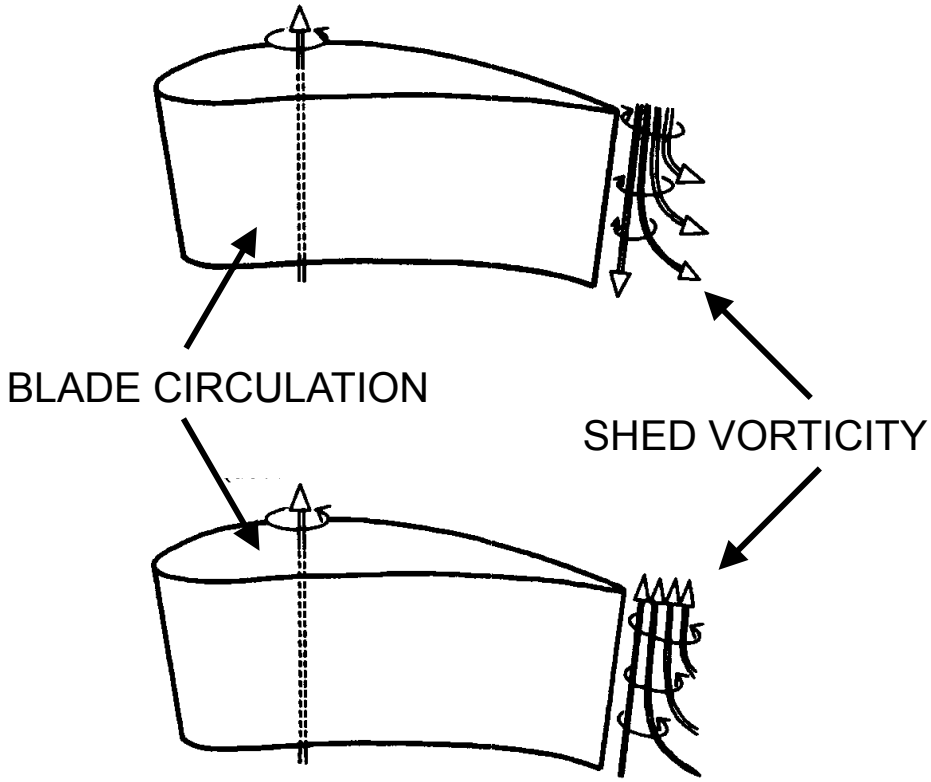

DECELERAZIONE

figure adattate da:

Y. Kinoue, T. Setoguchi, T.H. Kim, K. Kaneko, and M. Inoue. Mechanism of **hysteretic** characteristics of wells turbine for wave power conversion. *Journal of Fluids Engineering, Transactions of the ASME*, 125(2):302–307, 2003.

TURBINA WELLS - ISTERESI

Alcuni fenomeni dinamici:

DIVERSA DIMENSIONE
DEI VORTICI A
FERRO DI CAVALLO

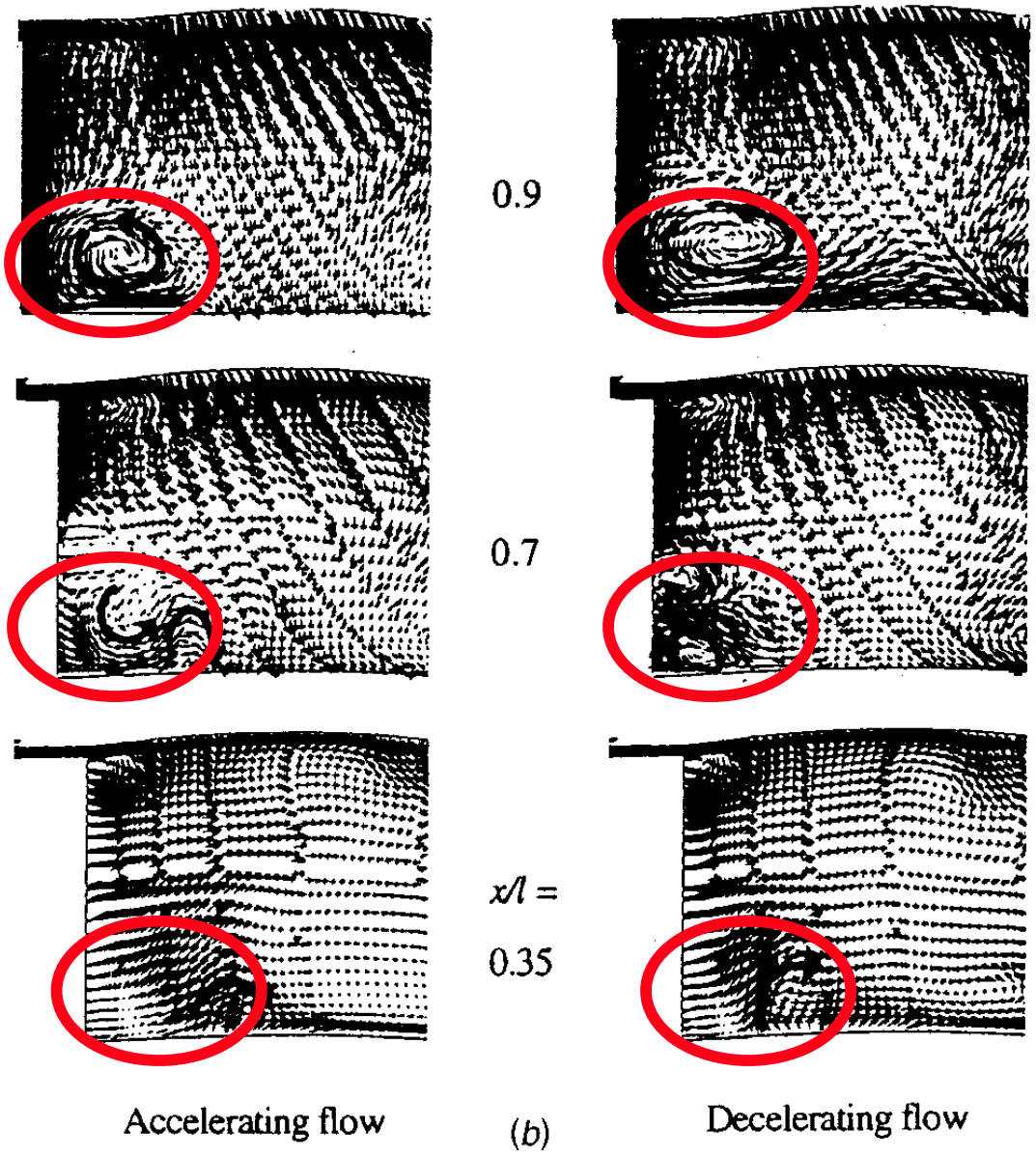

figure tratte da:

Y. Kinoue, T. Setoguchi, T.H. Kim, K. Kaneko, and M. Inoue. Mechanism of **hysteretic** characteristics of wells turbine for wave power conversion. *Journal of Fluids Engineering, Transactions of the ASME*, 125(2):302–307, 2003.

TURBINA WELLS - ISTERESI

Alcuni effetti dinamici:

PRESSIONI SUPERFICIALI SUL LATO IN PRESSIONE DELLA PALA

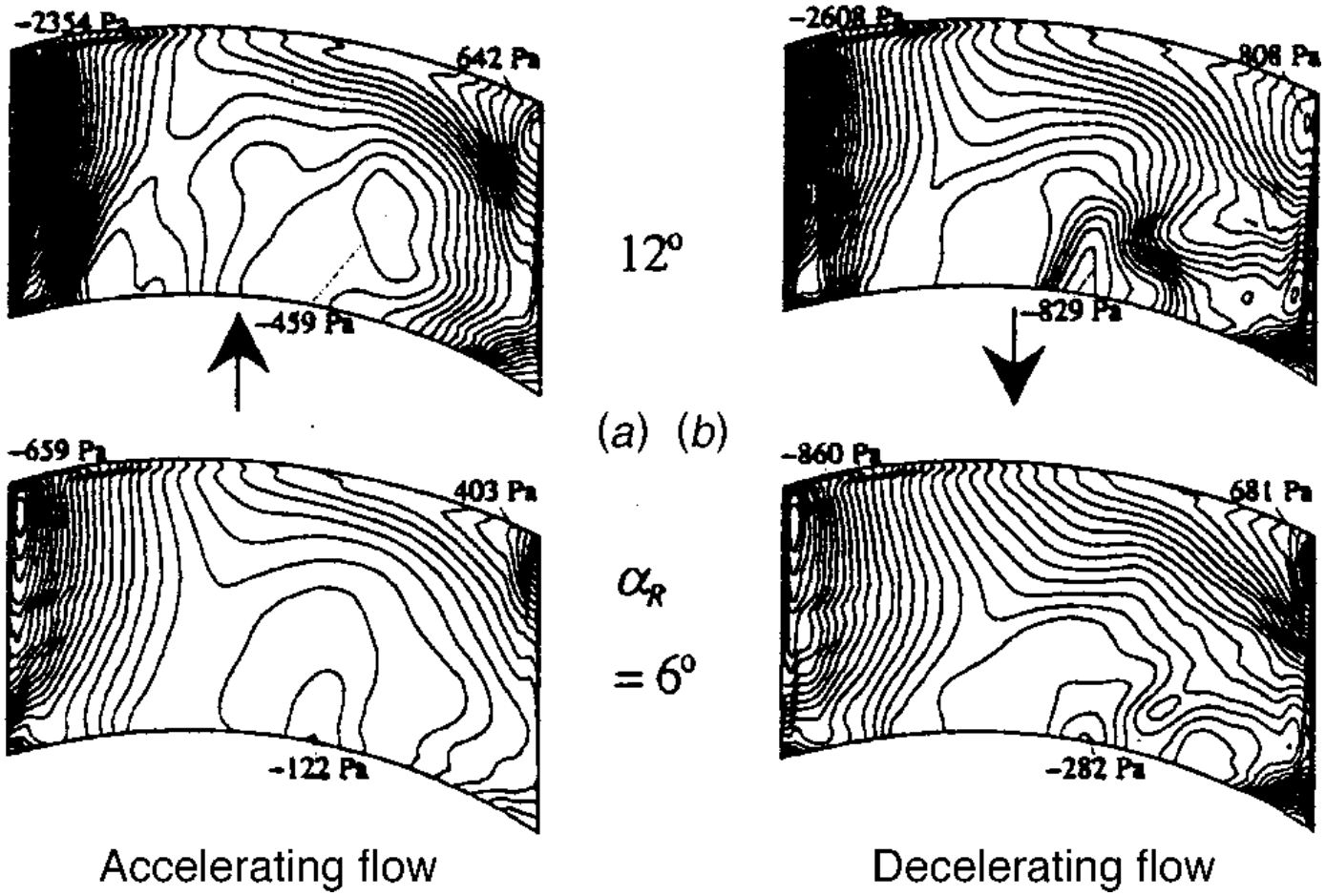

figure tratte da:

Y. Kinoue, T. Setoguchi, T.H. Kim, K. Kaneko, and M. Inoue. Mechanism of **hysteretic** characteristics of wells turbine for wave power conversion. *Journal of Fluids Engineering, Transactions of the ASME*, 125(2):302–307, 2003.

TURBINA WELLS - ISTERESI

Alcuni effetti dinamici

ACCELERAZIONE DECELERAZIONE

(STESSO COEFFICIENTE DI FLUSSO)

CONTORNI DI PRESSIONE

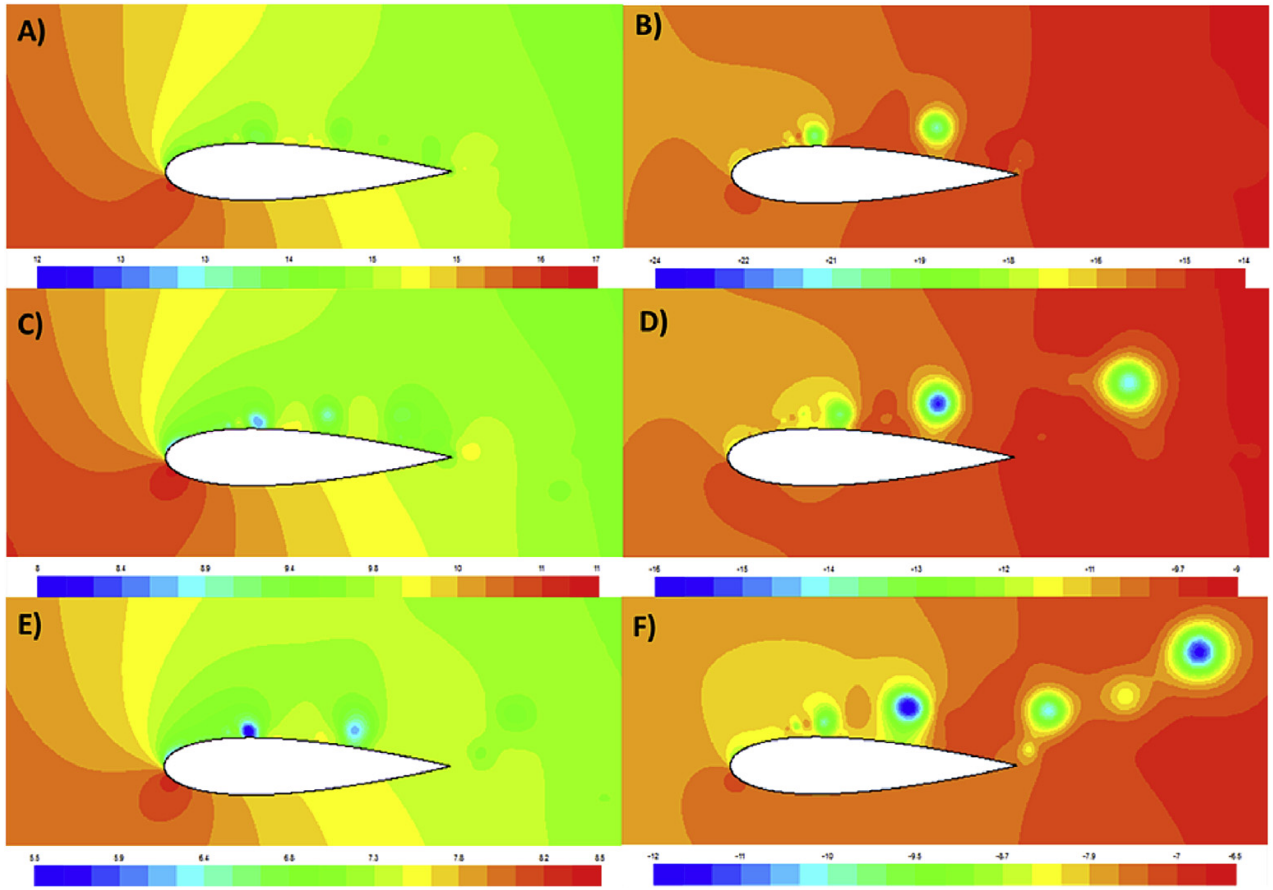

figure tratte da:

Ahmed S. Shehata, Qing Xiao, Mohamed El-Shaib, Ashraf Sharara, and Day Alexander. Comparative analysis of different wave turbine designs based on conditions relevant to northern coast of Egypt. *Energy*, 120:450–467, 2017.

TURBINA WELLS - ISTERESI

Abbiamo provato a riprodurre i risultati di questi articoli, senza successo

RISULTATI ORIGINALI

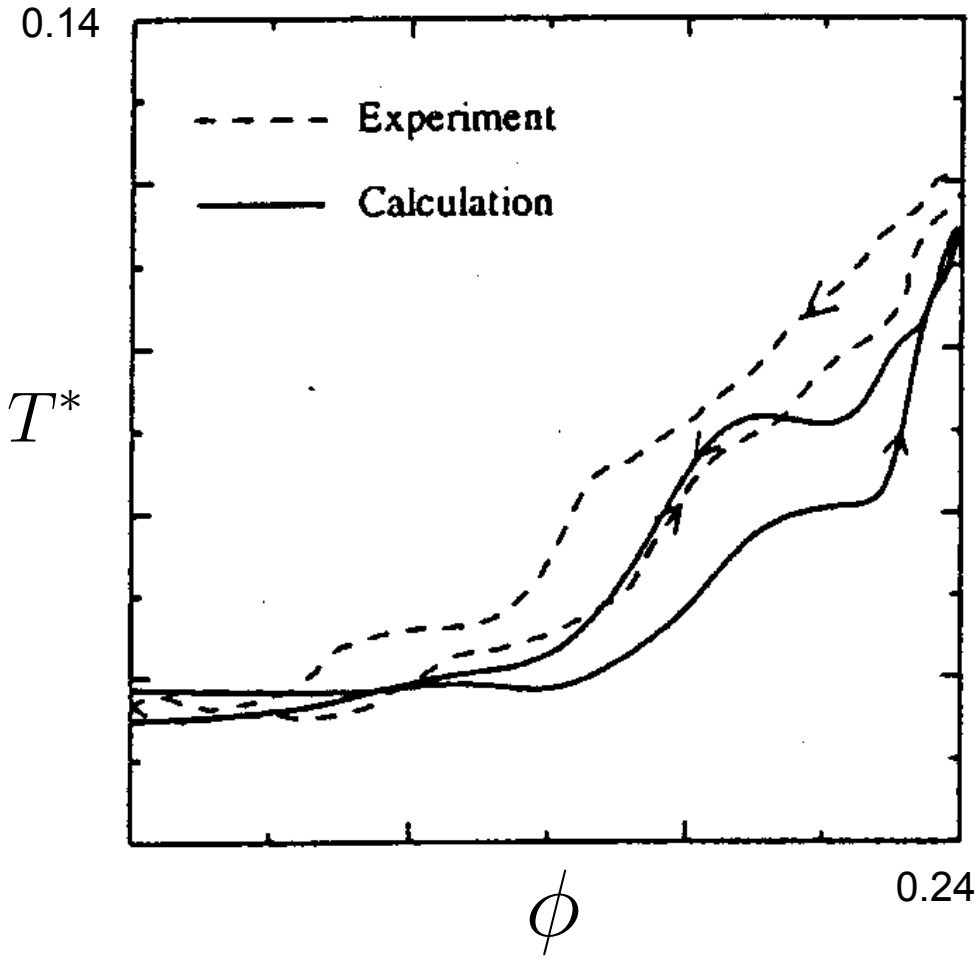

NOSTRI RISULTATI

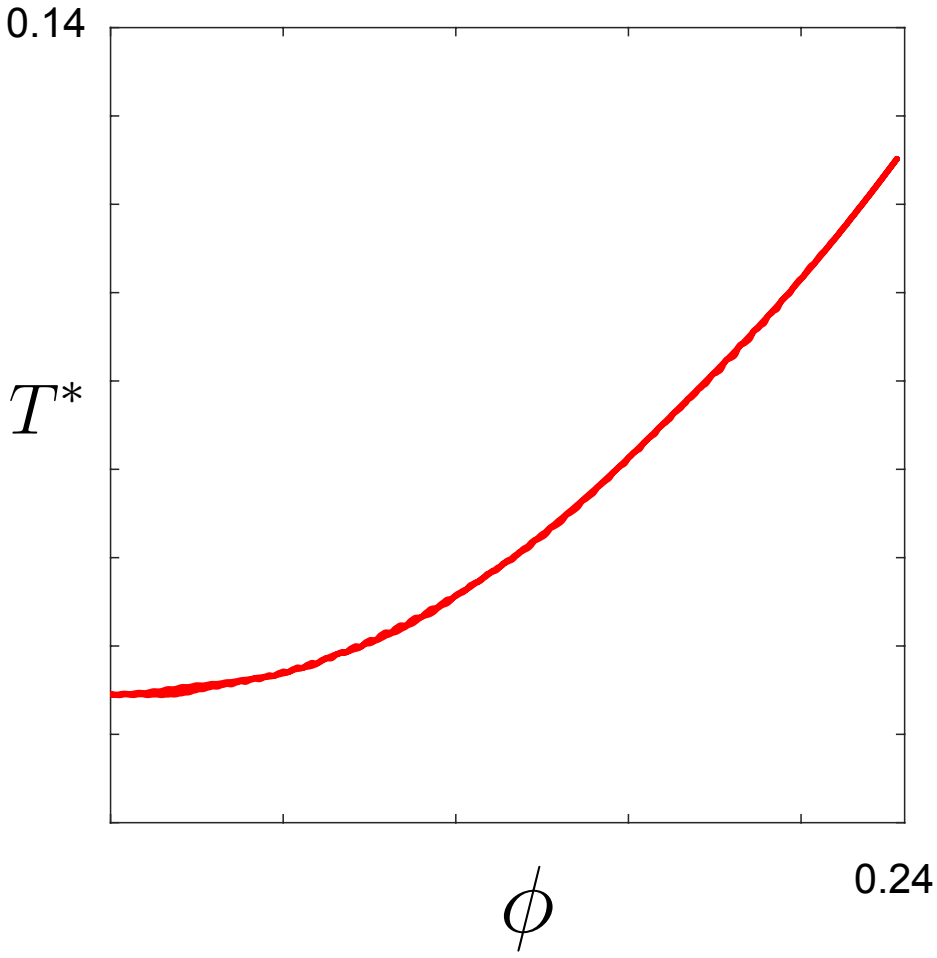

figure tratte da:

Y. Kinoue, T. Setoguchi, T.H. Kim, K. Kaneko, and M. Inoue. Mechanism of **hysteretic** characteristics of wells turbine for wave power conversion. *Journal of Fluids Engineering, Transactions of the ASME*, 125(2):302–307, 2003.

Abbiamo commesso qualche errore?

VERIFICA e VALIDAZIONE

MODELLO

DOMINIO DI CALCOLO:

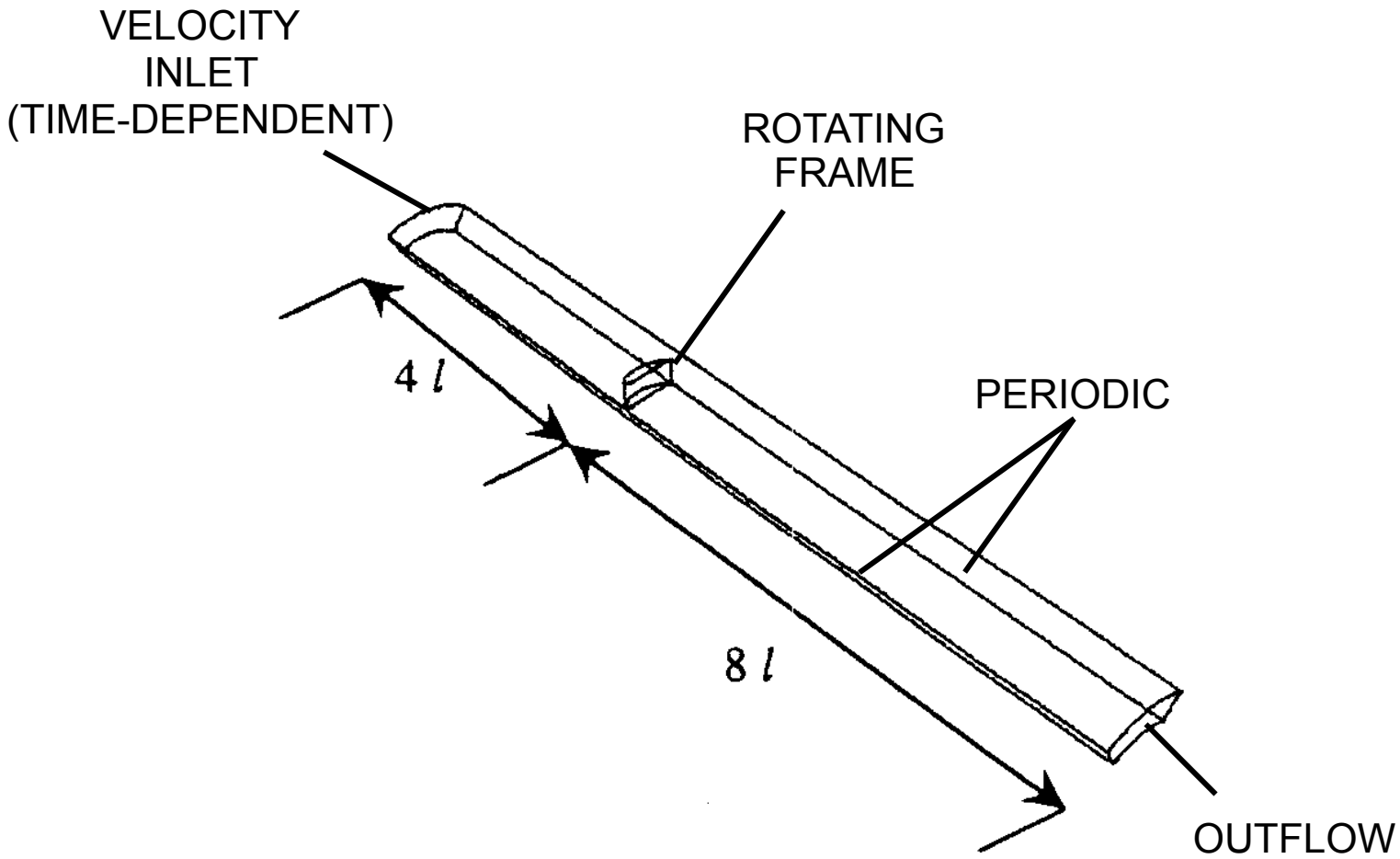

EQUAZIONI: RANS con $k - \omega$ per chiusura turbolenza

VERIFICA (Parte 1)

Utilizzando 3 GRIGLIE (1, 1.5 e 2 milioni di celle circa) abbiamo verificato la dipendenza dei risultati dalla discretizzazione spaziale.

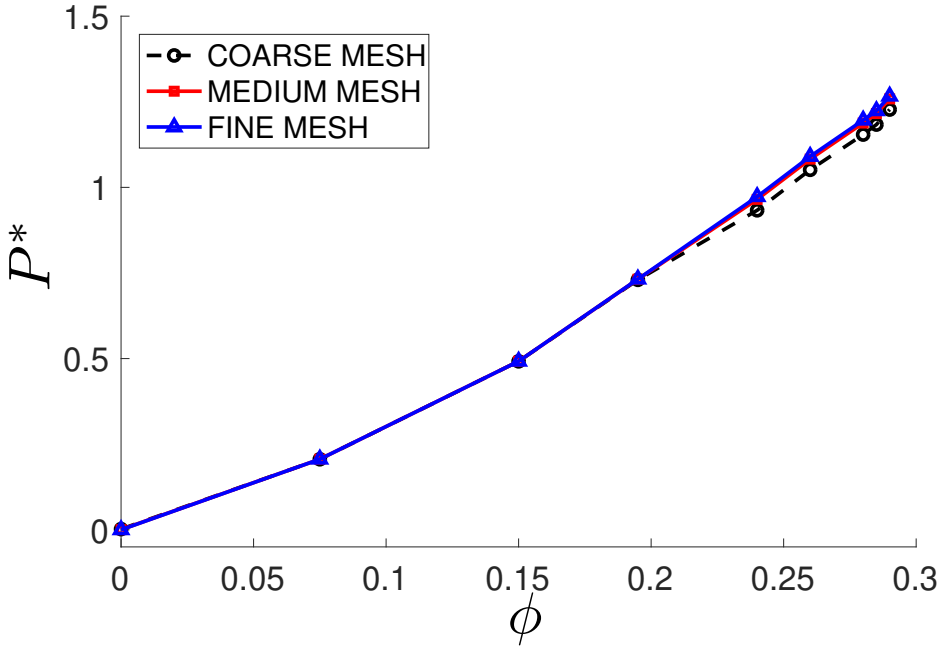

(a) Pressure drop coefficient

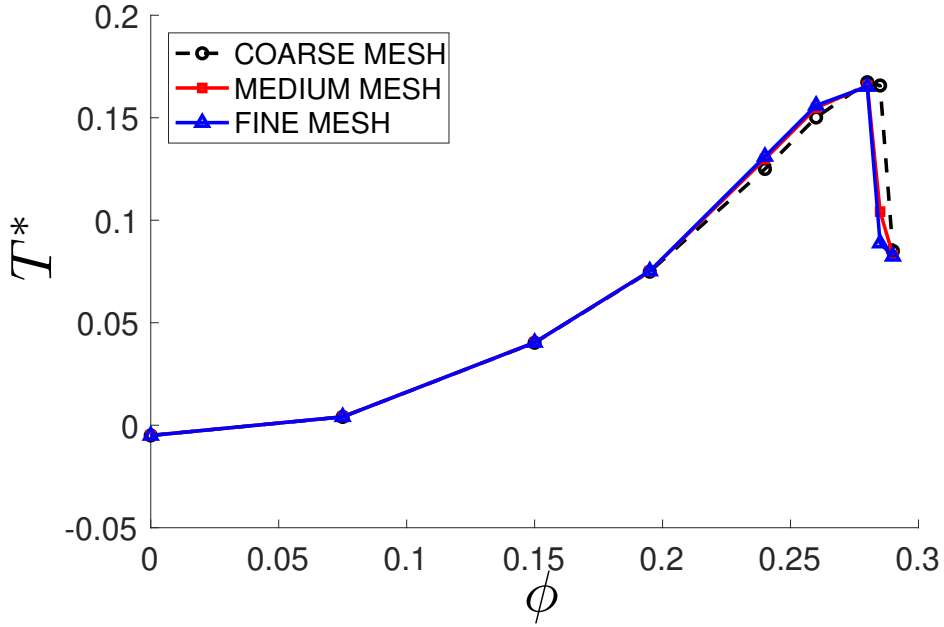

(b) Torque coefficient

VERIFICA (Parte 1)

Utilizzando 3 GRIGLIE (1, 1.5 e 2 milioni di celle circa) abbiamo verificato la dipendenza dei risultati dalla discretizzazione spaziale.

Abbiamo quindi calcolato l'errore di discretizzazione (e la relativa incertezza)

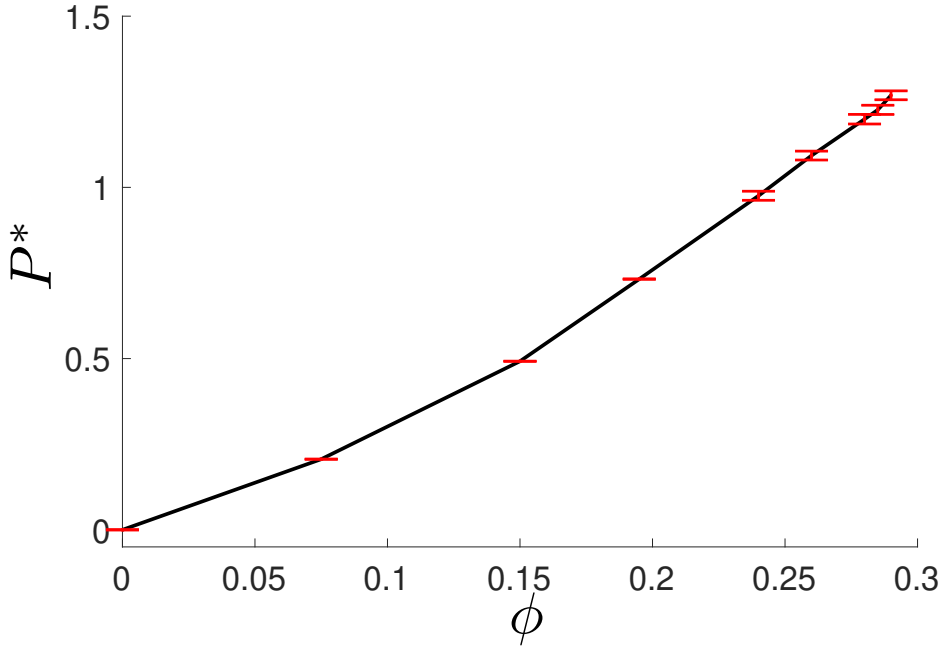

(a) Pressure drop coefficient

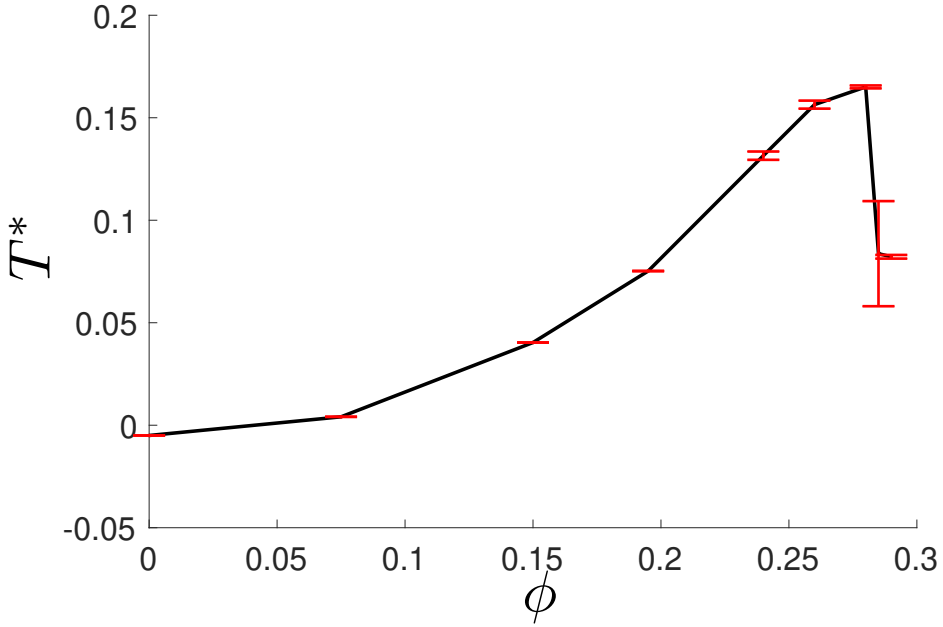

(b) Torque coefficient

Da notare come l'incertezza sia sempre molto contenuta, e aumenti per coefficienti di flusso vicini allo stallo.

VERIFICA (Parte 2)

Abbiamo quindi verificato la dipendenza della soluzione dalla discretizzazione temporale, utilizzando diversi valori del passo temporale

$$\Delta t_1 > \Delta t_2 > \Delta t_3 > \Delta t_4 > \Delta t_5$$

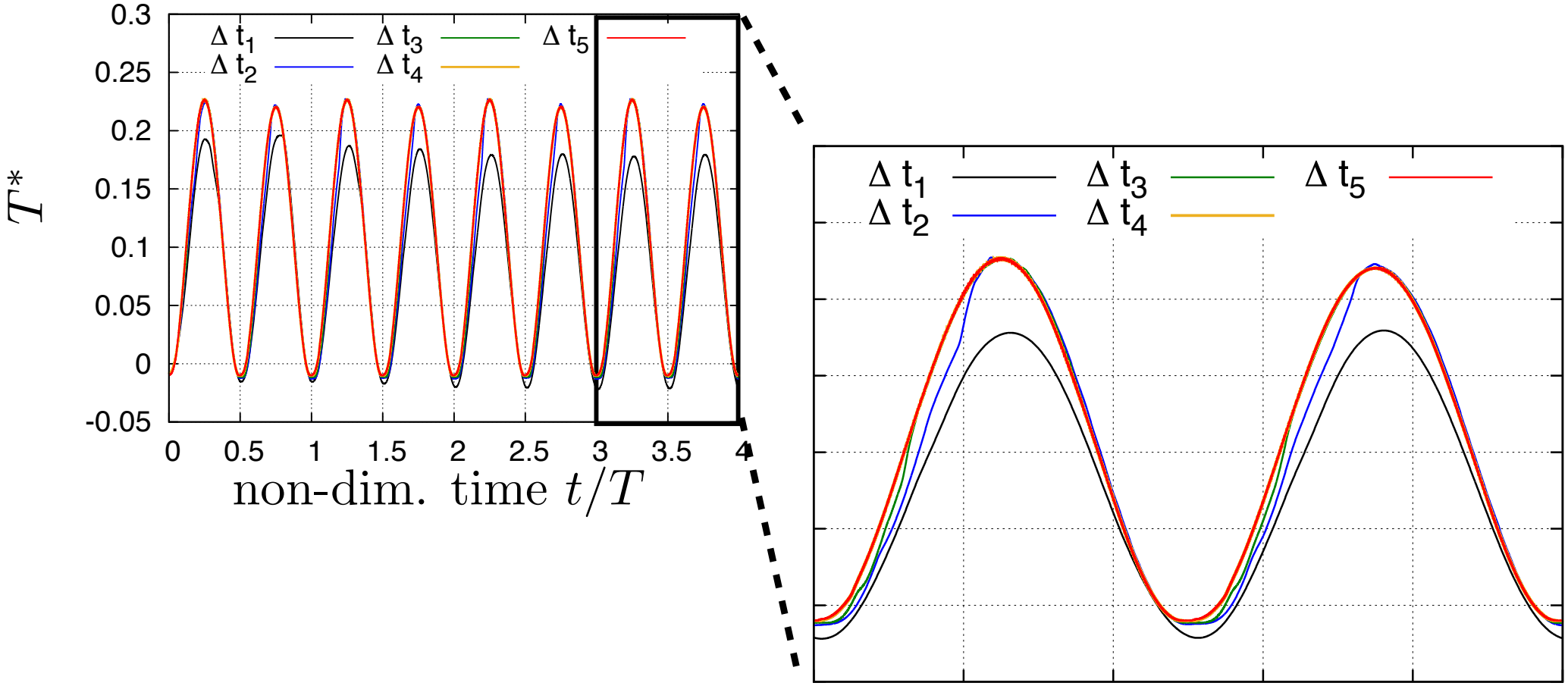

L'incertezza relativa sulla valutazione della fase e dell'ampiezza è 3 ordini di grandezza inferiore rispetto al valore misurato.

VERIFICA (Parte 2)

E’ interessante notare come l’utilizzo di una discretizzazione temporale troppo larga porti a un errore di fase, che si manifesta come una falsa isteresi.

SBAGLIATO

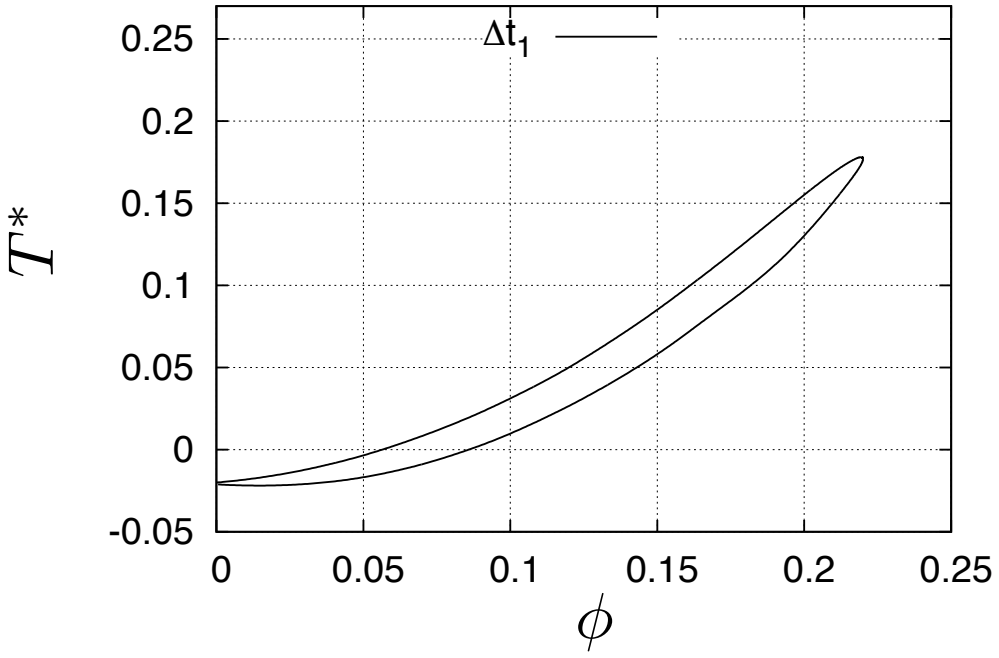

GIUSTO

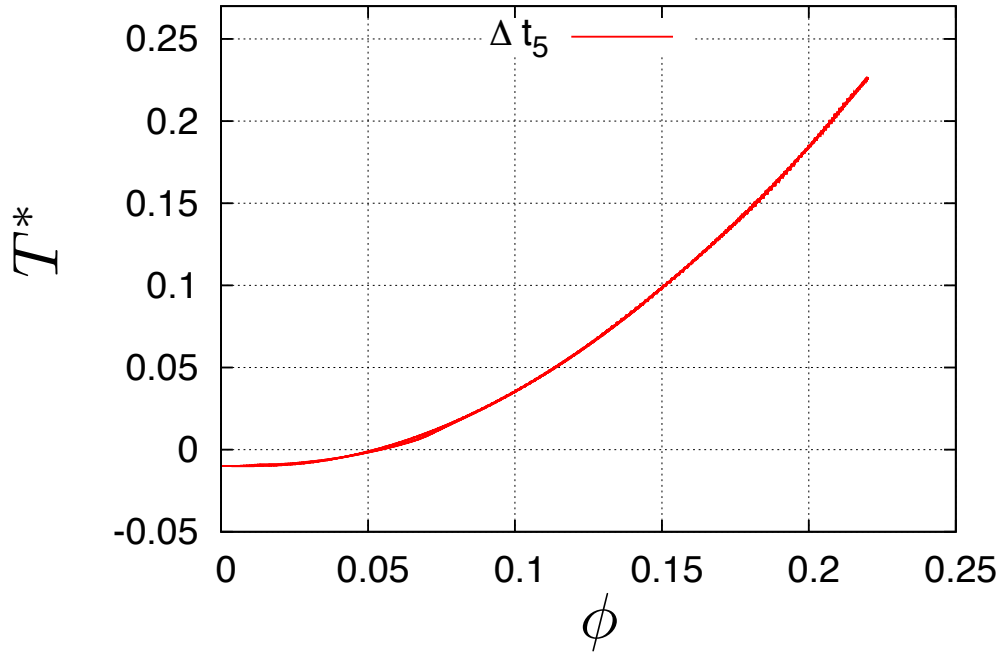

VALIDAZIONE

Confrontiamo i risultati numerici (una volta verificato che l'errore numerico è trascurabile) con i dati sperimentali. Sembra che si siamo allontani dalla soluzione (l'errore del modello è aumentato?)

SPERIMENTALE

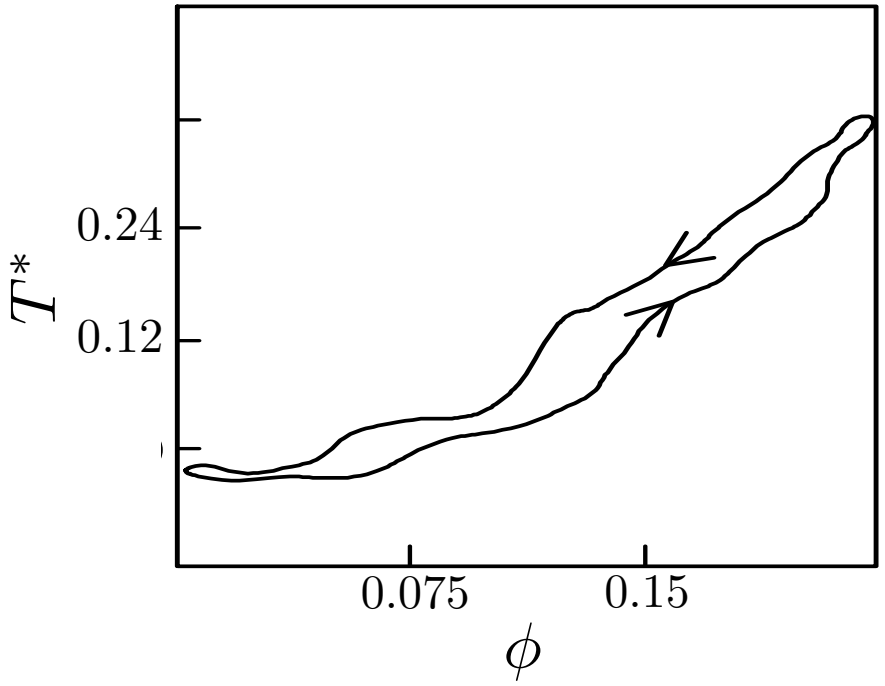

NUMERICO

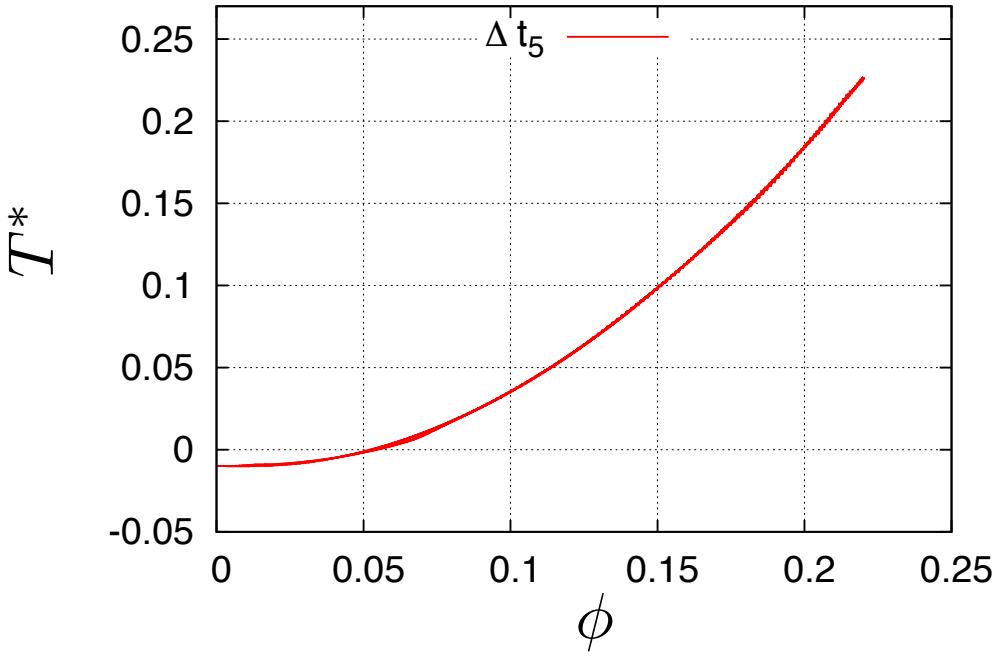

VERIFICA (Parte 2)

E’ interessante notare come l’utilizzo di una discretizzazione temporale troppo larga porti a un errore di fase, che si manifesta come una falsa isteresi.

SBAGLIATO

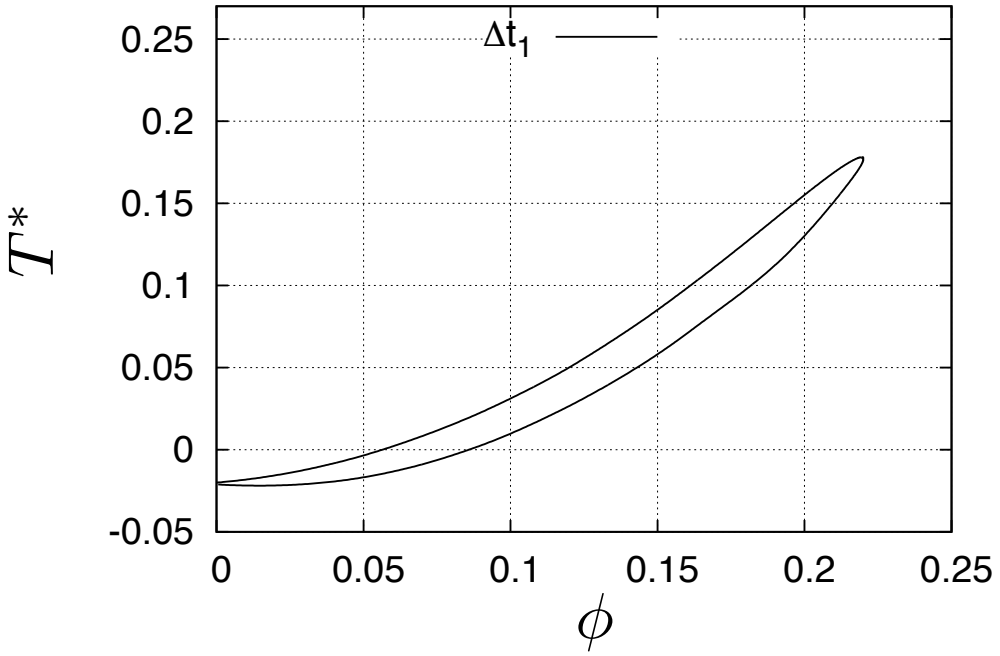

GIUSTO

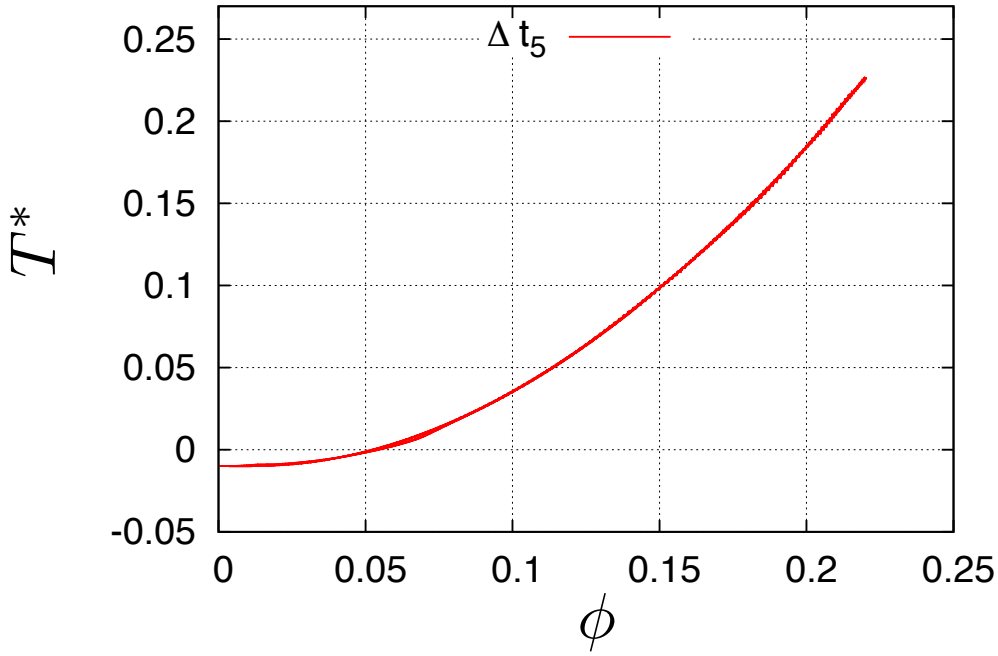

QUESTE FIGURE SONO INCOMPLETE!

VERIFICA (Parte 2)

E’ interessante notare come l’utilizzo di una discretizzazione temporale troppo larga porti a un errore di fase, che si manifesta come una falsa isteresi.

SBAGLIATO

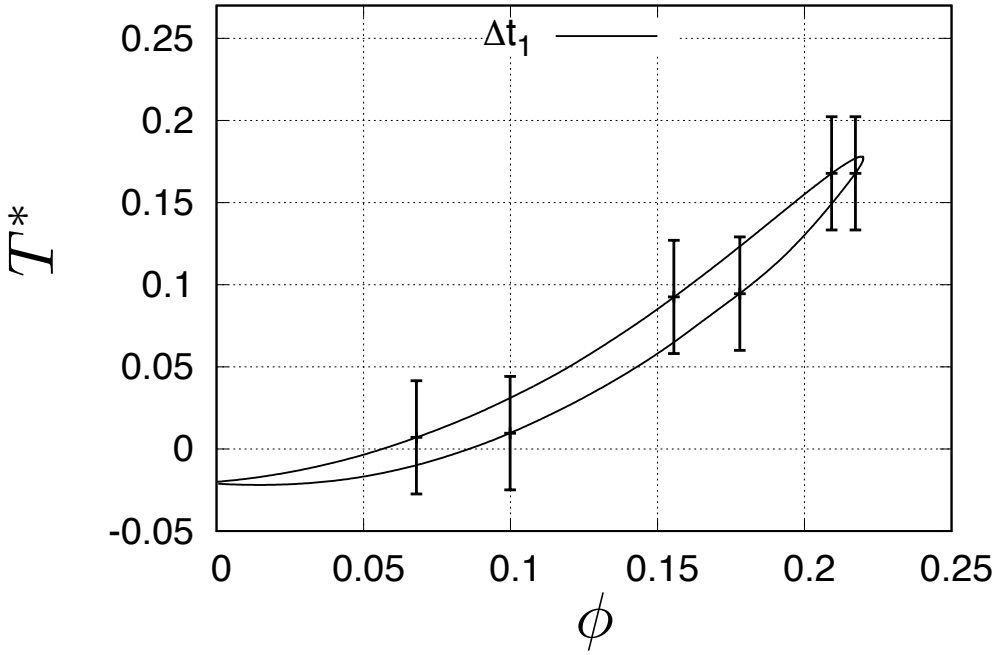

GIUSTO

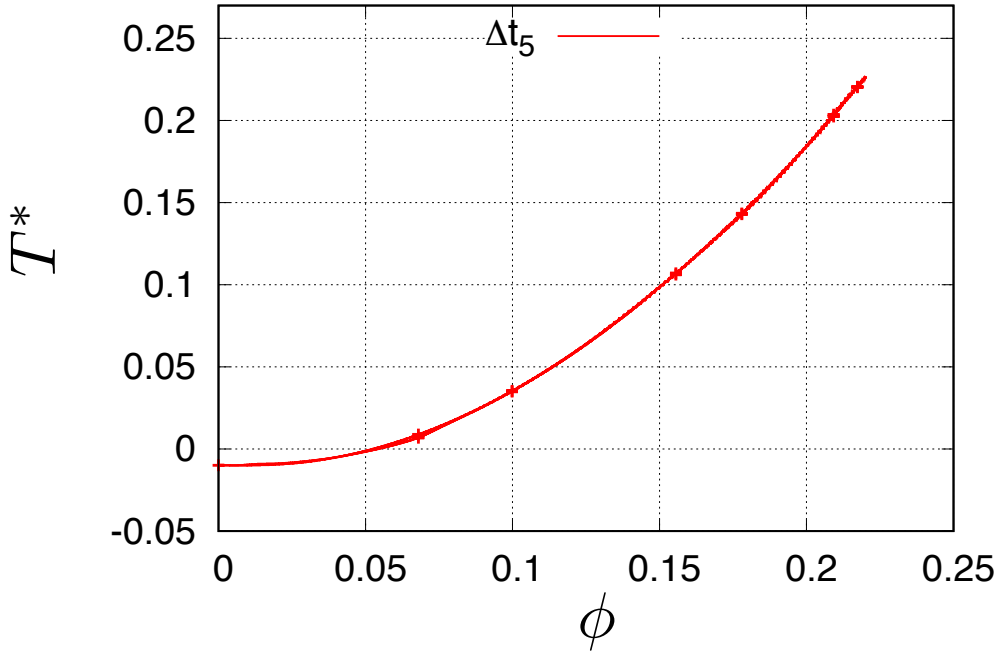

ERRORE E INCERTEZZA CONSIDEREVOLI
(MAGGIORI DI CIO’ CHE STIAMO VALUTANDO)

ERRORE E INCERTEZZA TRASCURABILI

ERRORE

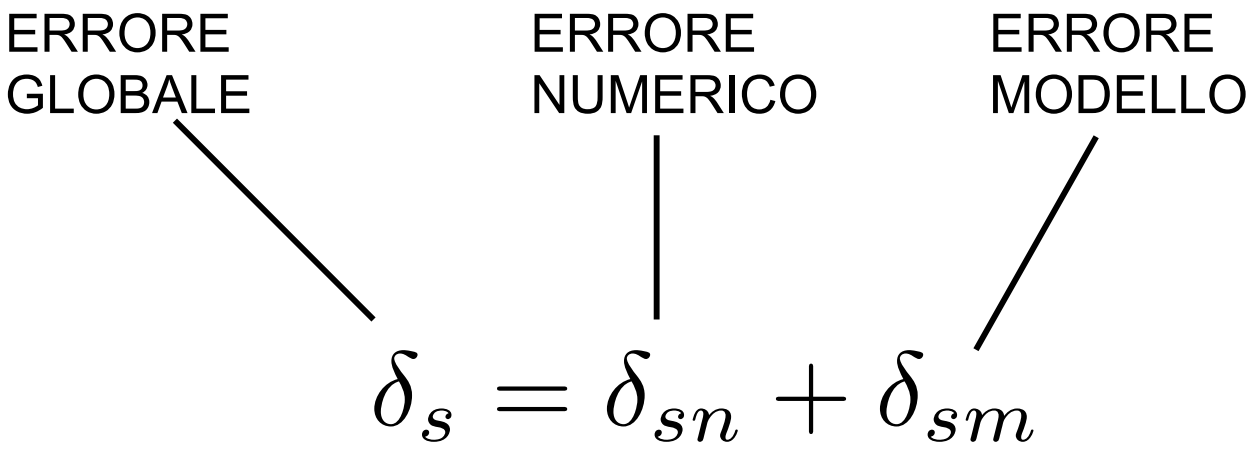

Abbiamo valutato e contenuto l'errore numerico, ma l'errore del modello?

In altri articoli, l'errore globale era limitato, ma non sappiamo (dubitiamo?) se sia stato verificato l'errore numerico.

Rivediamo il modello matematico …

MODELLO MATEMATICO

Consideriamo le semplificazioni introdotte nella determinazione del modello matematico:

ESPERIMENTO

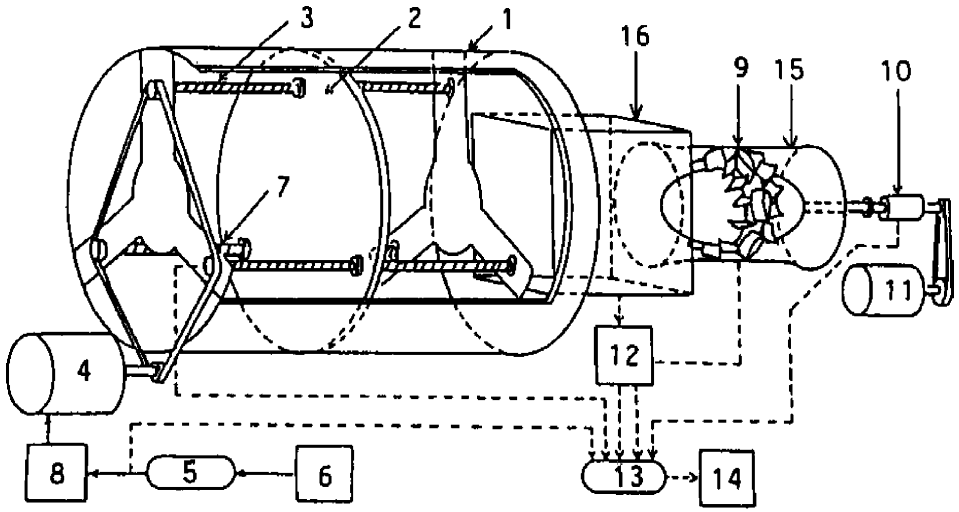

figure tratte da:

Y. Kinoue, T. Setoguchi, T.H. Kim, K. Kaneko, and M. Inoue. Mechanism of **hysteretic** characteristics of wells turbine for wave power conversion. *Journal of Fluids Engineering, Transactions of the ASME*, 125(2):302–307, 2003.

MODELLO MATEMATICO

Consideriamo le semplificazioni introdotte nella determinazione del modello matematico:

ESPERIMENTO

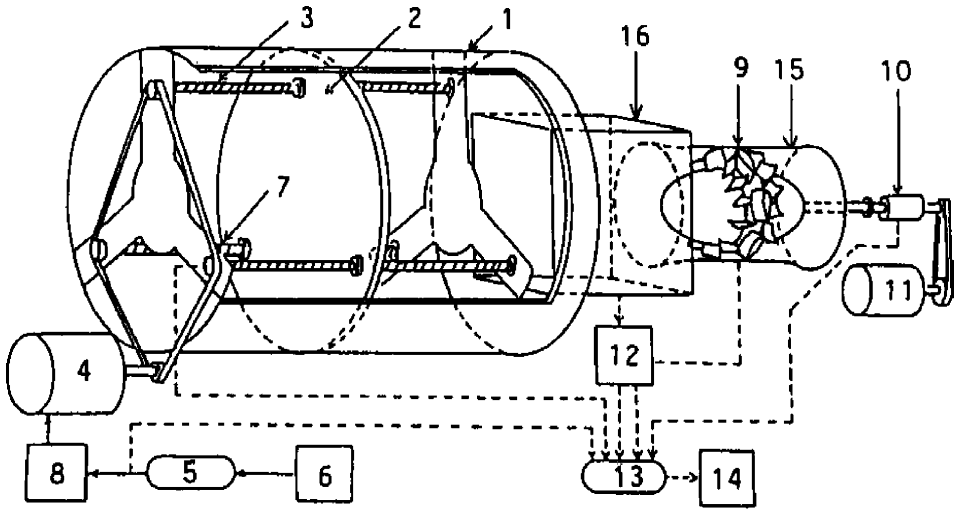

CFD

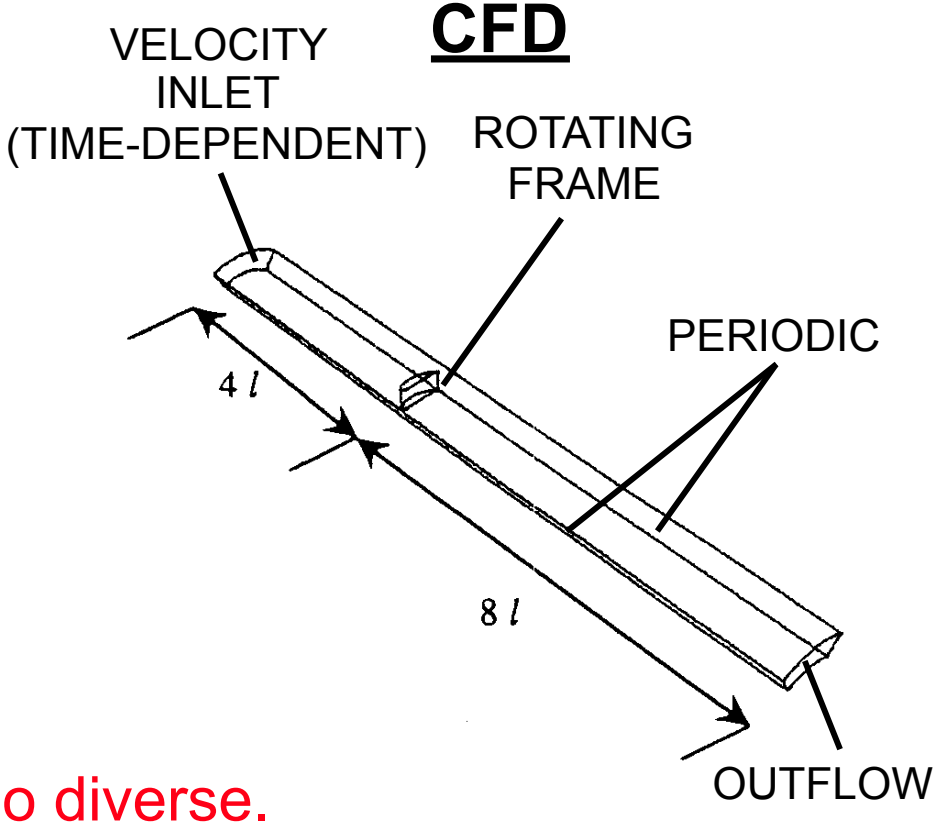

Geometria e condizioni al contorno sono diverse.

Nell'esperimento ϕ era valutato sulla base del moto del pistone, nel CFD era imposto come condizione al contorno.

figure tratte da:

Y. Kinoue, T. Setoguchi, T.H. Kim, K. Kaneko, and M. Inoue. Mechanism of **hysteretic** characteristics of wells turbine for wave power conversion. *Journal of Fluids Engineering, Transactions of the ASME*, 125(2):302–307, 2003.

MODELLO MATEMATICO

Prendiamo in considerazione un modello più vicino alla realtà:

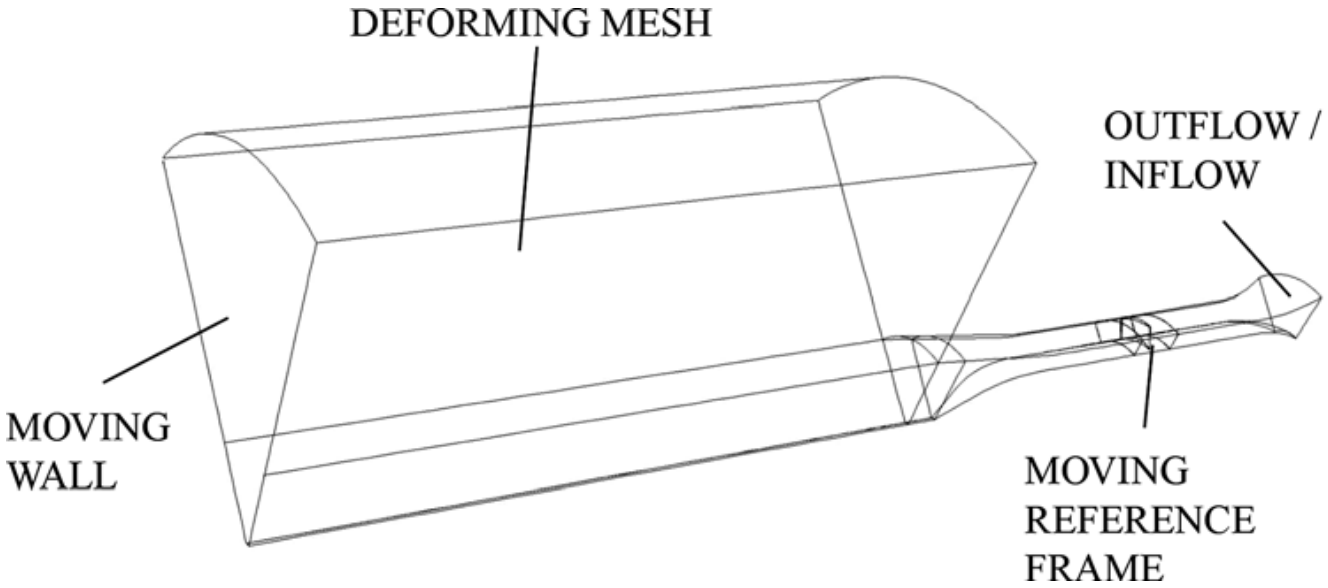

Geometrical and operating data for Setoguchi's experiments *	
chamber diameter [m]	1.4
rotor tip diameter [mm]	300
rotor hub diameter [mm]	210
tip clearance [mm]	1
chord length c [mm]	90
sweep ratio [-]	0.417
number of blades [-]	6
blade profile	NACA0020
solidity at tip radius σ [-]	0.57
rotational speed [rpm]	2500
operating frequency f [s^{-1}]	1/6
Reynolds number Re [-]	2×10^5
Mach number M [-]	0.1
turbine non-dimensional frequency k [-]	0.0014

* T. Setoguchi, M. Takao, K. Kaneko, Hysteresis on Wells turbine characteristics in reciprocating flow, International Journal of Rotating Machinery 4 (1) (1998) 17–24.

MODELLO MATEMATICO

Prendiamo in considerazione un modello più vicino alla realtà:

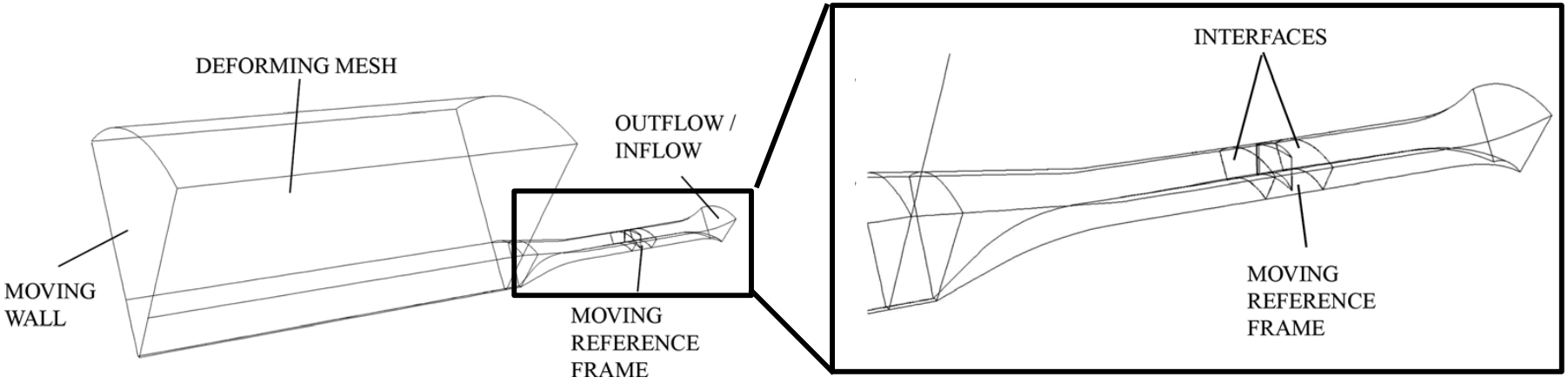

(Non senza prima VERIFICARE
i risultati numerici …)

VALIDAZIONE

Prendiamo in considerazione un modello più vicino alla realtà:

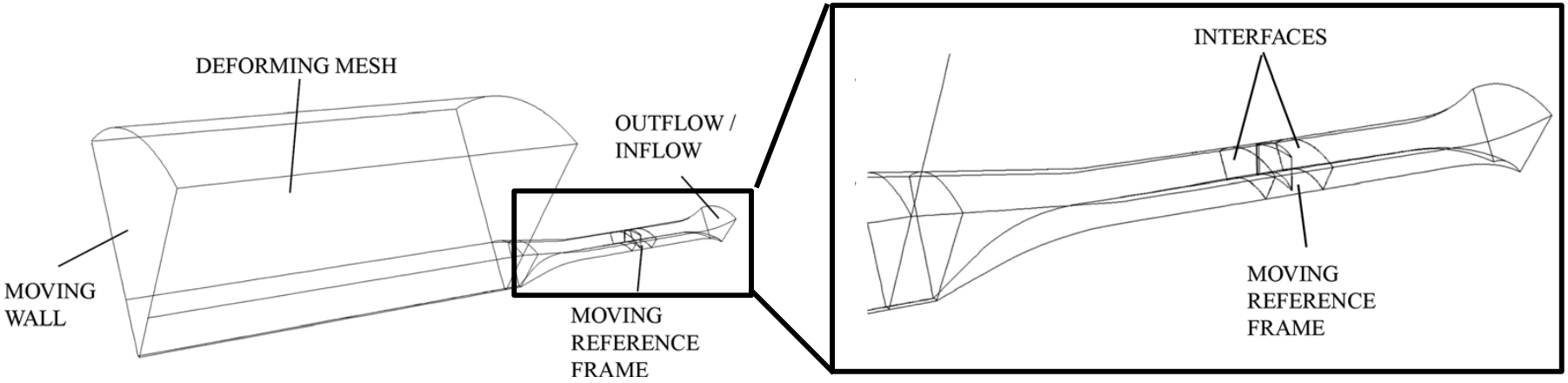

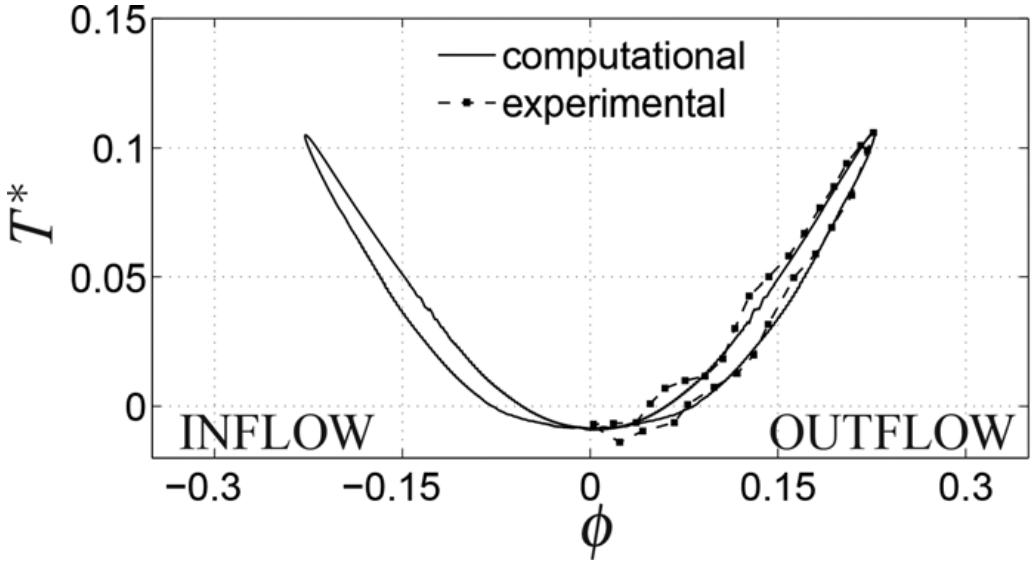

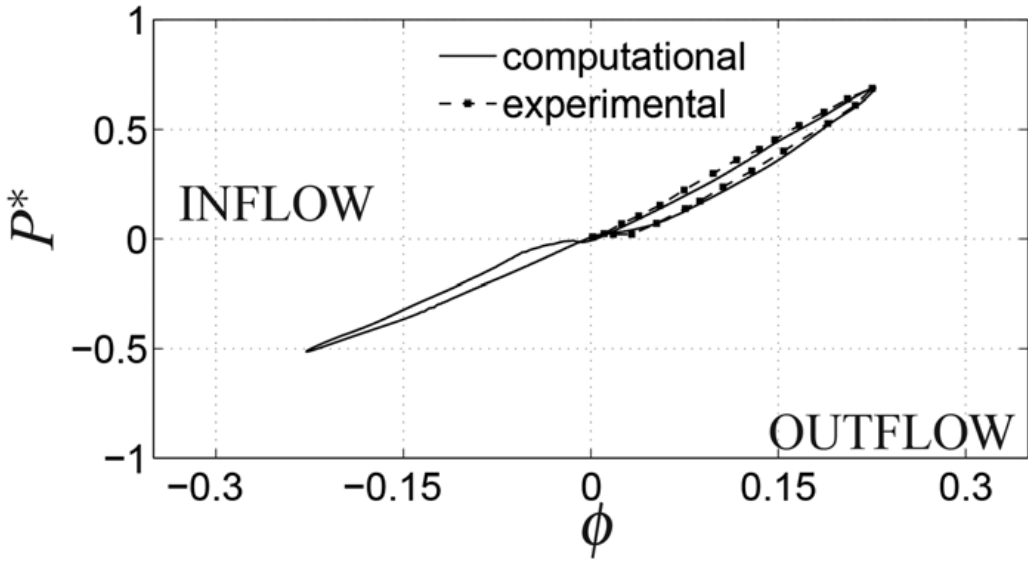

ϕ calcolato in base alla velocità del pistone.

dati sperimentali da:

Y. Kinoue, T. Setoguchi, T.H. Kim, K. Kaneko, and M. Inoue. Mechanism of **hysteretic** characteristics of wells turbine for wave power conversion. *Journal of Fluids Engineering, Transactions of the ASME*, 125(2):302–307, 2003.

ERRORE

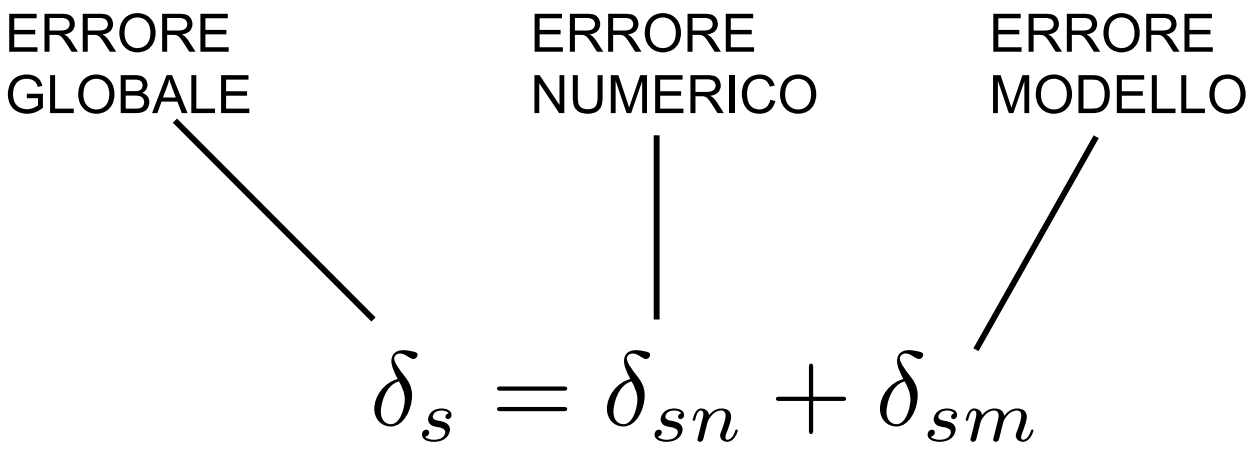

1) Abbiamo valutato e contenuto l'errore numerico

2) Possiamo valutare l'errore del modello (tramite confronto con i dati sperimentali) e concludere che il modello matematico è una buona approssimazione del problema fisico

ANALISI DEI RISULTATI

Analizziamo il comportamento della turbina:

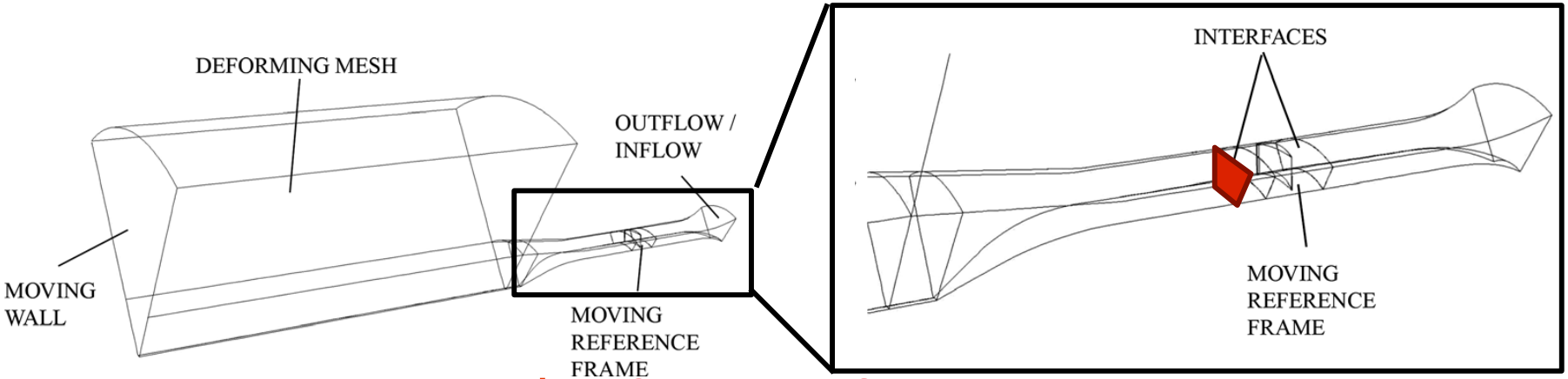

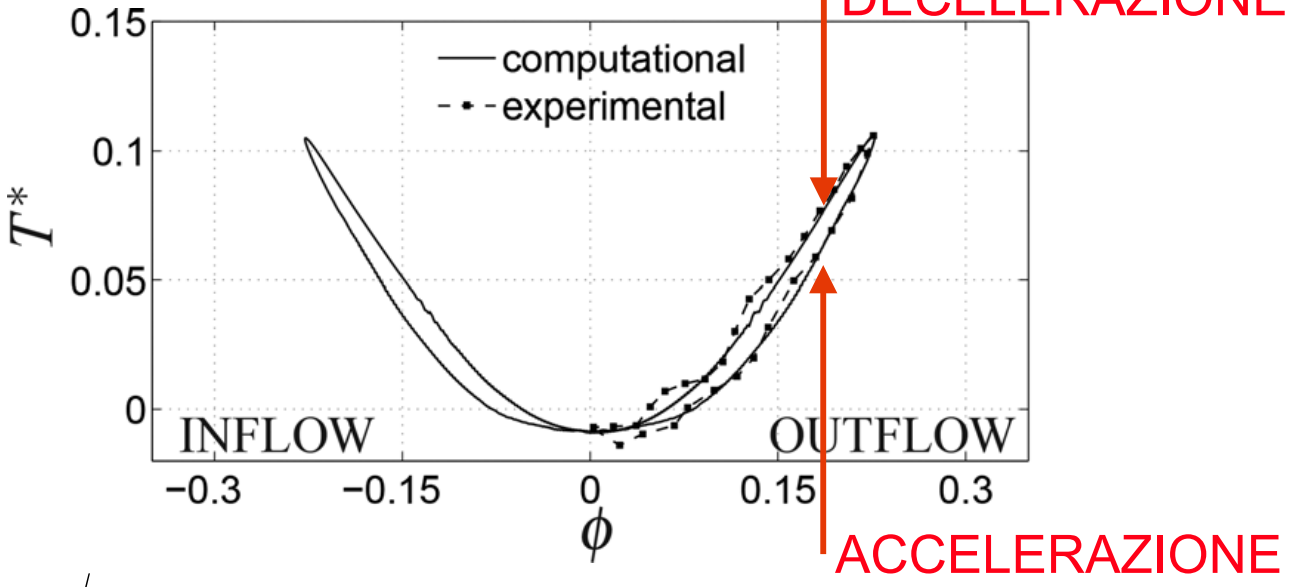

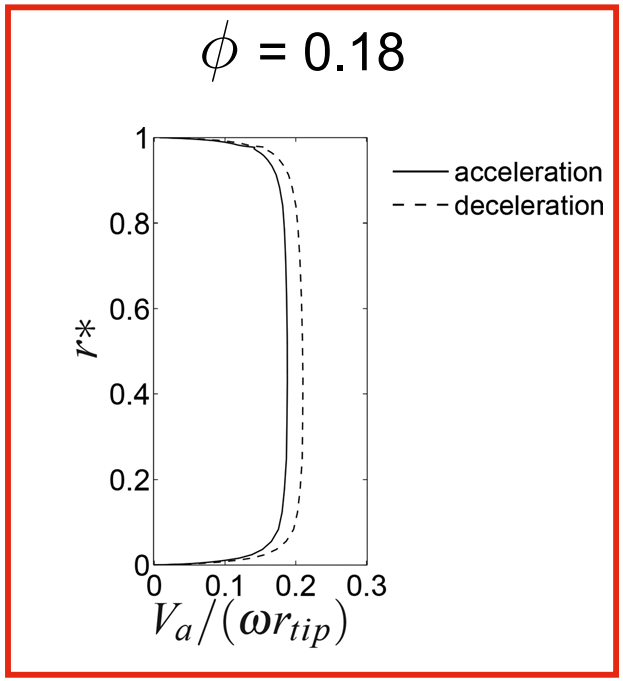

ϕ calcolato in base alla velocità del pistone.

dati sperimentali da:

Y. Kinoue, T. Setoguchi, T.H. Kim, K. Kaneko, and M. Inoue. Mechanism of **hysteretic** characteristics of wells turbine for wave power conversion. *Journal of Fluids Engineering, Transactions of the ASME*, 125(2):302–307, 2003.

ANALISI DEI RISULTATI

Analizzamo il comportamento della turbina:

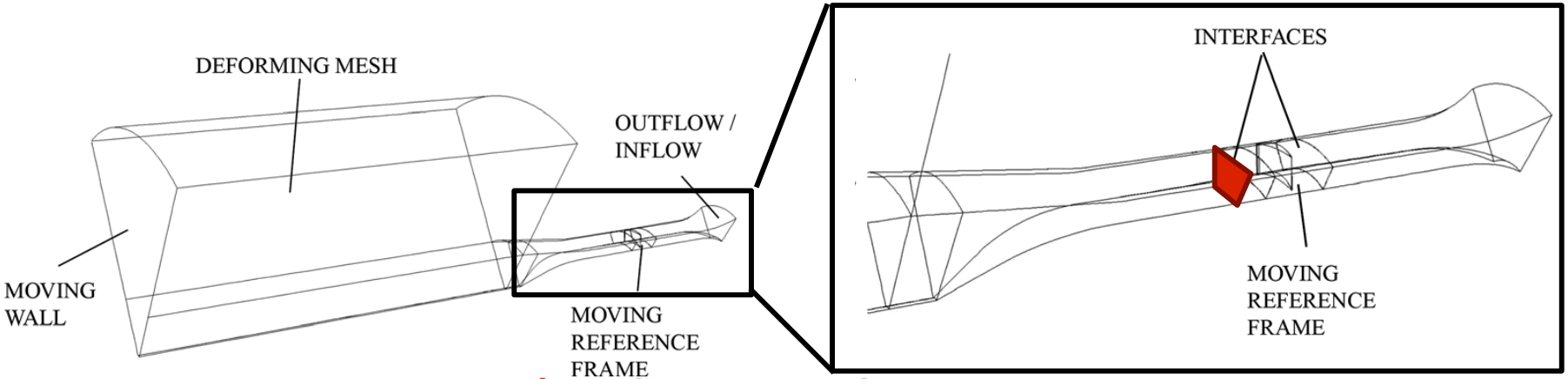

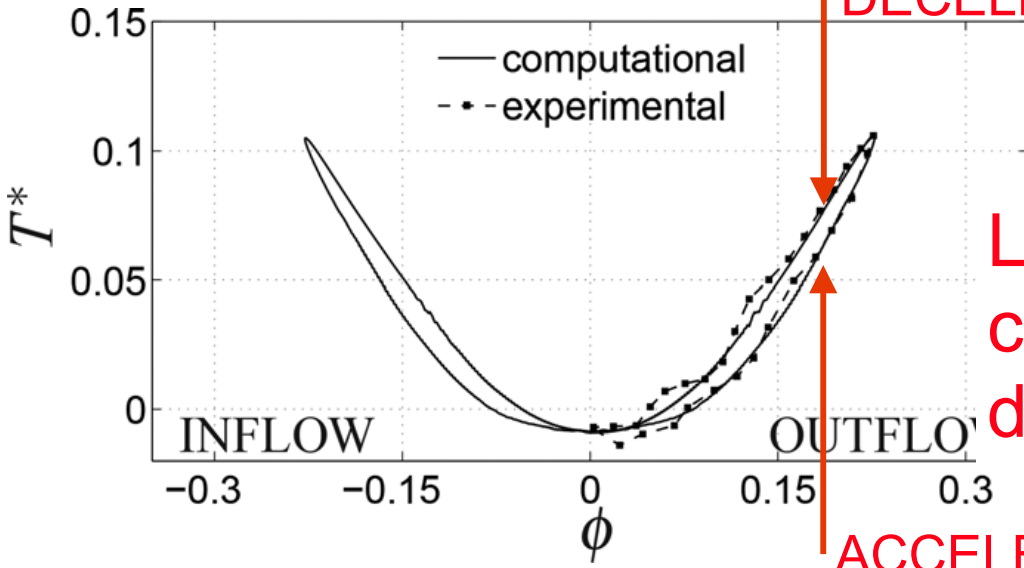

DECELERAZIONE

ACCELERAZIONE

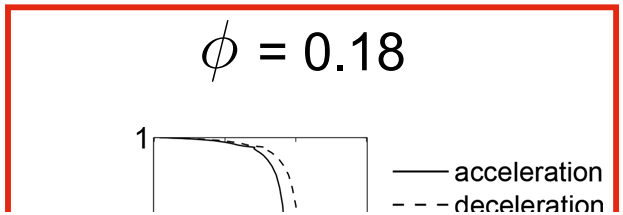

L'isteresi è causata dal comportamento capacitivo dell' OWC

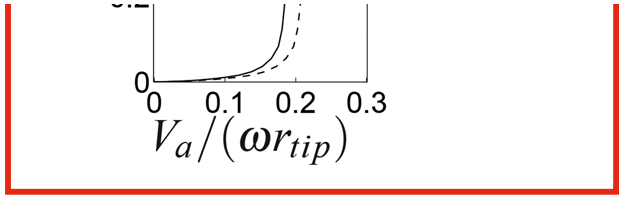

ϕ calcolato in base alla velocità del pistone.

dati sperimentali da:

Y. Kinoue, T. Setoguchi, T.H. Kim, K. Kaneko, and M. Inoue. Mechanism of **hysteretic** characteristics of wells turbine for wave power conversion. *Journal of Fluids Engineering, Transactions of the ASME*, 125(2):302–307, 2003.

ANALISI DEI RISULTATI

Analizziamo il comportamento della turbina:

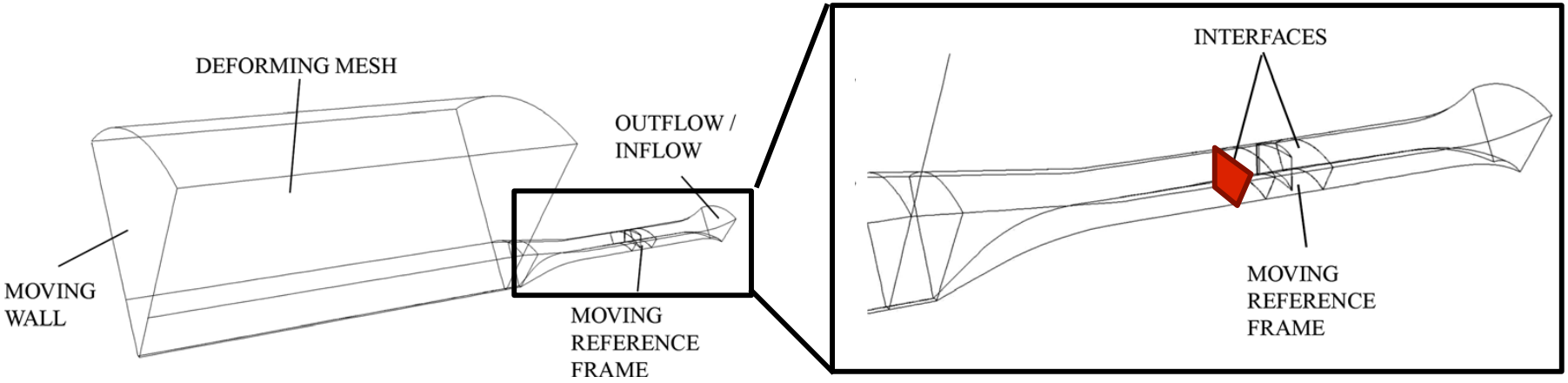

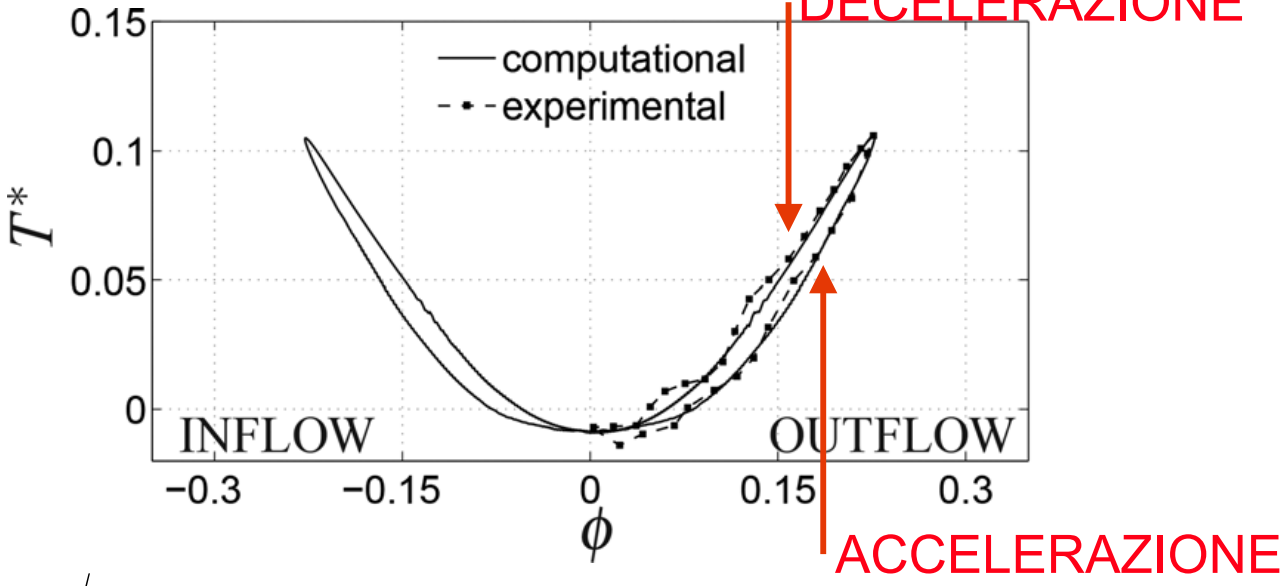

ϕ calcolato in base alla velocità del pistone.

ϕ = 0.18 (acceleration)
ϕ ~ 0.17 (deceleration)

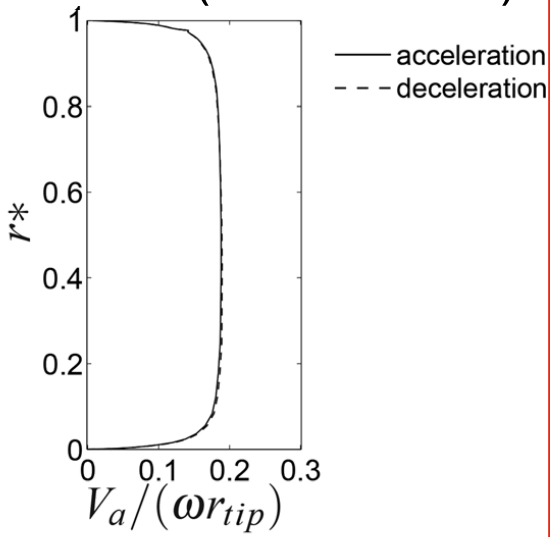

dati sperimentali da:

Y. Kinoue, T. Setoguchi, T.H. Kim, K. Kaneko, and M. Inoue. Mechanism of **hysteretic** characteristics of wells turbine for wave power conversion. *Journal of Fluids Engineering, Transactions of the ASME*, 125(2):302–307, 2003.

ANALISI DEI RISULTATI

Le differenze strutture fluide tra le fasi di accelerazione e decelerazione sono sparite

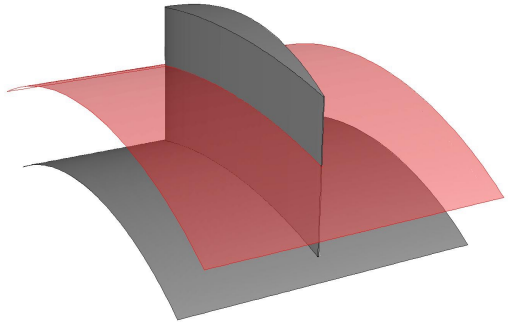

UGUALI PORTATE

CONTORNI DI VELOCITÀ RELATIVA

ACCEL.
ϕ = 0.18

DECEL.
ϕ ~ 0.17

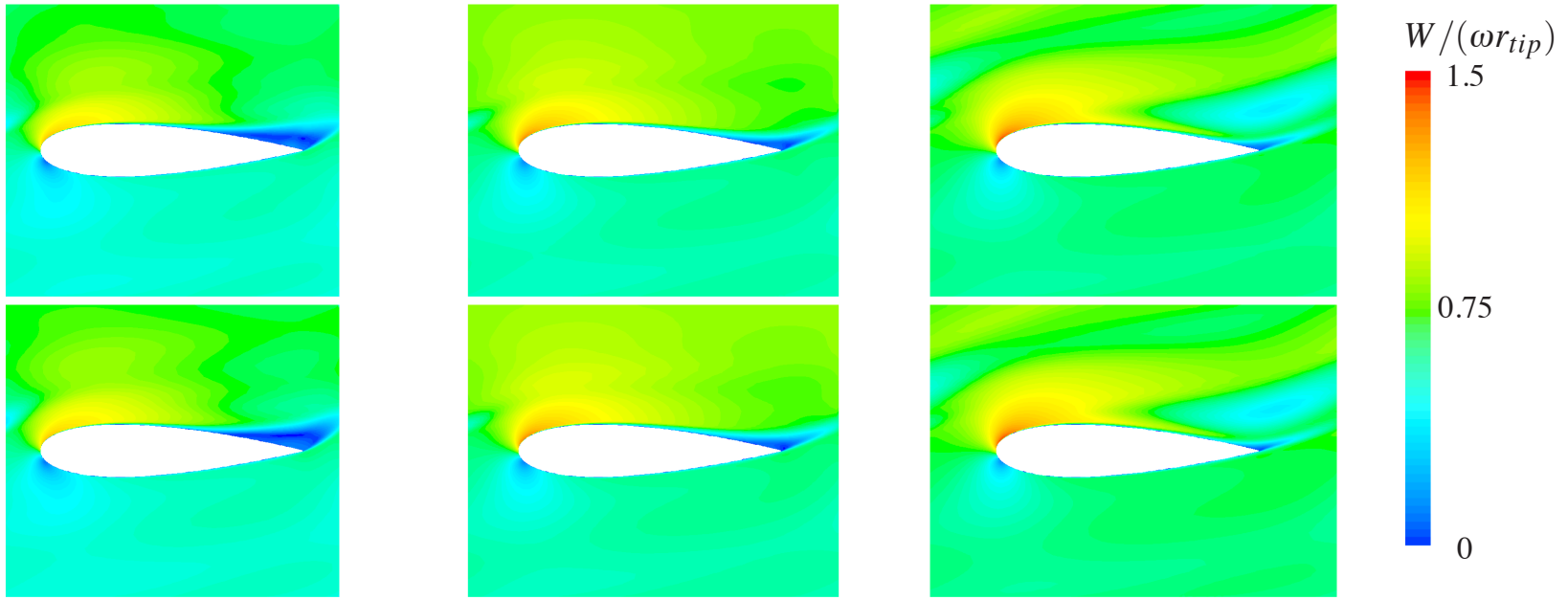

(a) $r^* = 0.2$ (b) $r^* = 0.5$ (c) $r^* = 0.8$

ANALISI DEI RISULTATI

Le differenze strutture fluide tra le fasi di accelerazione e decelerazione sono sparite

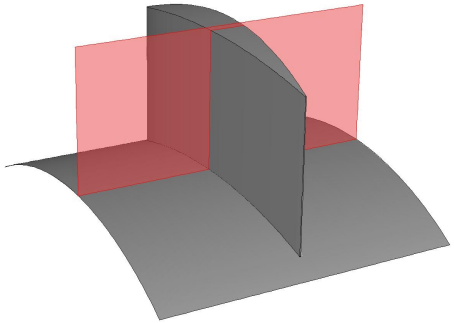

UGUALI PORTATE

CONTORNI DI VORTICITÀ

ACCEL.
ϕ = 0.18

DECEL.
ϕ ~ 0.17

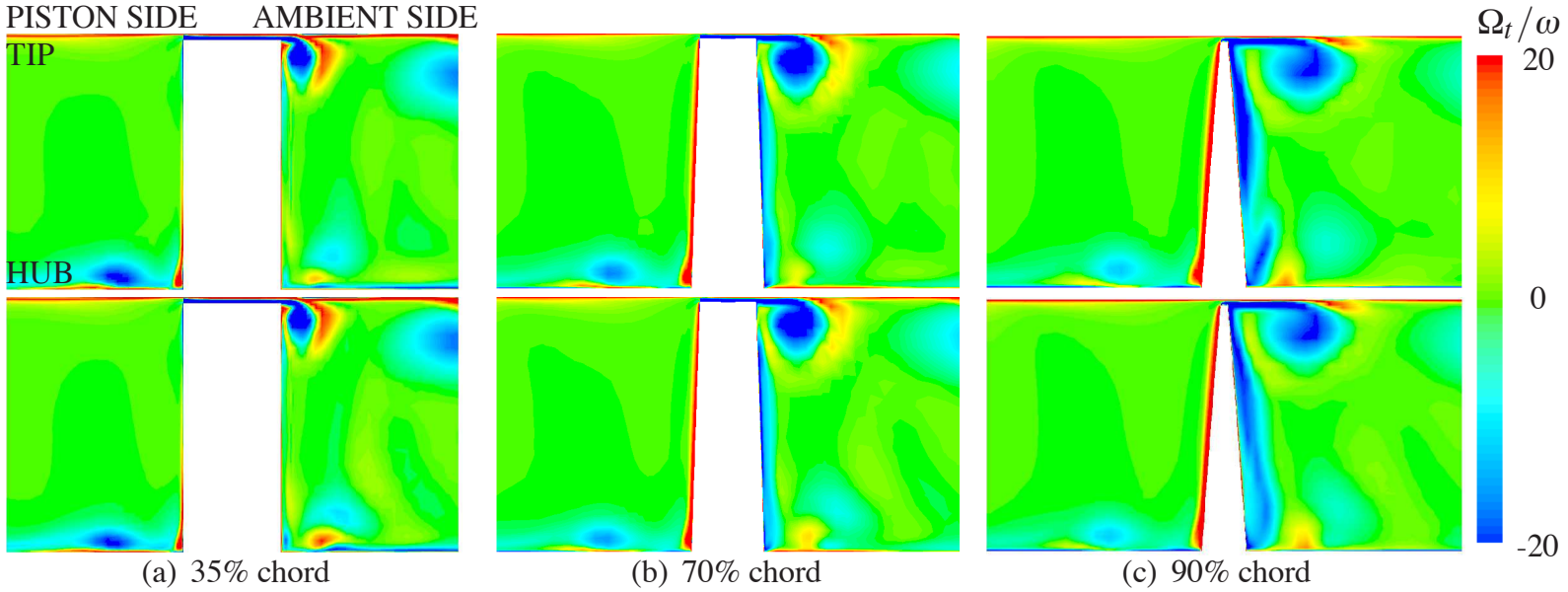

ANALISI DEI RISULTATI

Se vogliamo realmente studiare un'eventuale isteresi aerodinamica della turbina, dobbiamo analizzare le forze aerodinamiche in modo diverso

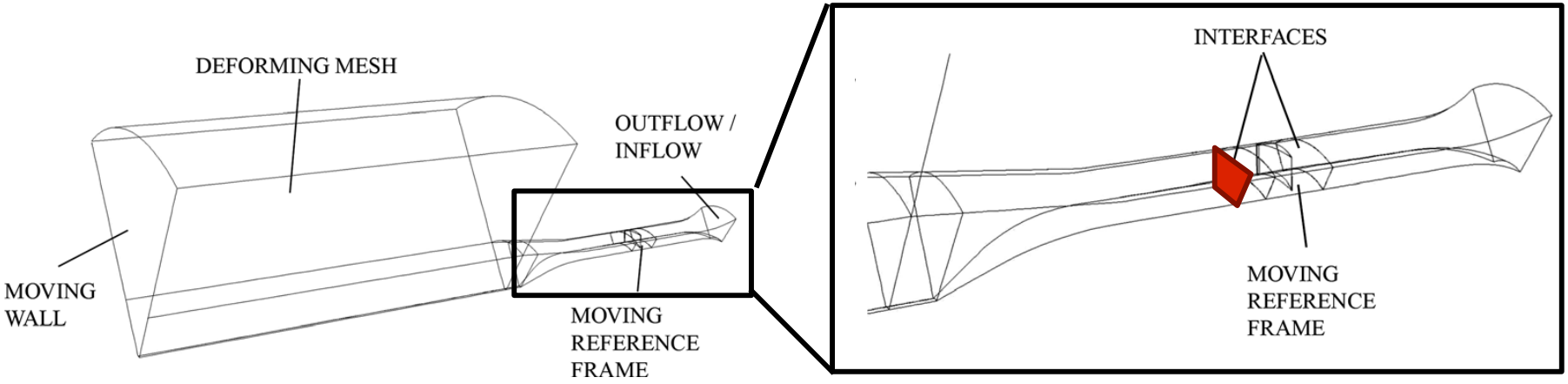

L'adimensionalizzazione "corretta" dei parametri di prestazione deve essere fatta utilizzando le velocità locali:

$$T^{**} = \frac{T}{\rho(W_t^2 + W_a^2)r_t^3}$$

$$P^{**} = \frac{\Delta P}{\rho(W_t^2 + W_a^2)}$$

$$\phi_l = \frac{W_a}{W_t}$$

ϕ_l RAPPRESENTA UN COEFFICIENTE DI FLUSSO EFFETTIVO

ANALISI DEI RISULTATI

Se vogliamo realmente studiare un'eventuale isteresi aerodinamica della turbina, dobbiamo analizzare le forze aerodinamiche in modo diverso

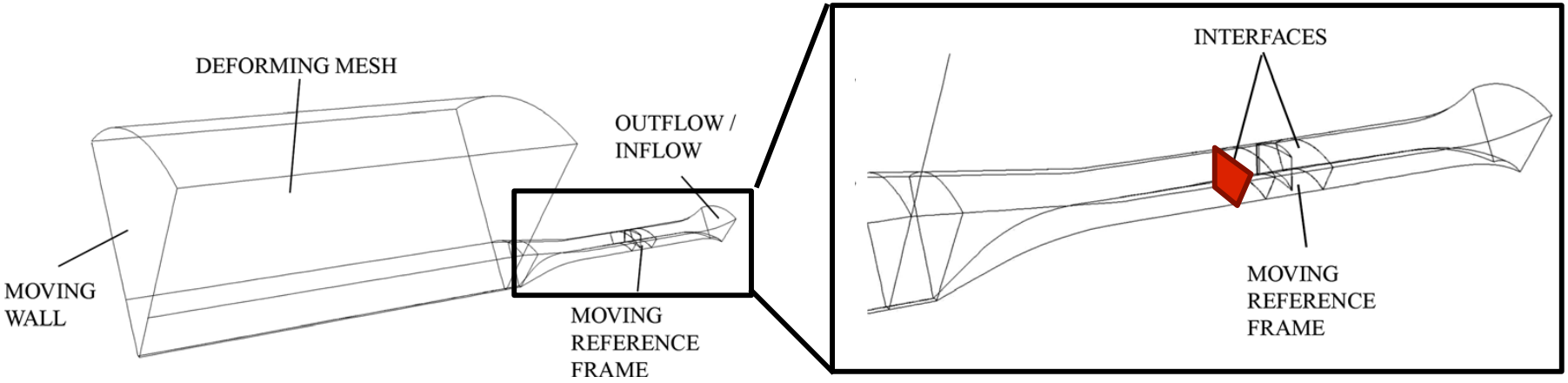

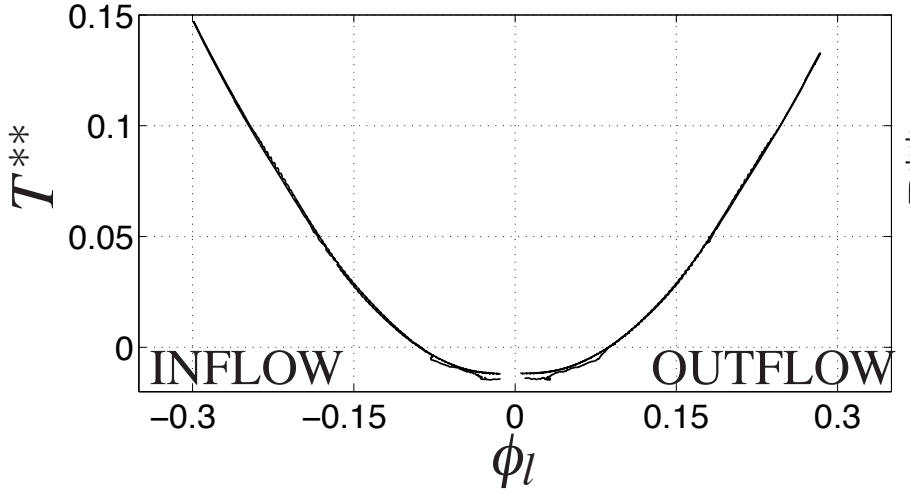

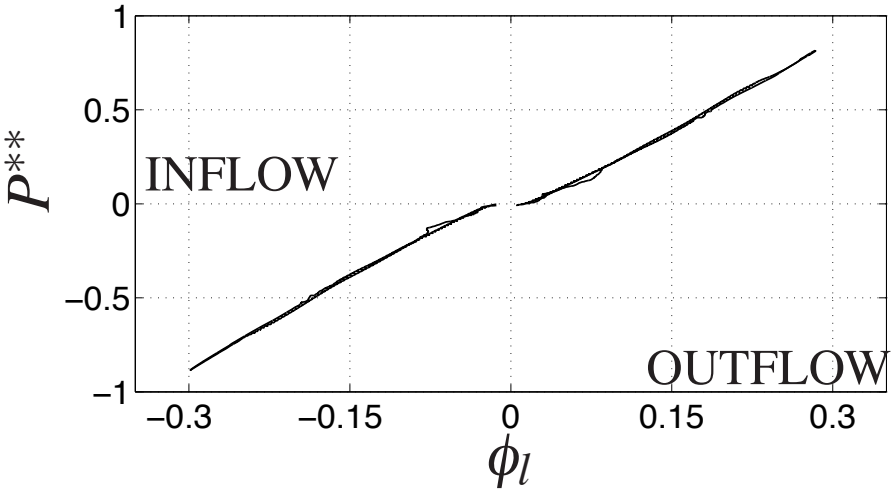

ϕ_l RAPPRESENTA UN COEFFICIENTE DI FLUSSO EFFETTIVO

Siamo convinti di questa spiegazione?

APPROCCIO ALTERNATIVO

Consideriamo le similarità tra il nostro sistema e altri strumenti che lavorano in condizioni dinamiche:

TRASDUTTORE DI PRESSIONE

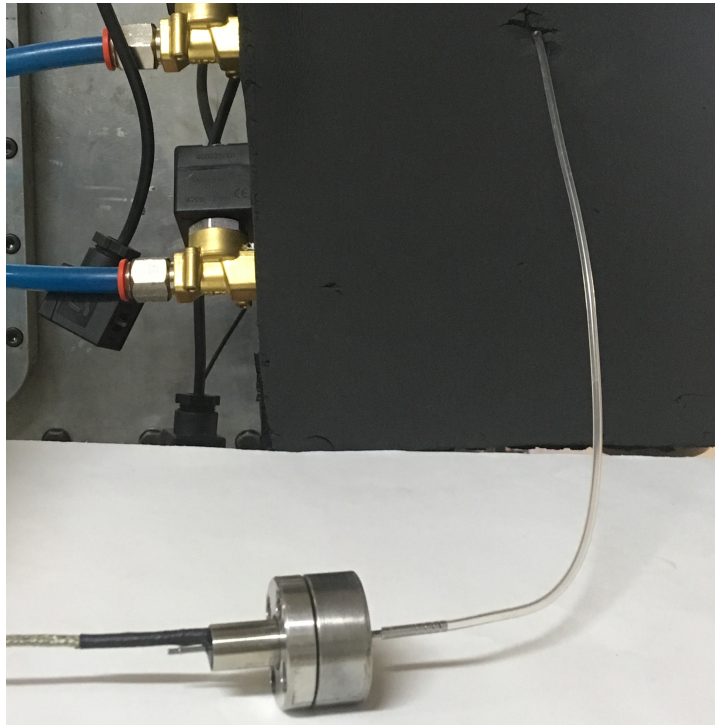

SISTEMA LINEA-CAVITA'

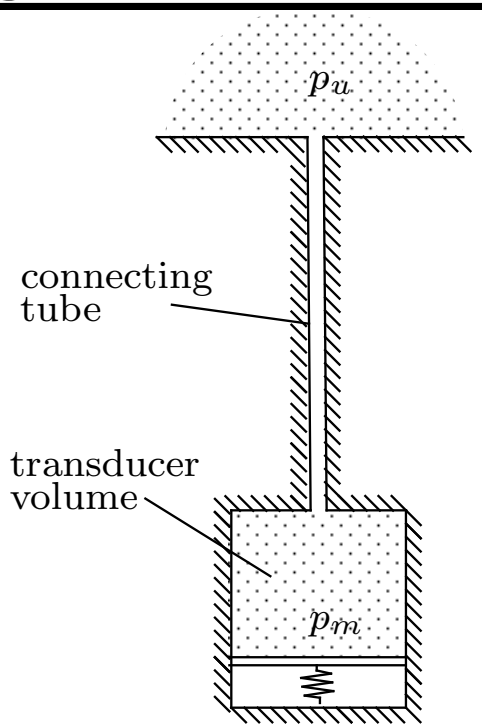

In una misura di pressione variabile nel tempo, la risposta dinamica del trasduttore deve essere considerata. Questo problema viene comunemente risolto con un modello a parametri concentrati.

* E. O. Doebelin, D. N. Manik, Measurement Systems: Application and Design, 5th Edition, McGraw-Hill series in Mechanical Engineering., Tata McGrawHill Education, New Delhi, 2007.

APPROCCIO ALTERNATIVO

Consideriamo le similarità tra il nostro sistema e altri strumenti che lavorano in condizioni dinamiche:

LAB. OWC

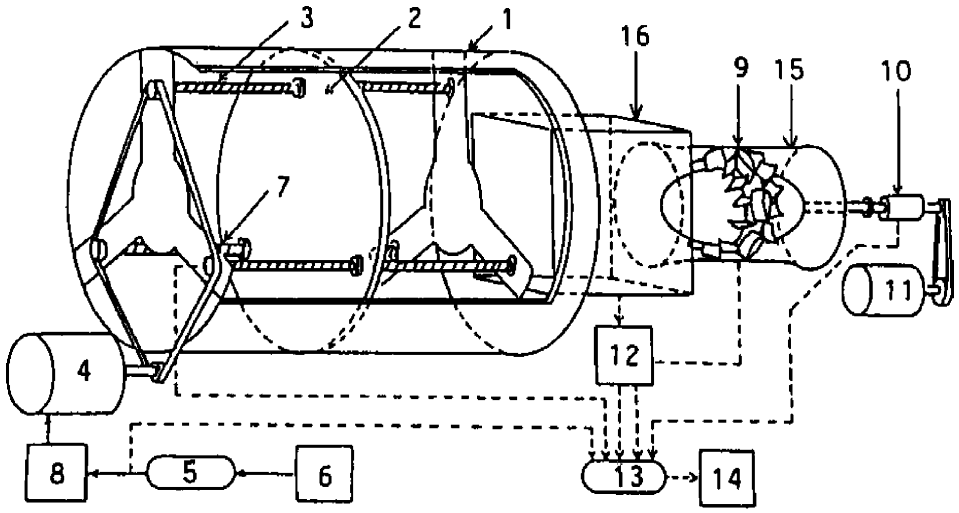

SISTEMA LINEA-CAVITA'

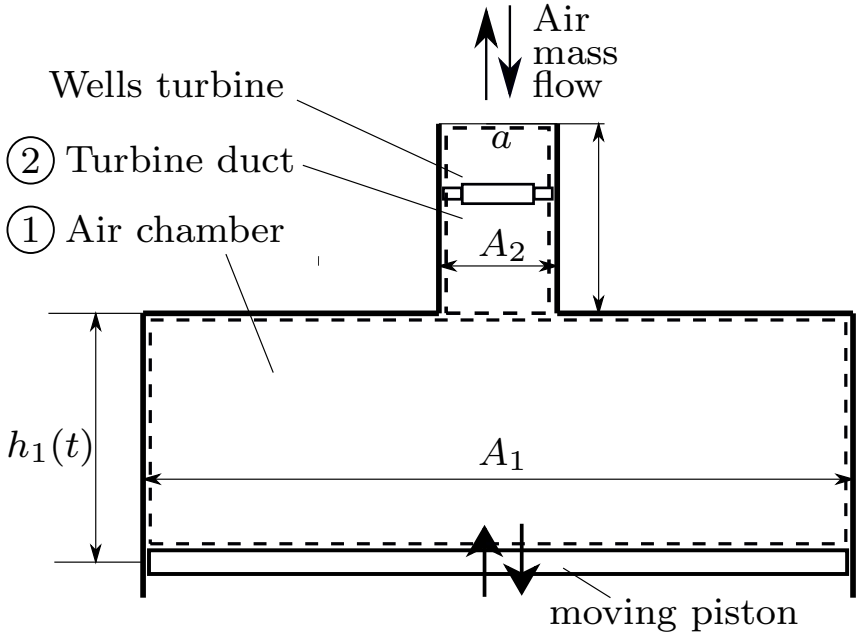

Possiamo usare lo stesso approccio per il nostro problema?

APPROCCIO ALTERNATIVO

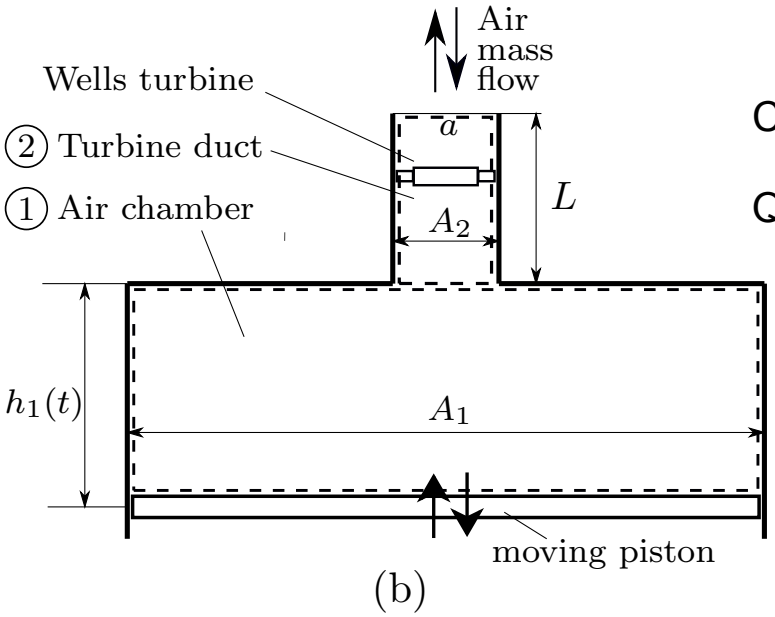

(b)

CONTINUITA' in 1:

Q. MOTO in 2:

$$\begin{cases} \dfrac{\mathrm{d}M_1}{\mathrm{d}t} = h_1 A_1 \dfrac{\mathrm{d}\rho_1}{\mathrm{d}t} + \rho_1 A_1 \dfrac{\mathrm{d}h_1}{\mathrm{d}t} = -\rho_a V_2 A_2 \\ \dfrac{\mathrm{d}(\rho_2 V_2 A_2 L)}{\mathrm{d}t} = (p_1 - p_a) A_2 + F_x \end{cases}$$

APPROCCIO ALTERNATIVO

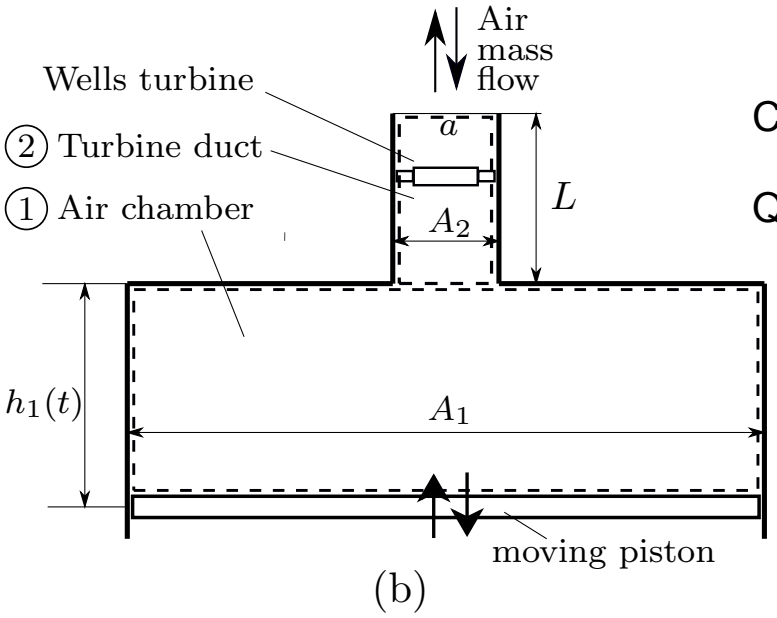

(b)

CONTINUITA' in 1:

Q. MOTO in 2:

$$\begin{cases} \dfrac{\mathrm{d}M_1}{\mathrm{d}t} = h_1 A_1 \dfrac{\mathrm{d}\rho_1}{\mathrm{d}t} + \rho_1 A_1 \dfrac{\mathrm{d}h_1}{\mathrm{d}t} = -\rho_a V_2 A_2 \\ \dfrac{\mathrm{d}(\rho_2 V_2 A_2 L)}{\mathrm{d}t} = (p_1 - p_a) A_2 + F_x \end{cases}$$

Dividiamo 1 per $(\rho_a \omega r_m A_2)$ e 2 per $(\rho_a (\omega r_m)^2 A_2)$:

$$\begin{cases} \dfrac{h_1}{r_m}\dfrac{A_1}{A_2}\dfrac{\mathrm{d}(\rho_1/\rho_a)}{\mathrm{d}(t\omega)} + \dfrac{\rho_1}{\rho_a}\dfrac{A_1}{A_2}\dfrac{\mathrm{d}(h_1/r_m)}{\mathrm{d}(t\omega)} = -\dfrac{V_2}{\omega r_m} \\ \dfrac{L}{r_m}\dfrac{\mathrm{d}(V_2/(\omega r_m))}{\mathrm{d}(t\omega)} = \dfrac{(p_1 - p_a)}{\rho_a(\omega r_m)^2} + \dfrac{F_x}{\rho_a(\omega r_m)^2 A_2} \end{cases}$$

APPROCCIO ALTERNATIVO

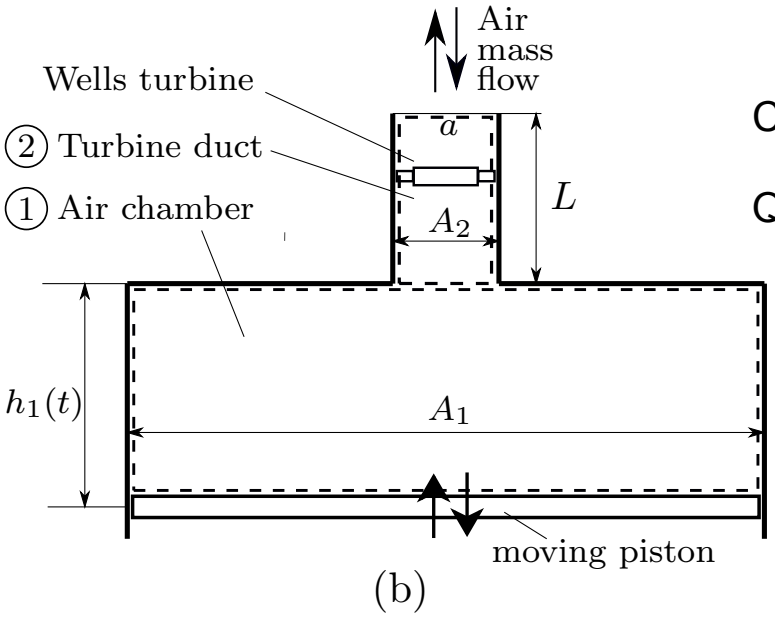

(b)

CONTINUITA' in 1:

Q. MOTO in 2:

$$\begin{cases} \dfrac{\mathrm{d}M_1}{\mathrm{d}t} = h_1 A_1 \dfrac{\mathrm{d}\rho_1}{\mathrm{d}t} + \rho_1 A_1 \dfrac{\mathrm{d}h_1}{\mathrm{d}t} = -\rho_a V_2 A_2 \\ \dfrac{\mathrm{d}(\rho_2 V_2 A_2 L)}{\mathrm{d}t} = (p_1 - p_a) A_2 + F_x \end{cases}$$

Dividiamo 1 per $(\rho_a \omega r_m A_2)$ e 2 per $(\rho_a (\omega r_m)^2 A_2)$:

PISTON-BASED FLOW COEFFICIENT

TURBINE FLOW COEFFICIENT

$$\begin{cases} \dfrac{h_1}{r_m}\dfrac{A_1}{A_2}\dfrac{\mathrm{d}(\rho_1/\rho_a)}{\mathrm{d}(t\omega)} + \dfrac{\rho_1}{\rho_a}\dfrac{A_1}{A_2}\dfrac{\mathrm{d}(h_1/r_m)}{\mathrm{d}(t\omega)} = -\dfrac{V_2}{\omega r_m} \\ \dfrac{L}{r_m}\dfrac{\mathrm{d}(V_2/(\omega r_m))}{\mathrm{d}(t\omega)} = \dfrac{(p_1 - p_a)}{\rho_a (\omega r_m)^2} + \dfrac{F_x}{\rho_a (\omega r_m)^2 A_2} \end{cases}$$

APPROCCIO ALTERNATIVO

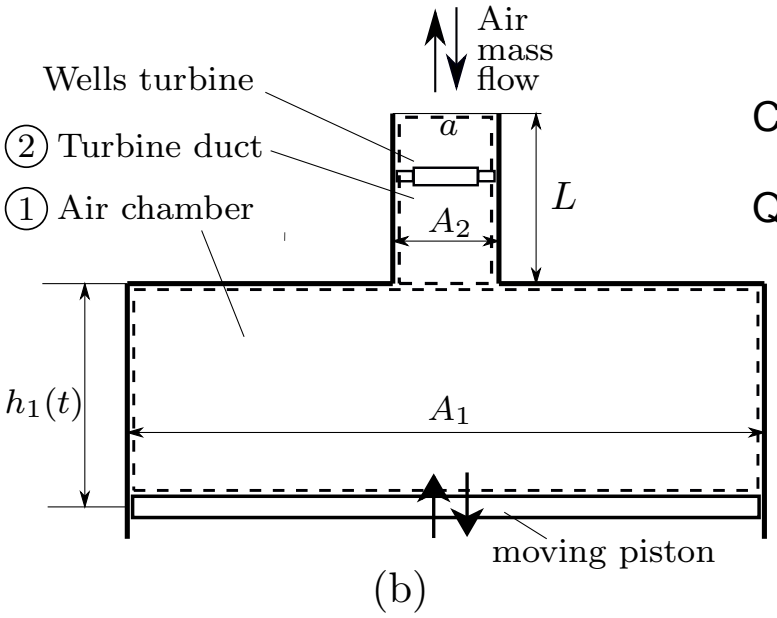

(b)

CONTINUITA' in 1:

Q. MOTO in 2:

$$\begin{cases} \dfrac{\mathrm{d}M_1}{\mathrm{d}t} = h_1 A_1 \dfrac{\mathrm{d}\rho_1}{\mathrm{d}t} + \rho_1 A_1 \dfrac{\mathrm{d}h_1}{\mathrm{d}t} = -\rho_a V_2 A_2 \\ \dfrac{\mathrm{d}(\rho_2 V_2 A_2 L)}{\mathrm{d}t} = (p_1 - p_a) A_2 + F_x \end{cases}$$

Dividiamo 1 per $(\rho_a \omega r_m A_2)$ e 2 per $(\rho_a (\omega r_m)^2 A_2)$:

PISTON-BASED FLOW COEFFICIENT

TURBINE FLOW COEFFICIENT

$$\begin{cases} \dfrac{h_1}{r_m}\dfrac{A_1}{A_2}\dfrac{\mathrm{d}(\rho_1/\rho_a)}{\mathrm{d}(t\omega)} + \dfrac{\rho_1}{\rho_a}\dfrac{A_1}{A_2}\dfrac{\mathrm{d}(h_1/r_m)}{\mathrm{d}(t\omega)} = -\dfrac{V_2}{\omega r_m} \\ \dfrac{L}{r_m}\dfrac{\mathrm{d}(V_2/(\omega r_m))}{\mathrm{d}(t\omega)} = \dfrac{(p_1 - p_a)}{\rho_a(\omega r_m)^2} + \dfrac{F_x}{\rho_a(\omega r_m)^2 A_2} \end{cases}$$

NON-DIMENSIONAL PRESSURE DROP

TURBINE AXIAL-FORCE COEFFICIENT

APPROCCIO ALTERNATIVO

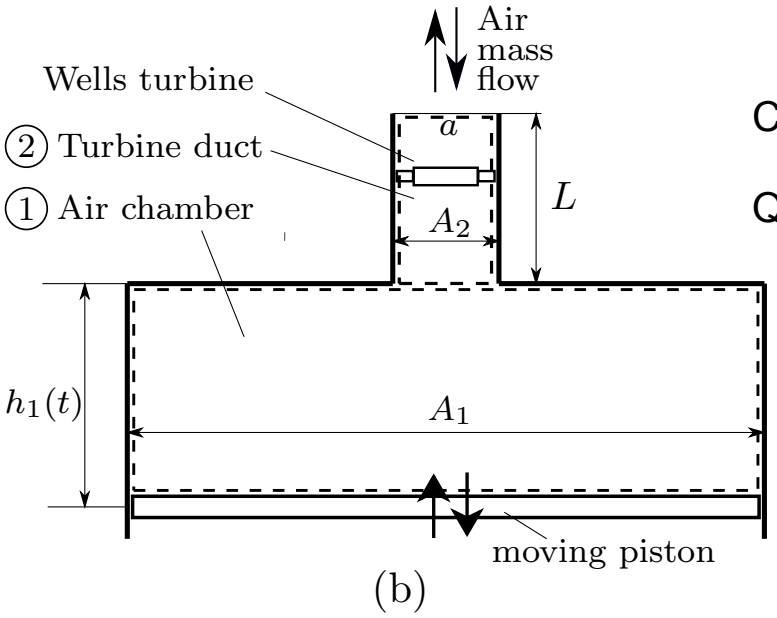

(b)

CONTINUITA' in 1:

Q. MOTO in 2:

$$\begin{cases} \dfrac{\mathrm{d}M_1}{\mathrm{d}t} = h_1 A_1 \dfrac{\mathrm{d}\rho_1}{\mathrm{d}t} + \rho_1 A_1 \dfrac{\mathrm{d}h_1}{\mathrm{d}t} = -\rho_a V_2 A_2 \\ \dfrac{\mathrm{d}(\rho_2 V_2 A_2 L)}{\mathrm{d}t} = (p_1 - p_a) A_2 + F_x \end{cases}$$

Dividiamo 1 per $(\rho_a \omega r_m A_2)$ e 2 per $(\rho_a (\omega r_m)^2 A_2)$:

PISTON-BASED FLOW COEFFICIENT

TURBINE FLOW COEFFICIENT

$$\begin{cases} \dfrac{h_1}{r_m}\dfrac{A_1}{A_2}\dfrac{\mathrm{d}(\rho_1/\rho_a)}{\mathrm{d}(t\omega)} + \dfrac{\rho_1}{\rho_a} \boxed{-\phi_P} = \boxed{-\phi_l} \\ \dfrac{L}{r_m}\dfrac{\mathrm{d}(V_2/(\omega r_m))}{\mathrm{d}(t\omega)} = \boxed{P^*} + \boxed{c_x} \end{cases}$$

NON-DIMENSIONAL PRESSURE DROP

TURBINE AXIAL-FORCE COEFFICIENT

APPROCCIO ALTERNATIVO

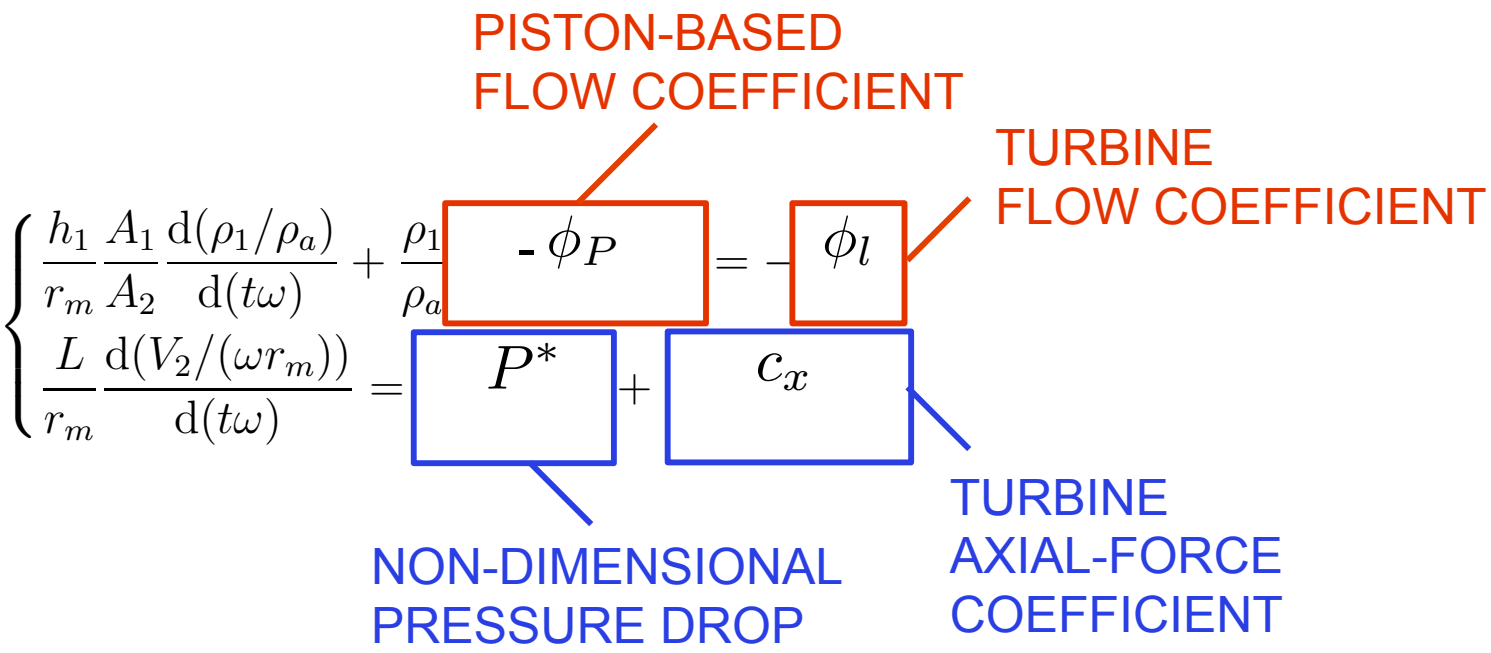

Alcune considerazioni:

1. Un ritardo tra c_x e P^* esiste, ed è proporzionale a $\frac{L}{r_m}\frac{\mathrm{d}(V_2/(\omega r_m))}{\mathrm{d}(t\omega)}$ (questo termine è **generalmente piccolo**)

2. Un ritardo tra ϕ_P e ϕ_l esiste, ed è proporzionale a $\frac{h_1}{r_m}\frac{A_1}{A_2}\frac{\mathrm{d}(\rho_1/\rho_a)}{\mathrm{d}(t\omega)}$ (questo termine è **generalmente abbastanza grande**)

APPROCCIO ALTERNATIVO

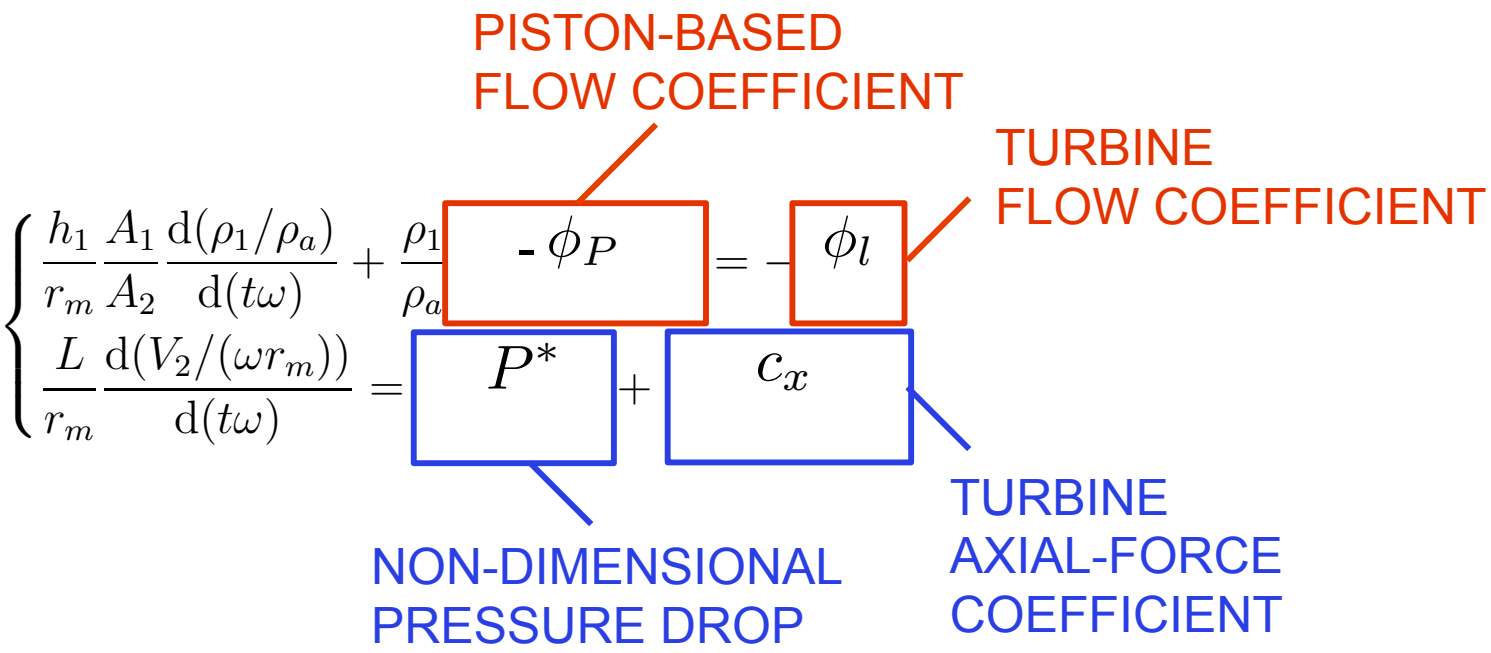

APPROCCIO NO 1. (**SOLUZIONE ANALITICA**)

1) Linearizziamo il sistema di equazioni ($c_x = c_{x,\phi}\phi_l$)

$$\frac{L}{r_m}\frac{\Omega}{\omega}\frac{\mathrm{d}^2\phi_l}{\mathrm{d}t^{*2}} + c_{x,\phi}\frac{\mathrm{d}\phi_l}{\mathrm{d}t^*} + \frac{a^2}{\gamma(\omega r_m)(h_{10}\Omega)}\frac{A_2}{A_1}\phi_l = \frac{a^2}{\gamma(\omega r_m)(h_{10}\Omega)}\frac{A_2}{A_1}\phi_p$$

2) Risolviamo analiticamente

APPROCCIO ALTERNATIVO

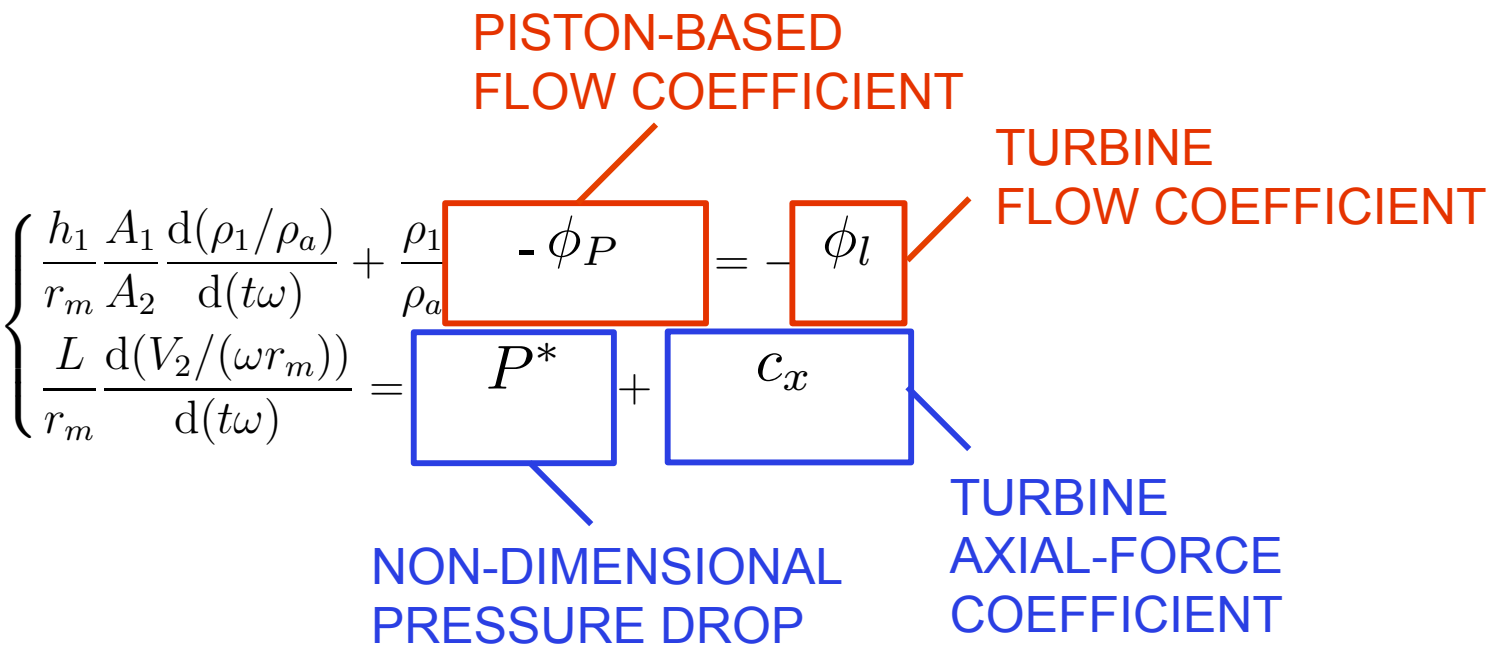

APPROCCIO NO 1. (**SOLUZIONE ANALITICA**)

1) Risolviamo numericamente (ovviamente stando attenti all'errore numerico (**VERIFICA**)

VALIDAZIONE

$\sigma = 0.57$

CURVE DI PRESTAZIONE (in funzione del coeff. di flusso basato sul pistone)

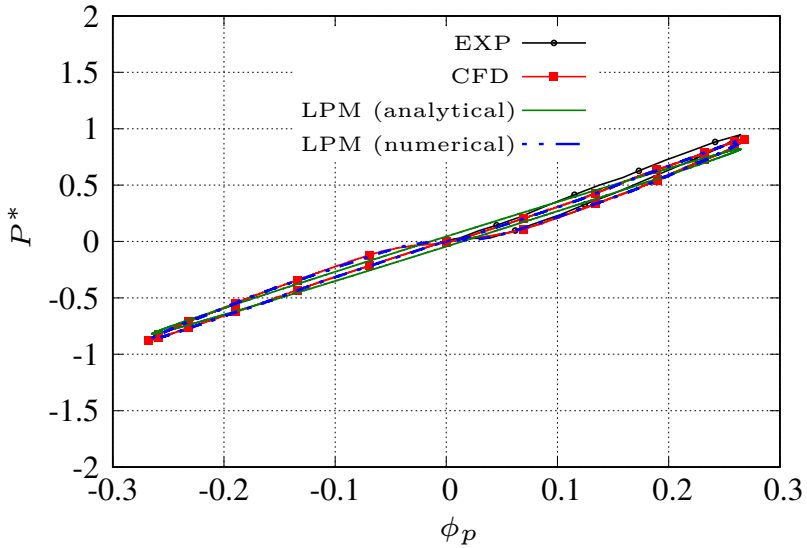

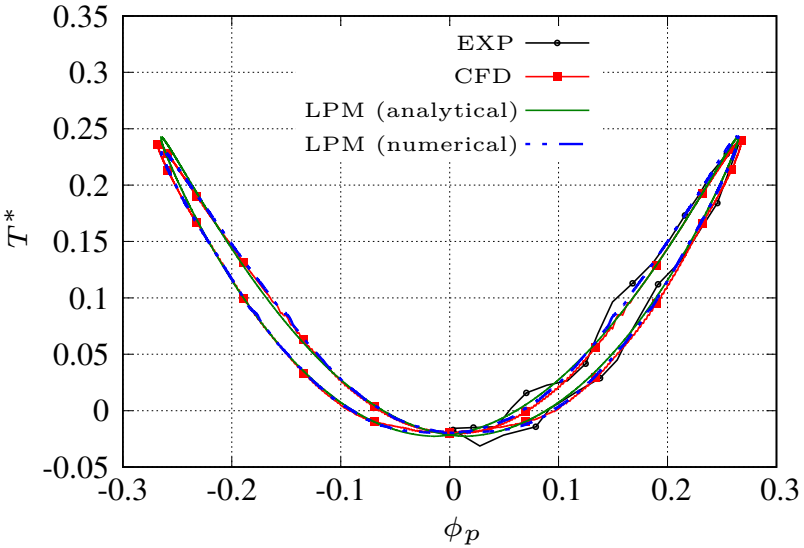

COEFFICIENTI DI FLUSSO GLOBALE E LOCALE

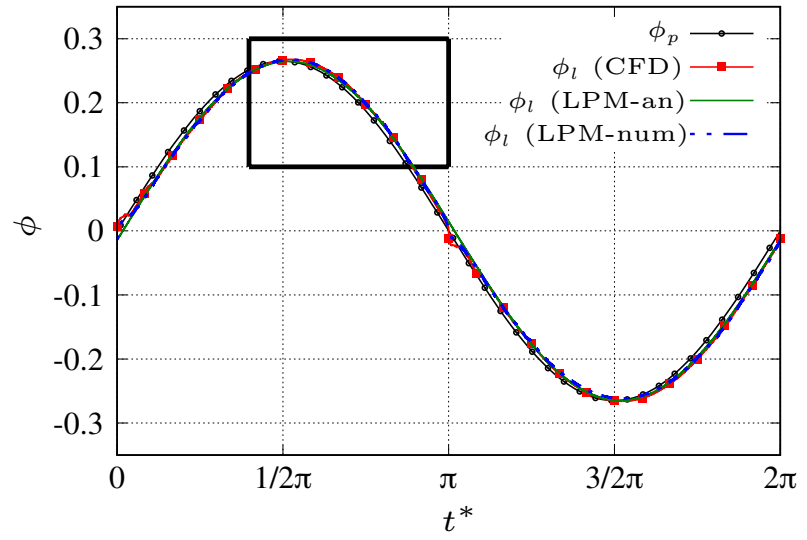

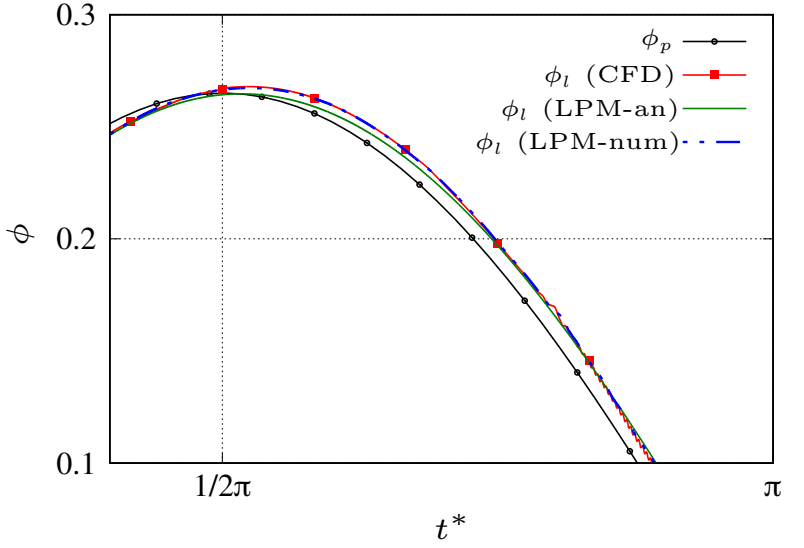

VALIDAZIONE

$\sigma = 0.67$

CURVE DI PRESTAZIONE (in funzione del coeff. di flusso basato sul pistone)

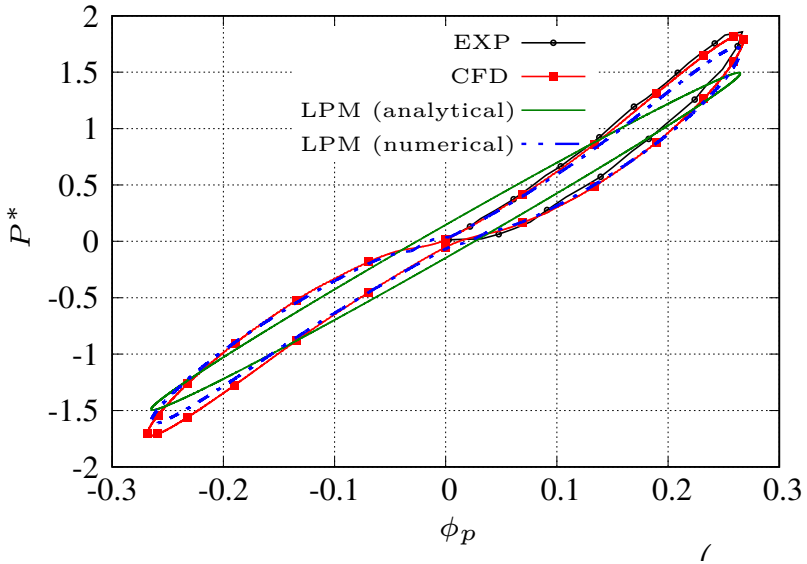

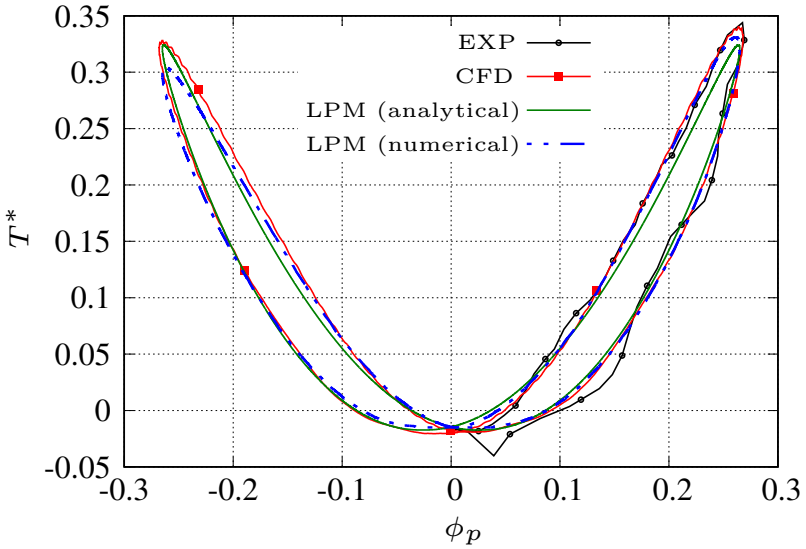

COEFFICIENTI DI FLUSSO GLOBALE E LOCALE

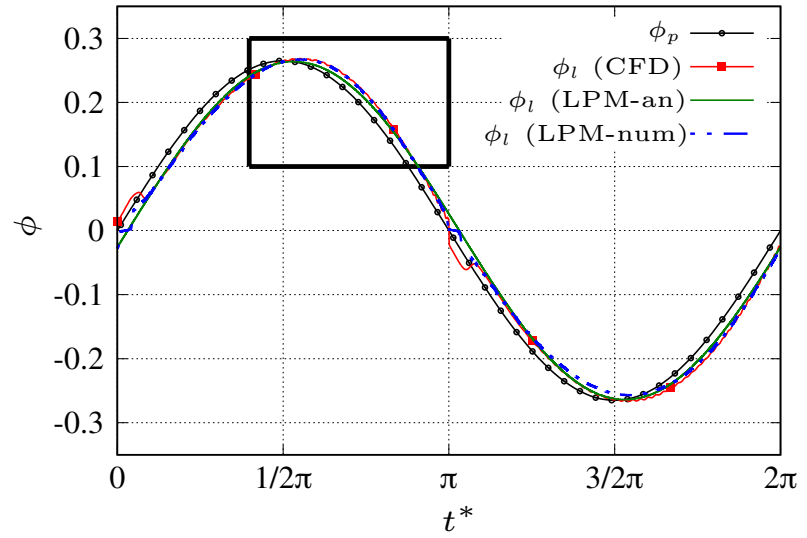

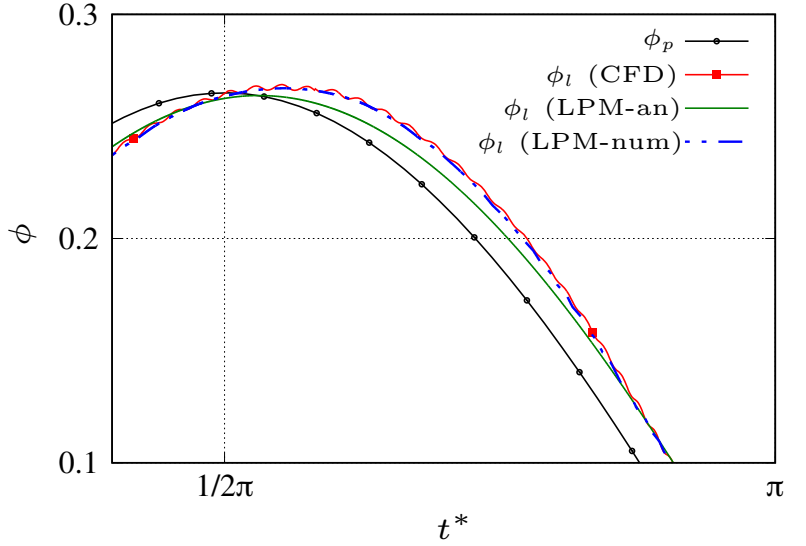

CONCLUSIONI

- Verifica e validazione sono due fasi FONDAMENTALI di una simulazione numerica (benché spesso trascurate)

- La verifica deve essere condotta tramite l'analisi dell'errore relativo al variare del passo di discretizzazione

- La verifica deve sempre precedere la validazione

- Una validazione non preceduta da verifica è inutile e rischiosa

- Non è sufficiente confrontare una soluzione numerica con dei dati sperimentali per essere sicuri di essere nel giusto

Journal of Fluids Engineering Editorial Policy
Statement on the Control of Numerical Accuracy

Although no standard method for evaluating numerical uncertainty is currently accepted by the CFD community, there are numerous methods and techniques available to the user to accomplish this task. The following is a list of guidelines, enumerating the criteria to be considered for archival publication of computational results in the *Journal of Fluids Engineering*.

1. Authors must be precise in describing the numerical method used; this includes an assessment of the formal order of accuracy of the truncation error introduced by individual terms in the governing equations, such as diffusive terms, source terms, and most importantly, the convective terms. It is not enough to state, for example, that the method is based on a "conservative finite-volume formulation," giving then a reference to a general CFD textbook.
2. The numerical method used must be at least formally second-order accurate in space (based on a Taylor series expansion) for nodes in the interior of the computational grid. The computational expense of second, third, and higher order methods are more expensive (per grid point) than first order schemes, but the computational efficiency of these higher order methods (accuracy per overall cost) is much greater. And, it has been demonstrated many times that, for first order methods, the effect of numerical diffusion on the solution accuracy is devastating.
3. Methods using a blending or switching strategy between first and second order methods (in particular, the well-known "hybrid," "power-law," and related exponential schemes) will be viewed as first-order methods, unless it can be demonstrated that their inherent numerical diffusion does not swamp or replace important modeled physical diffusion terms. A similar policy applies to methods invoking significant amounts of explicitly added artificial viscosity or diffusivity.
4. Solutions over a range of significantly different grid resolutions should be presented to demonstrate grid-independent or grid-convergent results. This criterion specifically addresses the use of improved grid resolution to systematically evaluate truncation error and accuracy. The use of error estimates based on methods such as Richardson extrapolation or those techniques now used in adaptive grid methods, may also be used to demonstrate solution accuracy.
5. Stopping criteria for iterative calculations need to be precisely explained. Estimates must be given for the corresponding convergence error.
6. In time-dependent solutions, temporal accuracy must be demonstrated so that the spurious effects of phase error are shown to be limited. In particular, it should be demonstrated that unphysical oscillations due to numerical dispersion are significantly smaller in amplitude than captured short-wavelength (in time) features of the flow.
7. Clear statements defining the methods used to implement boundary and initial conditions must be presented. Typically, the overall accuracy of a simulation is strongly affected by the implementation and order of the boundary conditions. When appropriate, particular attention should be paid to the treatment of inflow and outflow boundary conditions.
8. In the presentation of an existing algorithm or code, all pertinent references or other publications must be cited in the paper, thus aiding the reader in evaluating the code and its method without the need to redefine details of the methods in the current paper. However, basic features of the code must be outlined according to Item 1, above.
9. Comparison to appropriate analytical or well-established numerical benchmark solutions may be used to demonstrate accuracy for another class of problems. However, in general this does not demonstrate accuracy for another class of problems, especially if any adjustable parameters are involved, as in turbulence modeling.
10. Comparison with reliable experimental results is appropriate, provided experimental uncertainty is established. However, "reasonable agreement" with experimental data alone will not be enough to justify a given single-grid calculation, especially if adjustable parameters are involved.

These ten items lay down a set of criteria by which the editors and reviewers of this Journal will judge the archival quality of publications dealing with computational studies for the *Journal of Fluids Engineering*. We recognize that the effort to perform a thorough study of numerical accuracy may be great and that many practical engineering calculations will continue to be performed by first order methods, on a single fixed grid. However, such analyses would not be appropriate for presentation in this archival journal. With the gains in performance of low-end workstations, it is now reasonable to require papers on solutions by CFD to meet these fundamental criteria for archiving of a publication.

With the details of these ten criteria now presented, a shortened statement will appear as follows:

The Journal of Fluids Engineering will not consider any paper reporting the numerical solution of a fluids engineering problem that fails to address the task of systematic truncation error testing and accuracy estimation. Authors should address the following criteria for assessing numerical uncertainty.

1. The basic features of the method including formal truncation error of individual terms in the governing numerical equations must be described.
2. Methods must be at least second order accurate in space.
3. Inherent or explicit artificial viscosity (or diffusivity) must be assessed and minimized.
4. Grid independence or convergence must be established.
5. When appropriate, iterative convergence must be addressed.
6. In transient calculations, phase error must be assessed and minimized.
7. The accuracy and implementation of boundary and initial conditions must be fully explained.
8. An existing code must be fully cited in easily available references.
9. Benchmark solutions may be used for validation for a specific class of problems.
10. Reliable experimental results may be used to validate a solution.

Journal of Fluids Engineering Editorial Policy
Statement on the Control of Numerical Accuracy

Although no standard method for evaluating numerical uncertainty is currently accepted by the CFD community, there are numerous methods and techniques available to the user to accomplish this task. The following is a list of guidelines, enumerating the criteria to be considered for archival publication of computational results in the *Journal of Fluids Engineering*.

1. Authors must be precise in describing the numerical method used; this includes an assessment of the formal order of accuracy of the truncation error introduced by individual terms in the governing equations, such as diffusive terms, source terms, and most importantly, the convective terms. It is not enough to state, for example, that the method is based on a "conservative finite-volume formulation," giving then a reference to a general CFD textbook.
2. The numerical method used must be at least formally second-order accurate in space (based on a Taylor series expansion) for nodes in the interior of the computational grid. The computational expense of second, third, and higher order methods are more expensive (per grid point) than first order schemes, but the computational efficiency of these higher order methods (accuracy per overall cost) is much greater. And, it has been demonstrated many times that, for first order methods, the effect of numerical diffusion on the solution accuracy is devastating.
3. Methods using a blending or switching strategy between first and second order methods (in particular, the well-known "hybrid," "power-law," and related exponential schemes) will be viewed as first-order methods, unless it can be demonstrated that their inherent numerical diffusion does not swamp or replace important modeled physical diffusion terms. A similar policy applies to methods invoking significant amounts of explicitly added artificial viscosity or diffusivity.
4. Solutions over a range of significantly different grid resolutions should be presented to demonstrate grid-independent or grid-convergent results. This criterion specifically addresses the use of improved grid resolution to systematically evaluate truncation error and accuracy. The use of error estimates based on methods such as Richardson extrapolation or those techniques now used in adaptive grid methods, may also be used to demonstrate solution accuracy.
5. Stopping criteria for iterative calculations need to be precisely explained. Estimates must be given for the corresponding convergence error.
6. In time-dependent solutions, temporal accuracy must be demonstrated so that the spurious effects of phase error are shown to be limited. In particular, it should be demonstrated that unphysical oscillations due to numerical dispersion are significantly smaller in amplitude than captured short-wavelength (in time) features of the flow.
7. Clear statements defining the methods used to implement boundary and initial conditions must be presented. Typically, the overall accuracy of a simulation is strongly affected by the implementation and order of the boundary conditions. When appropriate, particular attention should be paid to the treatment of inflow and outflow boundary conditions.
8. In the presentation of an existing algorithm or code, all pertinent references or other publications must be cited in the paper, thus aiding the reader in evaluating the code and its method without the need to redefine details of the methods in the current paper. However, basic features of the code must be outlined according to Item 1, above.
9. Comparison to appropriate analytical or well-established numerical benchmark solutions may be used to demonstrate accuracy for another class of problems. However, in general this does not demonstrate accuracy for another class of problems, especially if any adjustable parameters are involved, as in turbulence modeling.
10. Comparison with reliable experimental results is appropriate, provided experimental uncertainty is established. However, "reasonable agreement" with experimental data alone will not be enough to justify a given single-grid calculation, especially if adjustable parameters are involved.

These ten items lay down a set of criteria by which the editors and reviewers of this Journal will judge the archival quality of publications dealing with computational studies for the *Journal of Fluids Engineering*. We recognize that the effort to perform a thorough study of numerical accuracy may be great and that many practical engineering calculations will continue to be performed by first order methods, on a single fixed grid. However, such analyses would not be appropriate for presentation in this archival journal. With the gains in performance of low-end workstations, it is now reasonable to require papers on solutions by CFD to meet these fundamental criteria for archiving of a publication.

With the details of these ten criteria now presented, a shortened statement will appear as follows:

The Journal of Fluids Engineering will not consider any paper reporting the numerical solution of a fluids engineering problem that fails to address the task of systematic truncation error testing and accuracy estimation. Authors should address the following criteria for assessing numerical uncertainty.

1. The basic features of the method including formal truncation error of individual terms in the governing numerical equations must be described.
2. Methods must be at least second order accurate in space.
3. Inherent or explicit artificial viscosity (or diffusivity) must be assessed and minimized.
4. Grid independence or convergence must be established.
5. When appropriate, iterative convergence must be addressed.
6. In transient calculations, phase error must be assessed and minimized.
7. The accuracy and implementation of boundary and initial conditions must be fully explained.
8. An existing code must be fully cited in easily available references.
9. Benchmark solutions may be used for validation for a specific class of problems.
10. Reliable experimental results may be used to validate a solution.

Journal of Fluids Engineering Editorial Policy
Statement on the Control of Numerical Accuracy

4. Solutions over a range of significantly different grid resolutions should be presented to demonstrate grid-independent or grid-convergent results. This criterion specifically addresses the use of improved grid resolution to systematically evaluate truncation error and accuracy. The use of error estimates based on methods such as Richardson extrapolation or those techniques now used in adaptive grid methods, may also be used to demonstrate solution accuracy.

6. In time-dependent solutions, temporal accuracy must be demonstrated so that the spurious effects of phase error are shown to be limited. In particular, it should be demonstrated that unphysical oscillations due to numerical dispersion are significantly smaller in amplitude than captured short-wavelength (in time) features of the flow.

10. Comparison with reliable experimental results is appropriate, provided experimental uncertainty is established. However, "reasonable agreement" with experimental data alone will not be enough to justify a given single-grid calculation, especially if adjustable parameters are involved.

Some recent articles:

[1] T. Ghisu, P. Puddu, and F. Cambuli. Numerical analysis of a wells turbine at different non-dimensional piston frequencies. *Journal of Thermal Science*, 24(6):535–543, 2015, doi:10.1007/s11630-015-0819-6.

[2] T. Ghisu, P. Puddu, and F. Cambuli. Physical explanation of the hysteresis in Wells turbines: A critical reconsideration. *Journal of Fluids Engineering, Transactions of the ASME*, 138(11), 2016, doi:10.1115/1.4033320.

[3] T. Ghisu, P. Puddu, and F. Cambuli. A detailed analysis of the unsteady flow within a Wells turbine. *Proceedings of the Institution of Mechanical Engineers, Part A: Journal of Power and Energy*, 231(3):197–214, 2017, doi:10.1177/0957650917691640.

[4] T. Ghisu, P. Puddu, F. Cambuli, N. Mandas, P. Seshadri, and G.T. Parks. Discussion on "Performance analysis of Wells turbine blades using the entropy generation minimization method" by Shehata, A. S., Saqr, K. M., Xiao, Q., Shahadeh, M. F. and Day, A. *Renewable Energy*, 118:386–392, 2018, doi:10.1016/j.renene.2017.10.107.

PHASE DELAY AND BODE DIAGRAMS

A LUMPED PARAMETER MODEL APPROACH

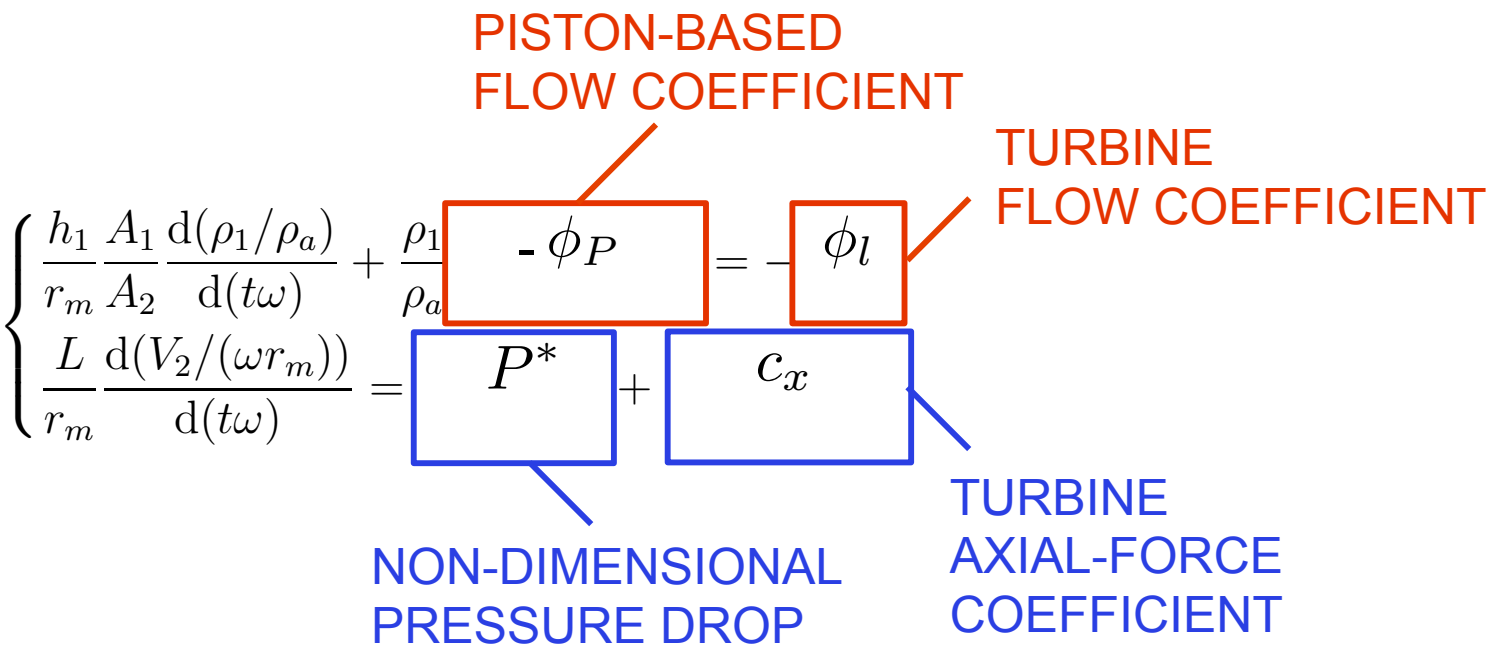

$$\underbrace{\frac{L}{r_m}\frac{\Omega}{\omega}}_{A}\frac{\mathrm{d}^2\phi_l}{\mathrm{d}t^{*2}} + \underbrace{c_{x,\phi}}_{B}\frac{\mathrm{d}\phi_l}{\mathrm{d}t^*} + \underbrace{\frac{a^2}{\gamma(\omega r_m)(h_{10}\Omega)}\frac{A_2}{A_1}}_{C}\phi_l = \underbrace{\frac{a^2}{\gamma(\omega r_m)(h_{10}\Omega)}\frac{A_2}{A_1}}_{D}\phi_p$$

A LUMPED PARAMETER MODEL APPROACH

I can see the solution in terms of the transfer function

$$G\left(\frac{\Omega}{\Omega_n}\right) = \frac{\phi_l}{\phi_p} = \frac{D}{-A + Bj + C} = \frac{\frac{D}{C}}{-\frac{A}{C} + \frac{B}{C}j + 1} = \frac{\frac{D}{C}}{-\left(\frac{\Omega}{\Omega_n}\right)^2 + 1 + 2\zeta\left(\frac{\Omega}{\Omega_n}\right)j}$$

$$\phi_p = \phi_{p0}\, e^{jt^*} \qquad\qquad \phi_l = \phi_{l0}\, e^{jt^* + \xi}$$

MODULE:

$$|\phi_l| = |\phi_p| \left|G\left(\frac{\Omega}{\Omega_n}\right)\right| = |\phi_p| \frac{D}{\sqrt{(C-A)^2 + B^2}} = \frac{1}{\left(\frac{\gamma h_{10} L}{a^2}\frac{A_1}{A_2} + 1\right)^2 + \frac{\gamma^2 h_{10}^2 (\omega r_m)^2}{a^4}\left(\frac{A_1}{A_2}\right)^2 c_{x,\phi}^2}$$

PHASE:

$$\xi = \tan^{-1}\left(\frac{-B}{C-A}\right) = \tan^{-1}\left(\frac{c_{x,\phi}}{\frac{L}{r_m}\frac{\Omega}{\omega} - \frac{a^2}{\gamma(\omega r_m)(h_{10}\Omega)}\frac{A_2}{A_1}}\right)$$

Table 1: Geometrical and operating data for Setoguchi's experiments*

chamber diameter [m]	1.4
rotor tip diameter [mm]	300
rotor hub diameter [mm]	210
tip clearance [mm]	1
chord length c [mm]	90
sweep ratio [-]	0.417
number of blades [-]	6
blade profile	NACA0020
solidity at tip radius σ [-]	0.57
rotational speed [rpm]	2500
operating frequency f [s^{-1}]	1/6
Reynolds number Re [-]	2×10^5
Mach number M [-]	0.1
turbine non-dimensional frequency k [-]	0.0014

*T. Setoguchi, M. Takao, K. Kaneko, Hysteresis on Wells turbine characteristics in reciprocating flow, International Journal of Rotating Machinery 4 (1) (1998) 17–24.

A LUMPED PARAMETER MODEL APPROACH

ND PERFORMANCE PARAMETERS

$\sigma = 0.57$

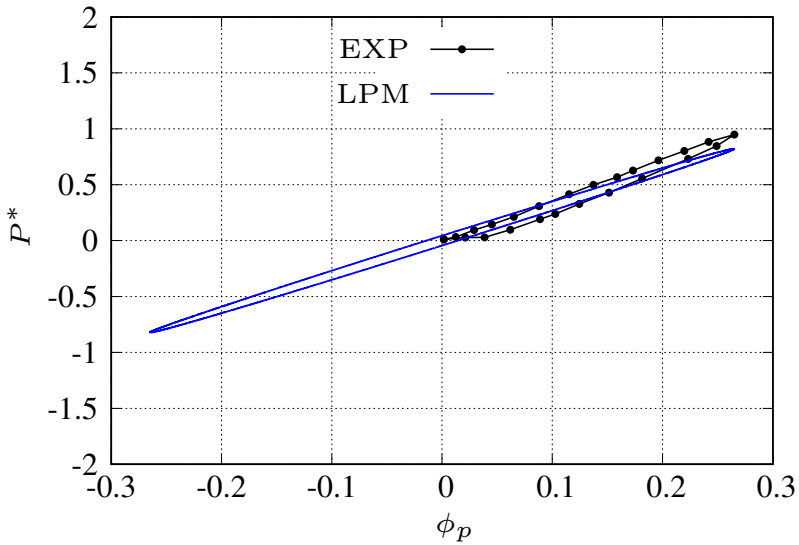

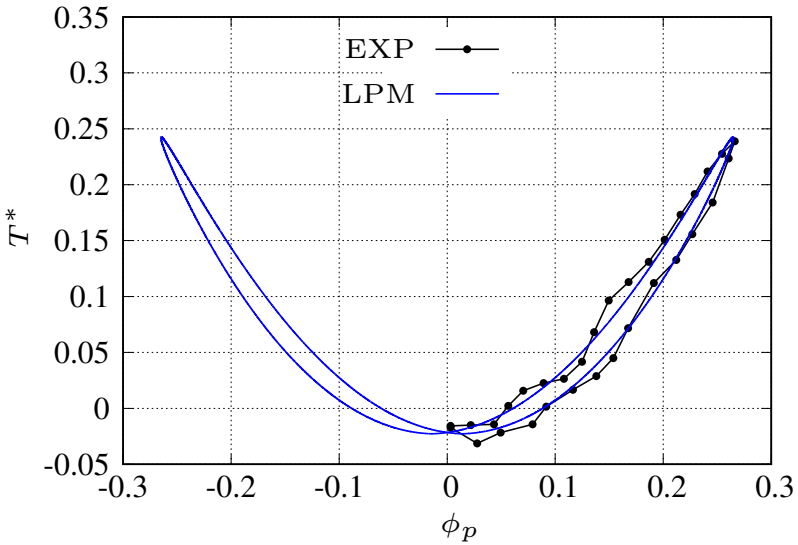

$\sigma = 0.67$

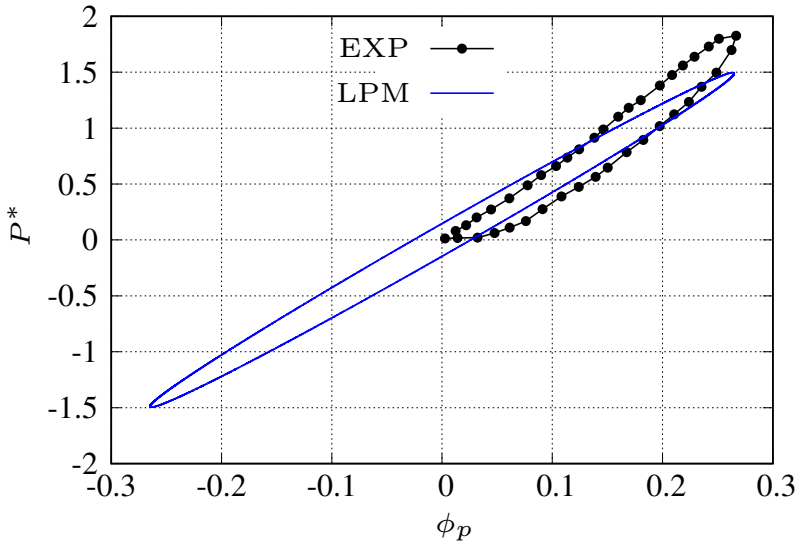

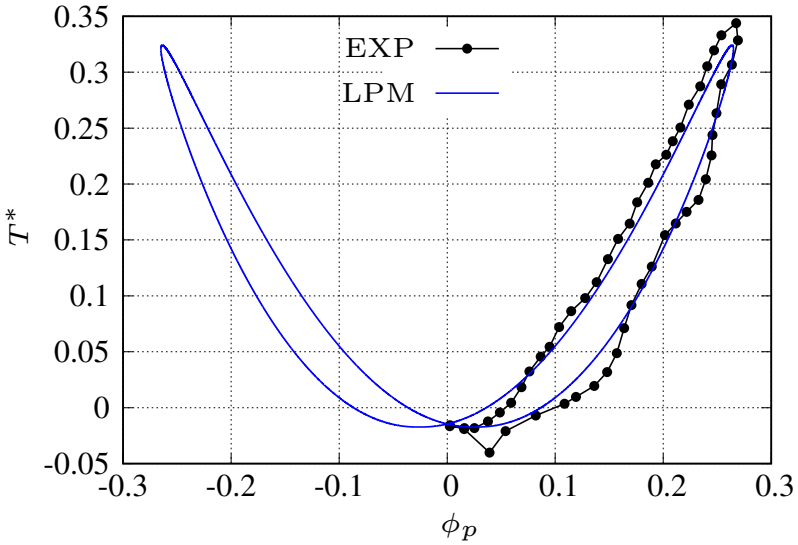

A LUMPED PARAMETER MODEL APPROACH

TIME HISTORIES

$\sigma = 0.57$

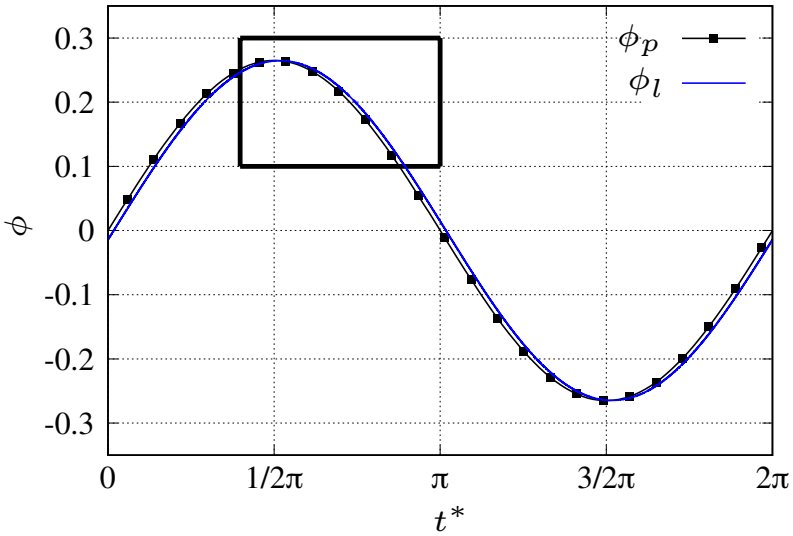

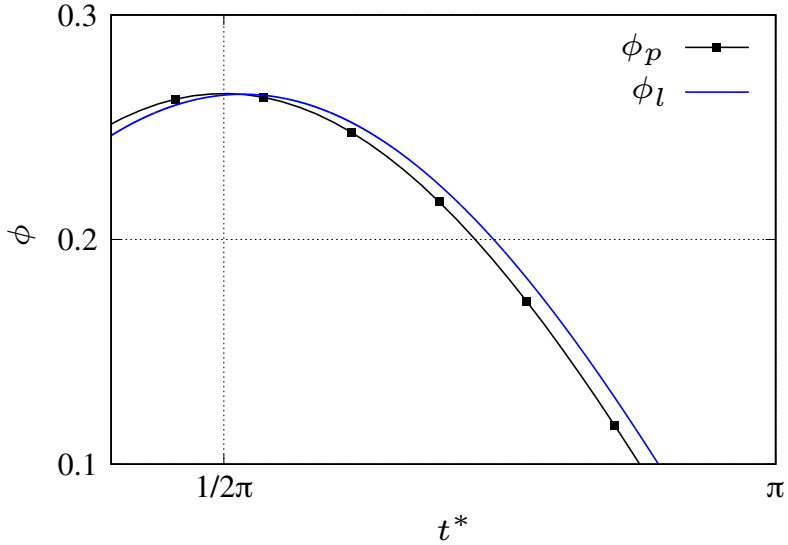

$\sigma = 0.67$

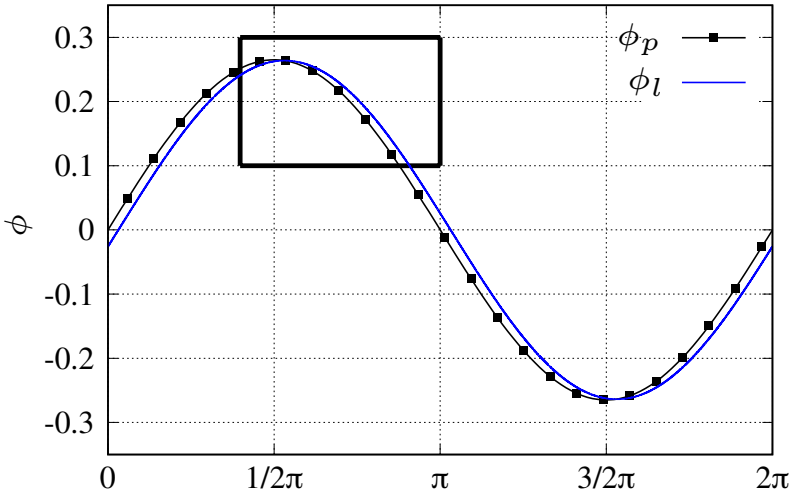

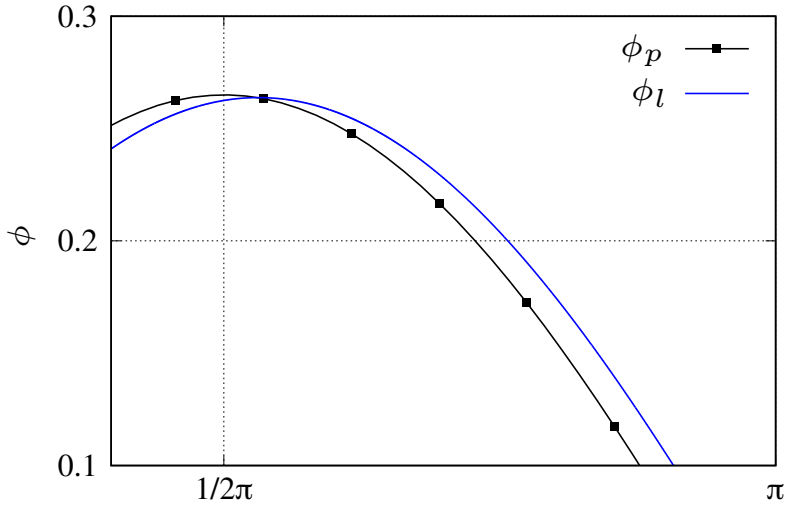

A LUMPED PARAMETER MODEL APPROACH

I can analyse the solution in terms of the BODE DIAGRAMS of the system

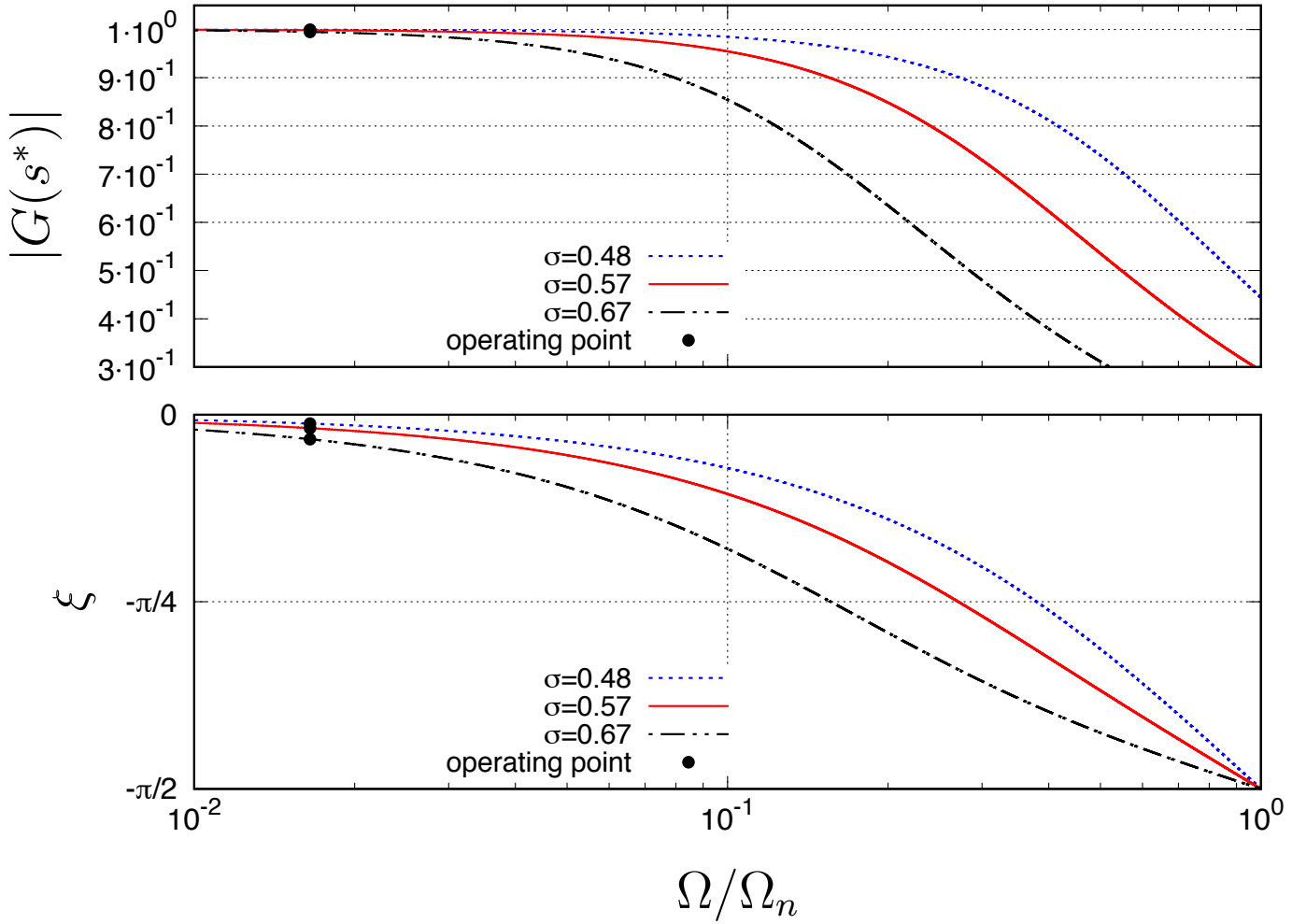

AIRFOIL PITCHING AND PLUNGING (true hysteresis)

RAPIDLY OSCILLATING AIRFOILS

PLUNGING

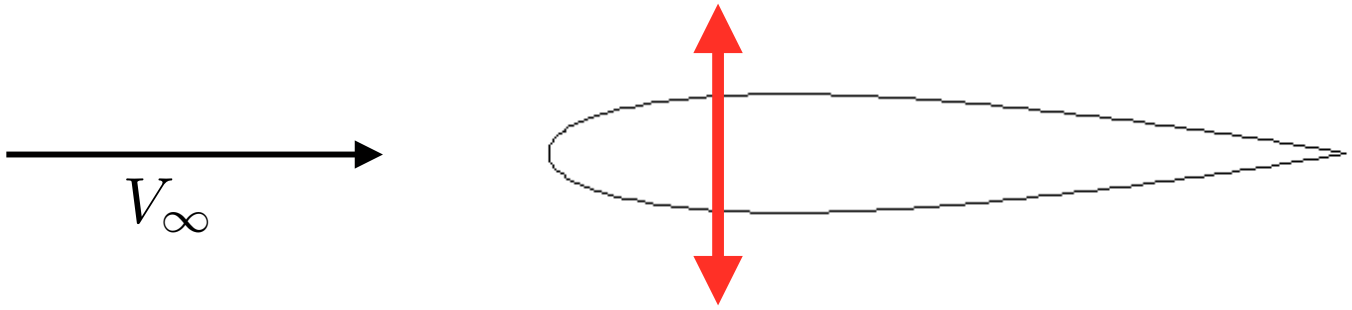

PITCHING

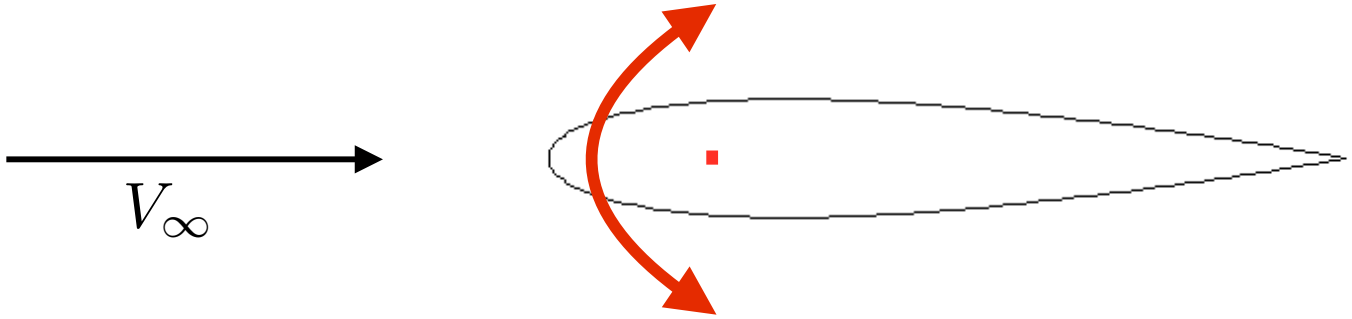

RAPIDLY OSCILLATING AIRFOILS

Hysteresis in oscillating airfoils has been studied for decades.

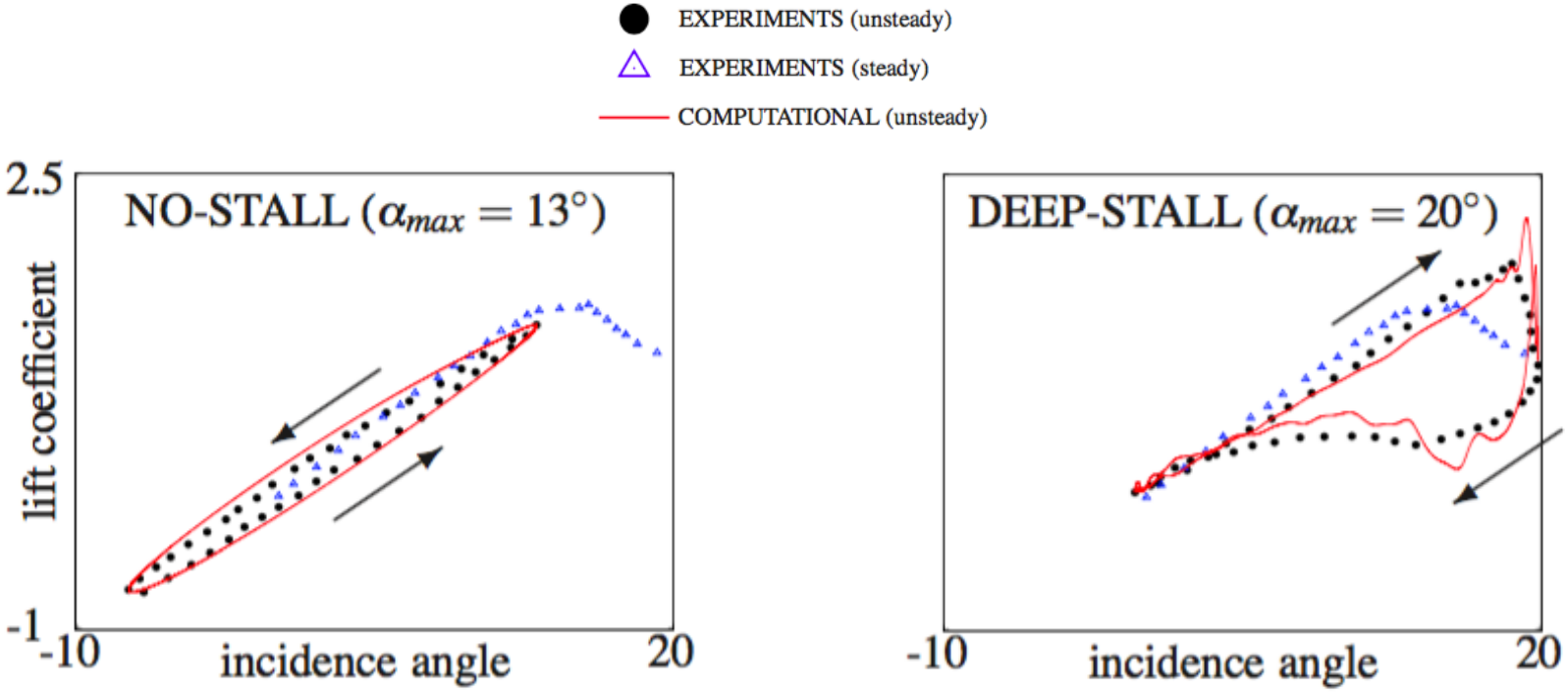

NON-DIMENSIONAL FREQUENCY $\overline{f} = \frac{\omega c}{2V_\infty} = 1E-1$

IN WELLS TURBINES $\overline{f} < 1E-3$

RAPIDLY OSCILLATING AIRFOILS

What happens at lower non-dimensional frequencies?

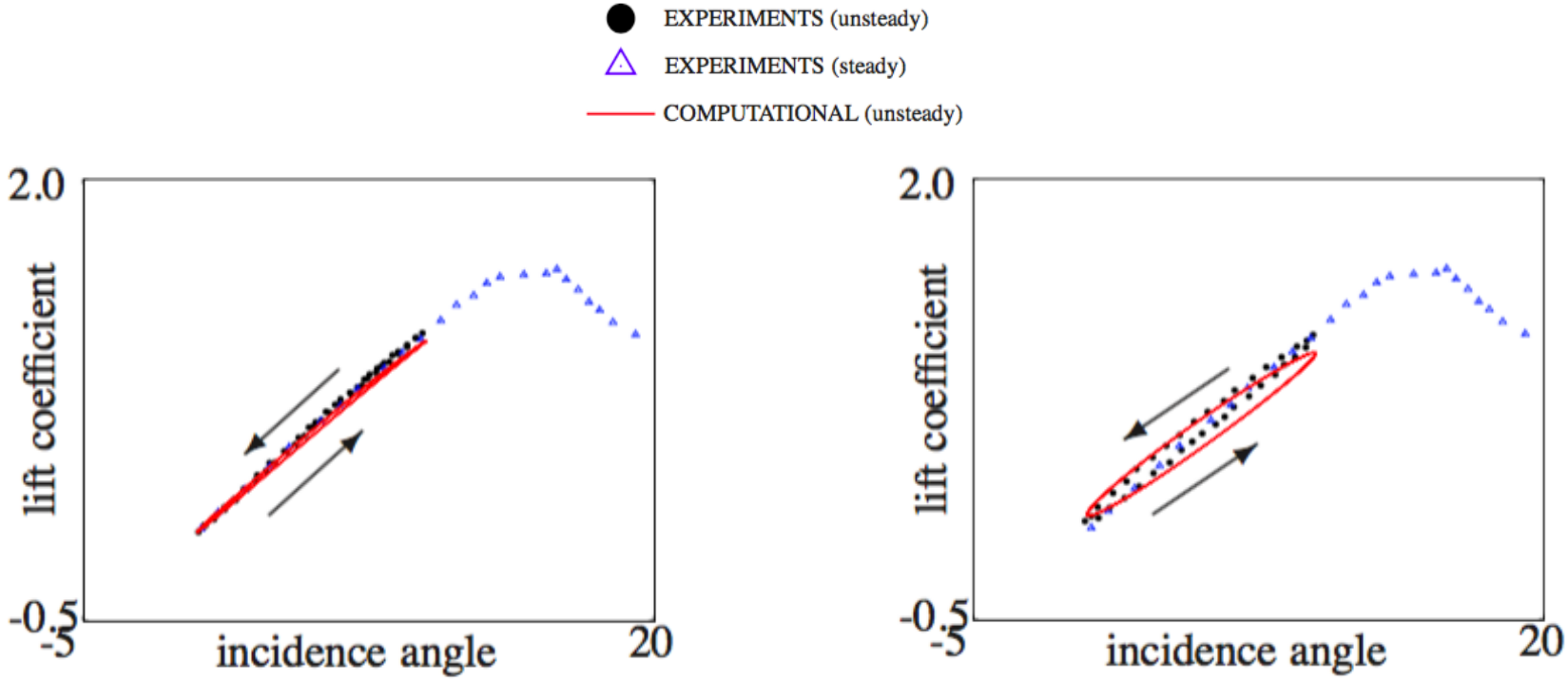

$\overline{f} = 1E-2$ $\overline{f} = 1E-1$

NO STALL

RAPIDLY OSCILLATING AIRFOILS

Hysteresis in oscillating airfoils has been studied for decades.

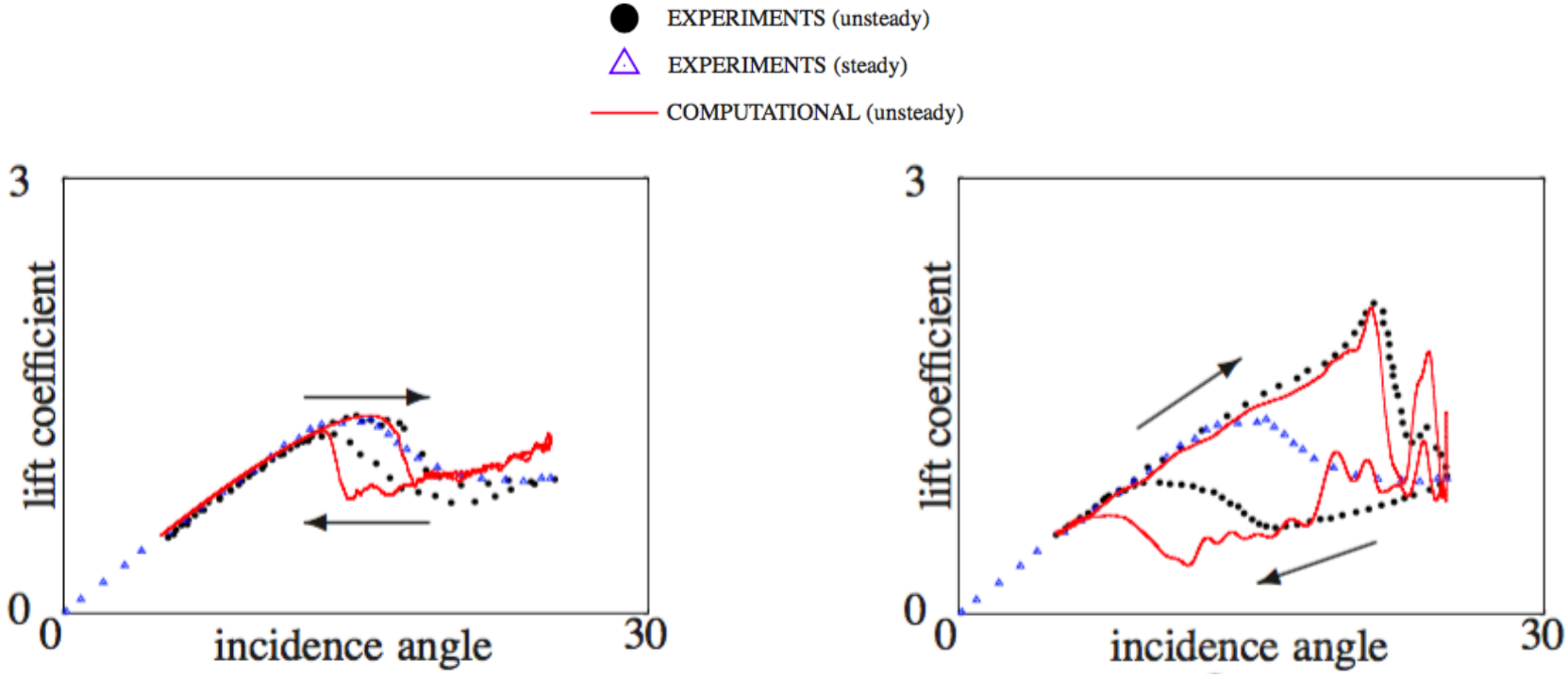

$\overline{f} = 4E - 3$

$\overline{f} = 5E - 2$

STALL

EXPERIMENTAL RESULTS

UNICA SETUP

Experimental setup

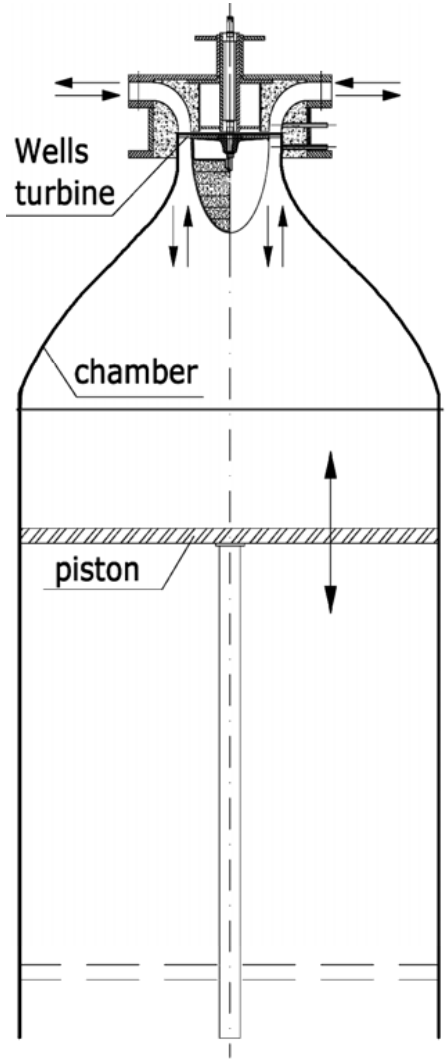

HYSTERESIS IN WELLS TURBINE

EXPERIMENTAL

PISTON-BASED

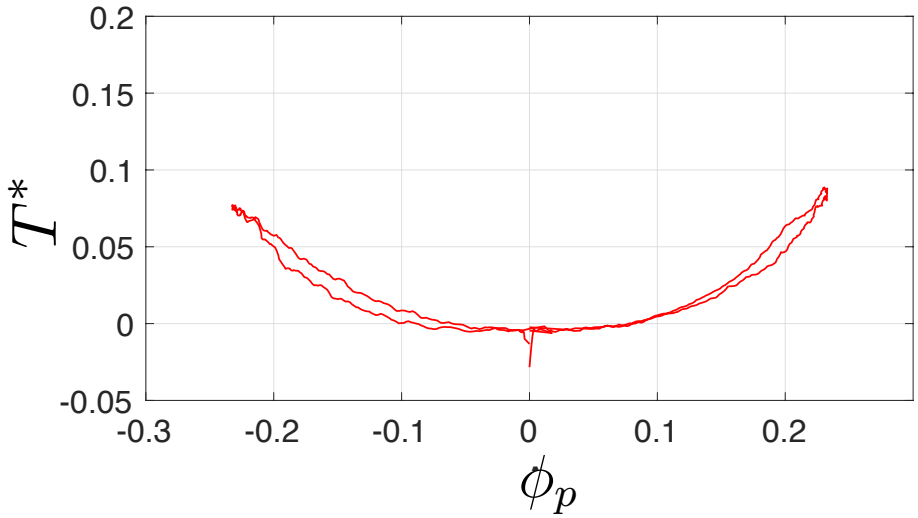

LOCAL-BASED

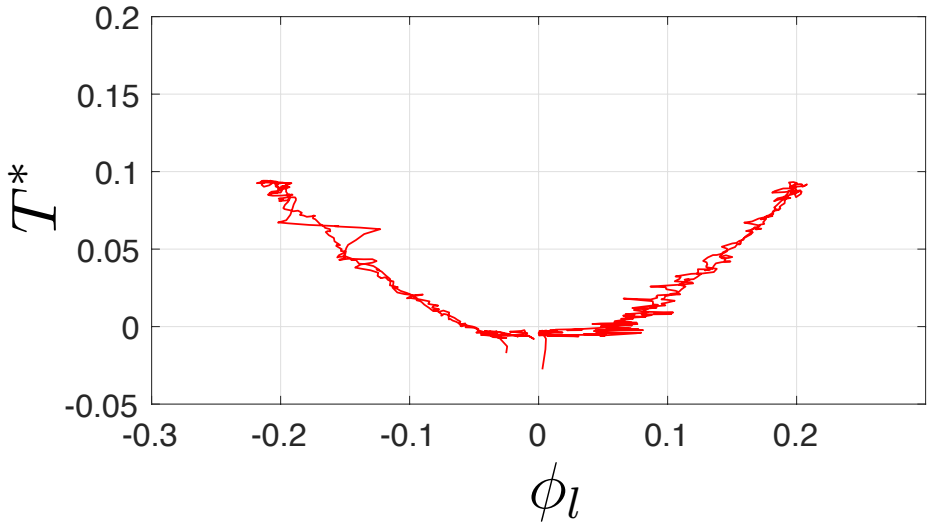

M. Paderi and P. Puddu. Experimental investigation in a Wells turbine under bi-directional flow. *Renewable Energy*, 57:570–576, 2013, doi:10.1016/j.renene.2013.02.016.

HYSTERESIS IN WELLS TURBINE

NUMERICAL

PISTON-BASED

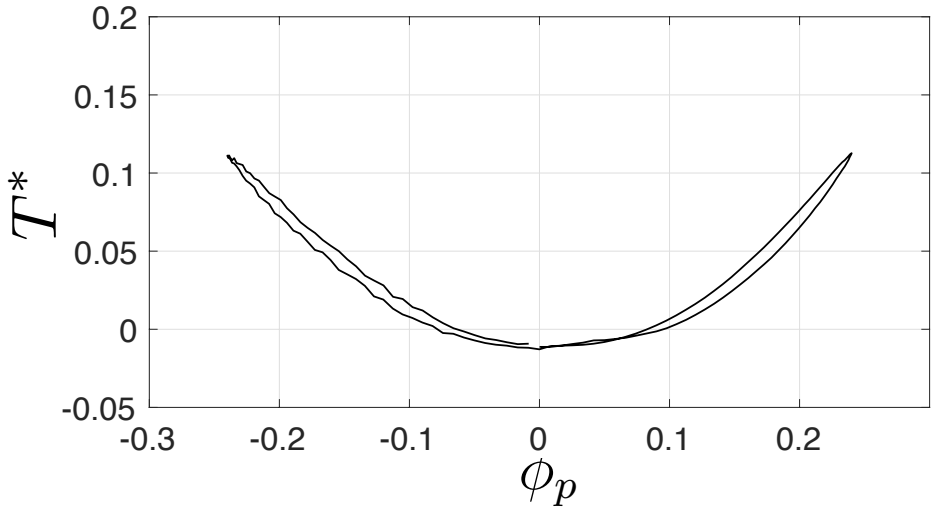

LOCAL-BASED

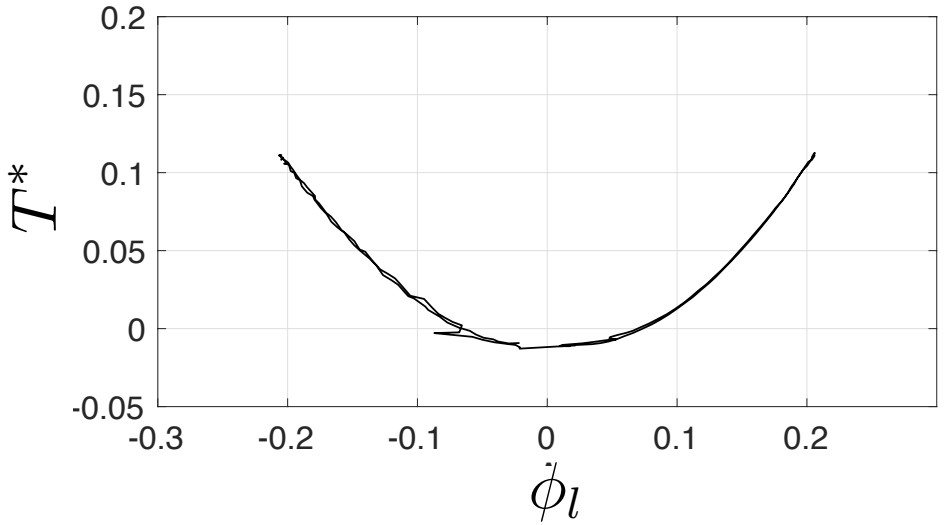

T. Ghisu, P. Puddu, and F. Cambuli. A detailed analysis of the unsteady flow within a Wells turbine. *Proceedings of the Institution of Mechanical Engineers, Part A: Journal of Power and Energy*, 231(3):197–214, 2017, doi:10.1177/0957650917691640.

HYSTERESIS IN WELLS TURBINE

EXPERIMENTAL

PISTON-BASED

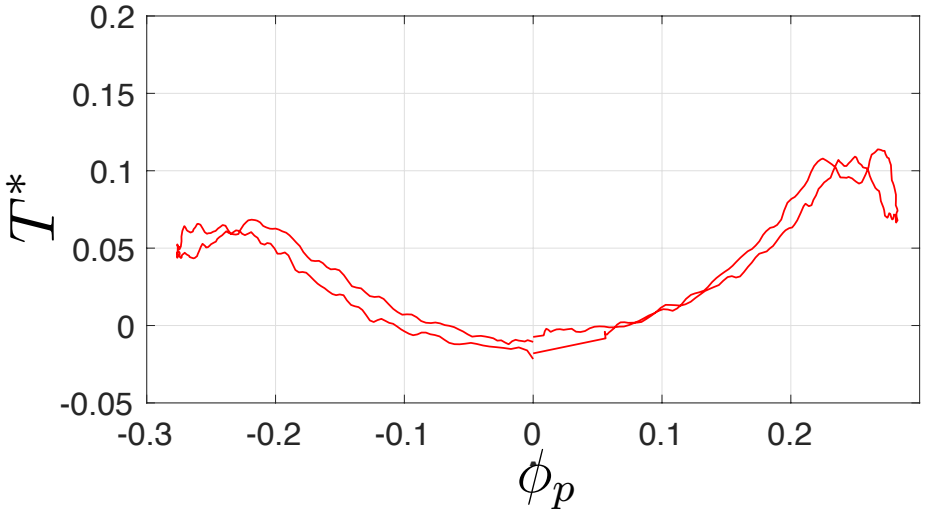

LOCAL-BASED

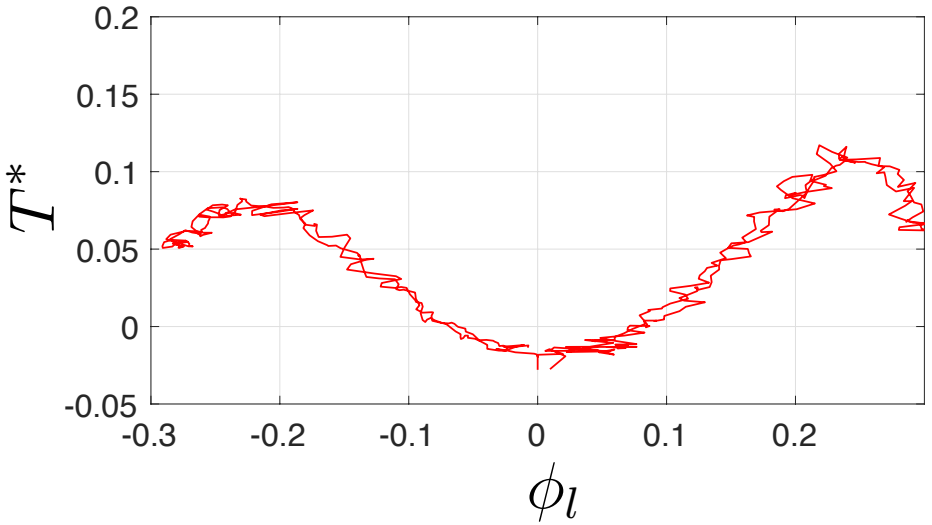

M. Paderi and P. Puddu. Experimental investigation in a Wells turbine under bi-directional flow. *Renewable Energy*, 57:570–576, 2013, doi:10.1016/j.renene.2013.02.016.

HYSTERESIS IN WELLS TURBINE

NUMERICAL

PISTON-BASED

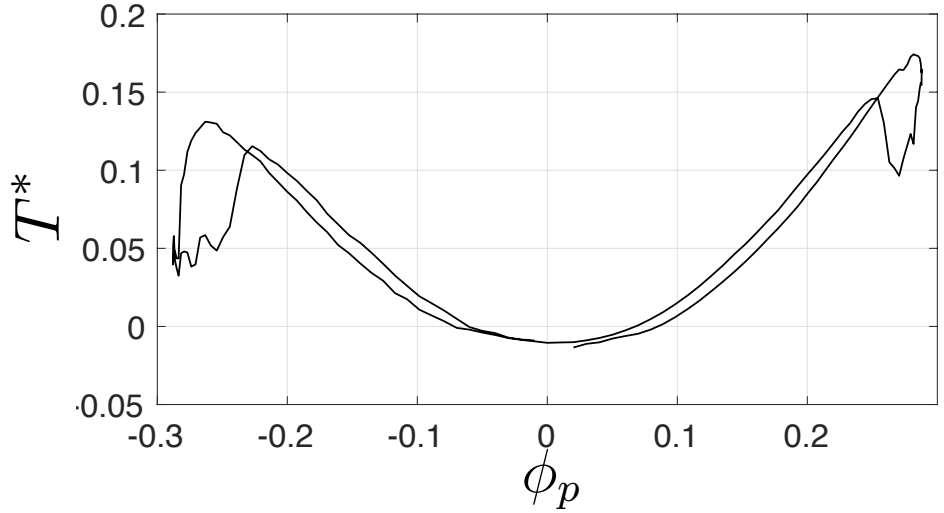

LOCAL-BASED

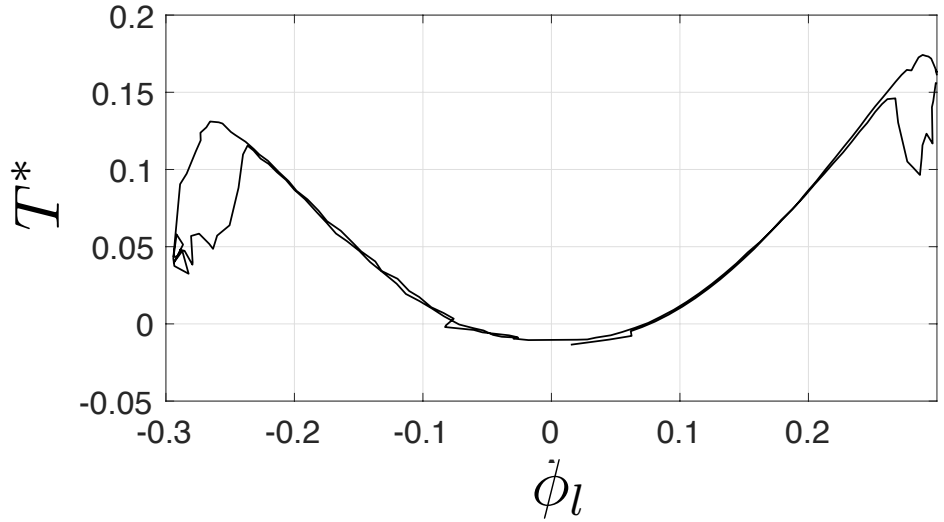

T. Ghisu, P. Puddu, and F. Cambuli. A detailed analysis of the unsteady flow within a Wells turbine. *Proceedings of the Institution of Mechanical Engineers, Part A: Journal of Power and Energy*, 231(3):197–214, 2017, doi:10.1177/0957650917691640.

NUMERICAL VERIFICATION

SETOGUCHI'S NUMERICAL EXPERIMENT

Where is the difference between their and our results?

$$\Delta t_1 > \Delta t_2 > \Delta t_3 > \Delta t_4 > \Delta t_5$$

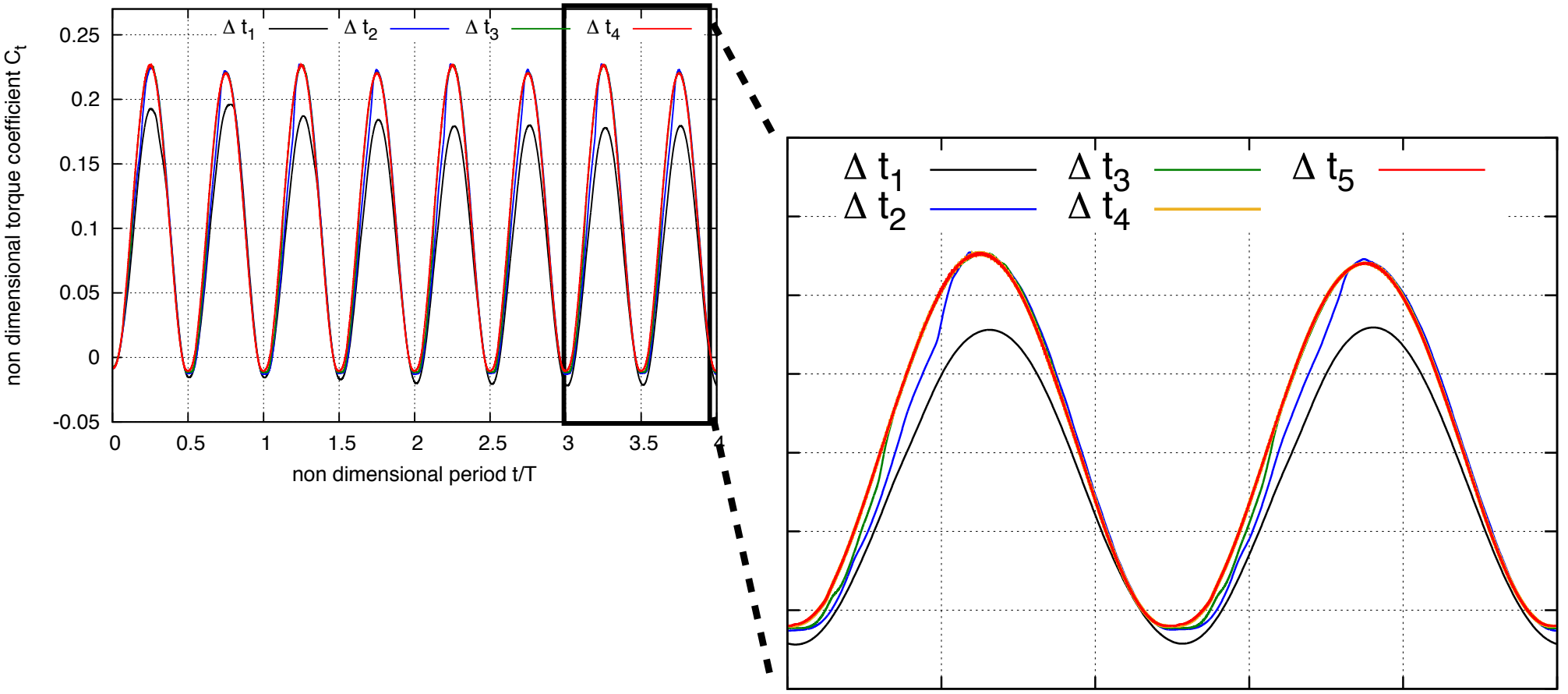

SETOGUCHI'S NUMERICAL EXPERIMENT

Where is the difference between their and our results?

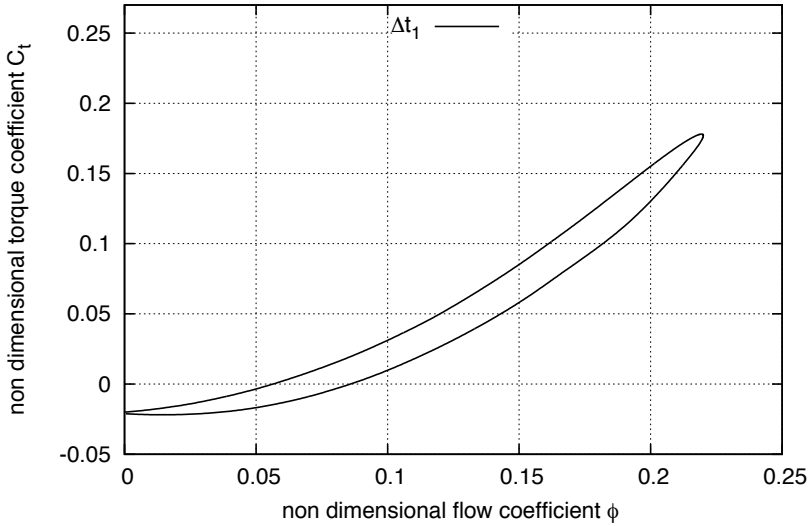

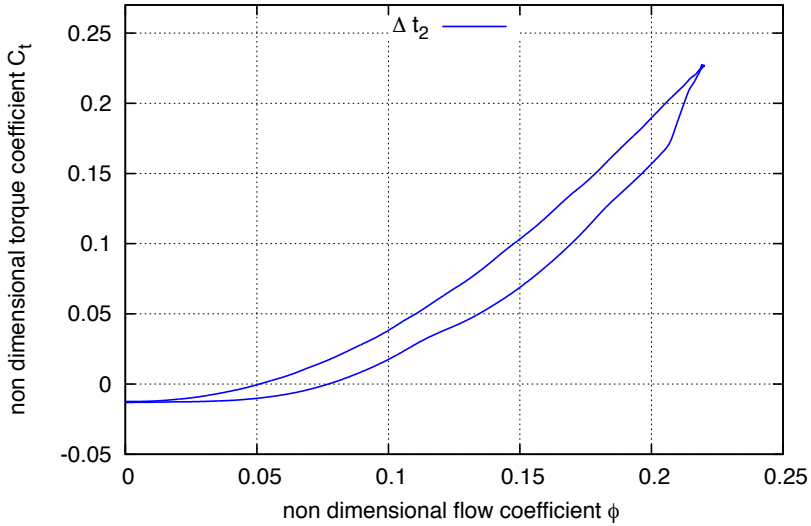

Figure 4

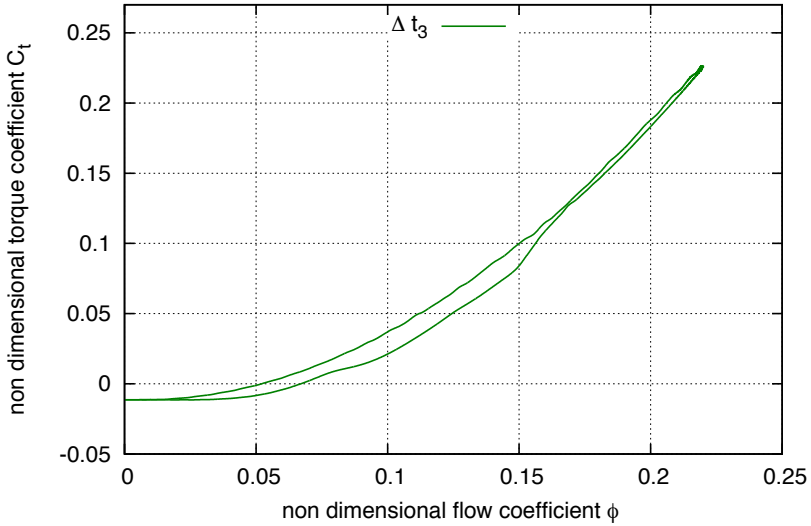

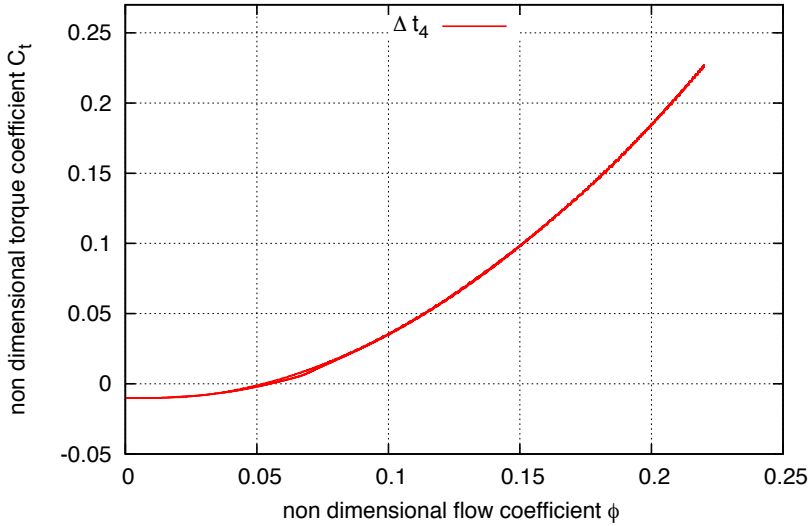

RAPIDLY OSCILLATING AIRFOILS

Hysteresis in oscillating airfoils has been studied for decades.

PLUNGING

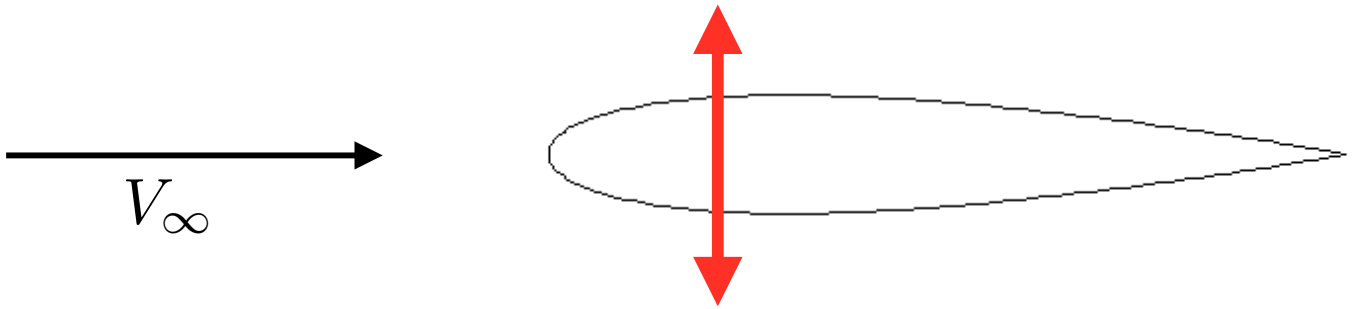

PITCHING

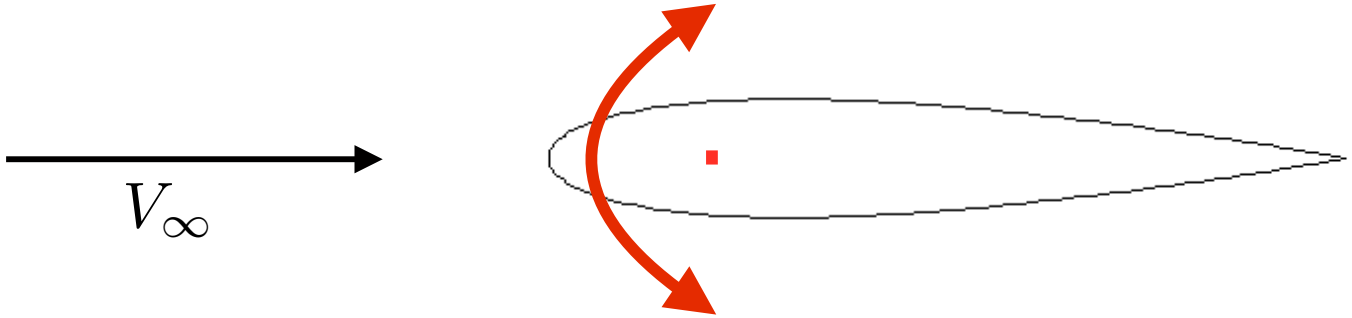

RAPIDLY OSCILLATING AIRFOILS

Hysteresis in oscillating airfoils has been studied for decades.

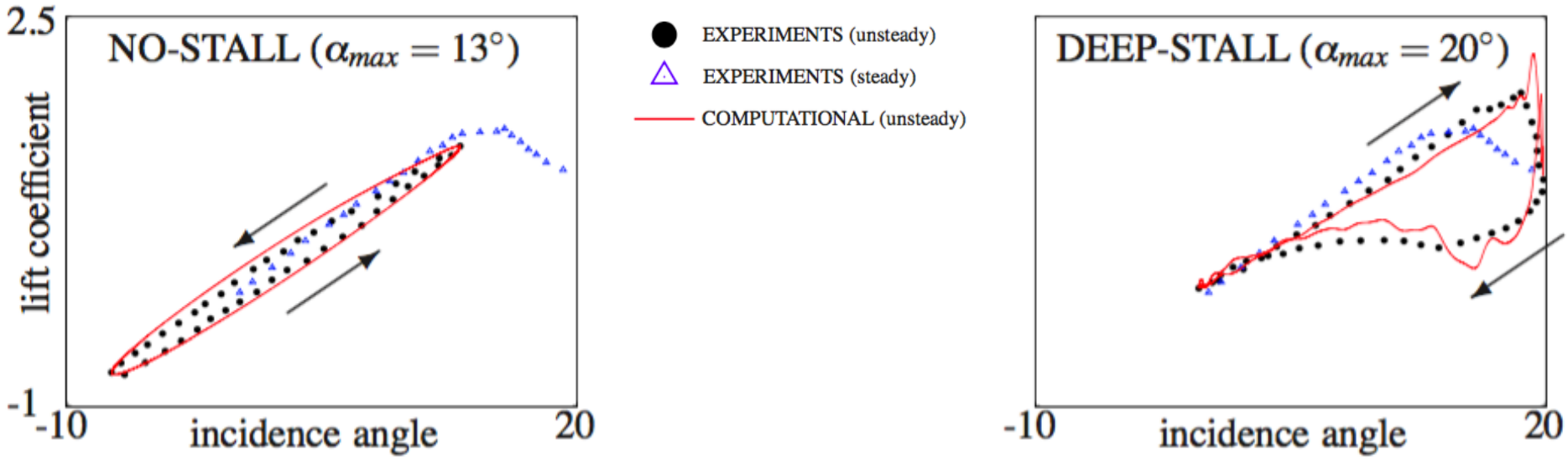

NON-DIMENSIONAL FREQUENCY $$k = \frac{\Omega c}{2U_\infty} = 1E-1$$

IN WELLS TURBINES $$k < 1E-3$$

In oscillating airfoils, no hysteresis is produced for $k < 1E-2$

SETOGUCHI'S NUMERICAL EXPERIMENT

The explanation has been derived with a CFD analysis that was able to capture the "right" trends for blade forces.

EXPERIMENT

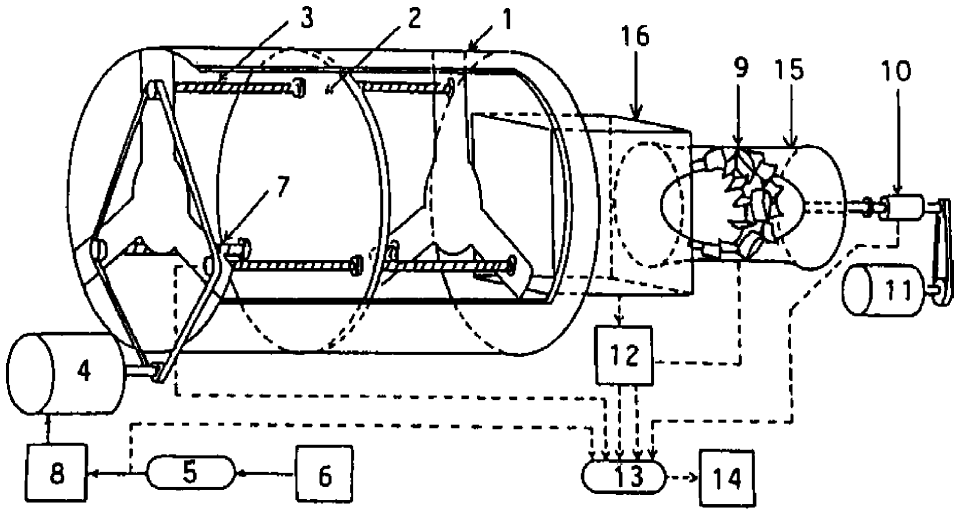

CFD

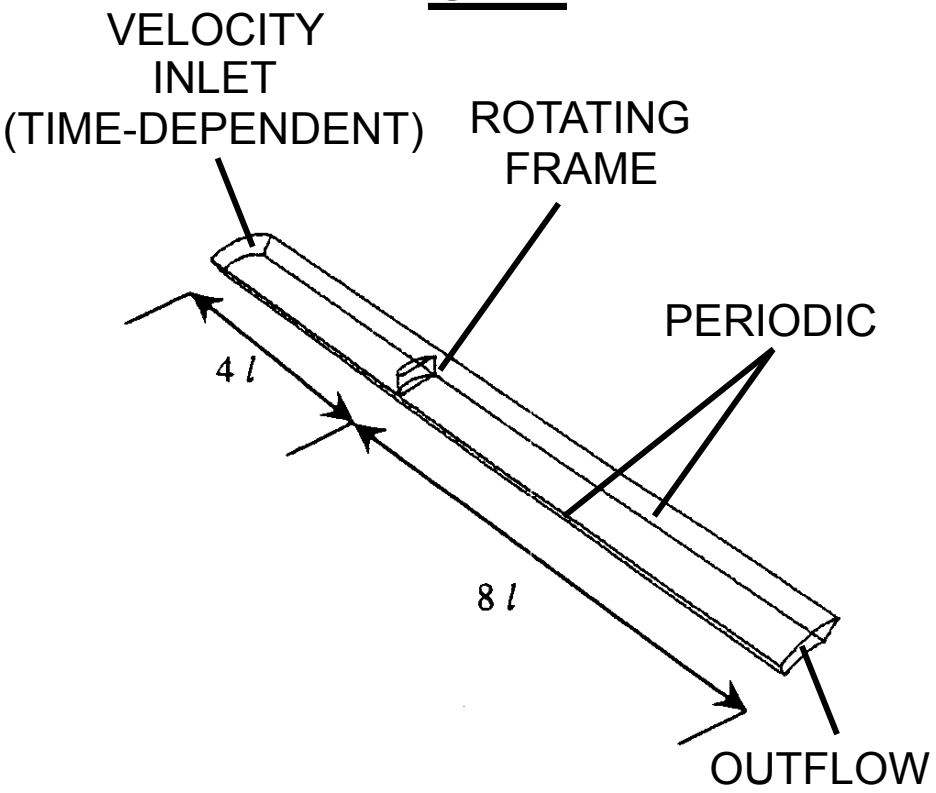

figures adapted from:

Y. Kinoue, T. Setoguchi, T.H. Kim, K. Kaneko, and M. Inoue. Mechanism of **hysteretic** characteristics of wells turbine for wave power conversion. *Journal of Fluids Engineering, Transactions of the ASME*, 125(2):302–307, 2003.